



Sudan University of Science and Technology
College of Graduate Studies



Optical Properties of Nano-Crystalline ZnO-AL₂ O₃ Thin Films

(الخواص الضوئية لشريحة بلورات اكسيد الزنك - اكسيد الالمونيوم النانوية
الرقيقة)

A Thesis Submitted To Graduate College For Fulfillment For The Requirements
Of The Degree Of. Ph.D.

By:

Zohl Ebnouf Mohamed Ebnouf

Supervisor:

Dr. Ahmed Elhassan Elfaki Idries

Co-Supervisor:

Prof. Mubarak Dirar Abdallah

April. 2019

الآية

قَالَ تَعَالَى:

﴿ وَاللَّهُ أَخْرَجَكُمْ مِنْ بُطُونِ أُمَّهَاتِكُمْ لَا تَعْلَمُونَ شَيْئًا وَجَعَلَ
لَكُمْ السَّمْعَ وَالْأَبْصَرَ وَالْأَفْئِدَةَ لَعَلَّكُمْ تَشْكُرُونَ ﴾ (٧٨)

سورة النحل: ٧٨



Dedication

To all those who are enlightened by the knowledge of the mind of others or guided by the correct answer puzzled by his patients, he showed with his tolerance humility of scientists and his blessing knowledge. Who taught me success and patience to those whom I missed to confront difficulties that faced me in my world to have some of his affection.

My father and to those whom my words are unable to describe them also my words extended to those who taught me and suffered and overcome all these difficulties to get to where I am and when I am bored I swim in the sea of tenderness to ease my pain.

.My mother, brothers and sisters:

To me who would light the way for me and support me and give up their rights to satisfy me and live in their joy. My brothers and sisters my love to you like if you pass on the barren land it will burst out of springs of love.

I also thank all the members of my family, specially my beloved husband who support me and helped me to accomplish this research and I owe them all my love and appreciation. And whoever taught me a character, or gave me advice or backed me, and to those who strengthen me, so I am very grateful to them all with great thanks and gratitude.

Acknowledgment

My special thanks and appreciation to everyone who contributed with me to this research, the family of the University of Sudan for Science and Technology Prof. Mubarak Dirar Abdallah, Dr. Ahmed Hassan Al-faki and Department of Physics, Department of Chemistry. University of Neeline represented by Dr. Abdul-Sakhi. And everyone who gave me help and support.

Abstract

In this study preparing eleventh samples of Zinc oxide doping by Aluminum oxide by formula $(ZnO)_x(Al_2O_3)_{1-x}$. Then study the effect of difference concentrations on the optical, electrical and morphology. Properties of Al_2O_3 on the ZnO thin films, prepared on glass slides by Sol-gel method. The optical characteristics of the prepared thin films have been investigated by UV-VIS spectrophotometer in the wavelength range (200 – 800) nm. The morphology characteristics of the prepared thin films have been investigated by XRD and used optical method to calculate the electrical properties. The films have a direct allowed electronic transition with optical energy (E_g) the value of untreated sample (ZnO) obtained was (3.615) eV while for other untreated sample (Al_2O_3) obtained was (3.511) eV. The value of (E_g) was decreased from (3.615) eV to (3.511) eV. The decreasing of (E_g) related to decreasing Aluminum Oxide index for $(Al_2O_3)_{1-x}$ on the samples. The maximum value of (n) is (2.13) for all samples at the difference wavelength which is agreement with red shift when the Aluminum Oxide index for $(Al_2O_3)_{1-x}$ increased for all samples of $(ZnO)_x(Al_2O_3)_{1-x}$. Dislocation density decreases and the number of unit cells increases with increasing in the calcinations $(ZnO)_x(Al_2O_3)_{1-x}$ ratio that leads to increase the crystal growth and decreasing the defects in crystallites. The crystallite size increases with increasing the (Al_2O_3) ratio. The relation between the ratio of $(ZnO)_x(Al_2O_3)_{1-x}$ and d -spacing. On the other hand, it's noticed that the ratio of (ZnO) increasing with decreases of the d -spacing and construction to larger clusters. Dislocation density decreases and the number of unit cells increases with increasing in the calcination $(ZnO)_x(Al_2O_3)_{1-x}$ ratio that leads to increase the crystal growth and decreasing the defects in crystallites. The high magnitude of optical conductivity $(1.3 \times 10^{11}) \Omega^{-1} \text{ cm}^{-1}$ confirms the presence of very high photo-

response of the eleven samples prepared by $(\text{ZnO})_x (\text{Al}_2\text{O}_3)_{1-x}$ form . The increased of optical conductivity at high photon energies is due to the high absorbance of eleven samples prepared by $(\text{ZnO})_x (\text{Al}_2\text{O}_3)_{1-x}$ form and may be due to electron excitation by photon energy. The results indicate the films have good characteristics for optoelectronic applications.

المستخلص

في هذه الدراسة تم تحضير إحدى عشر عينة من ZnO مطعمة بواسطة ALO وفقاً للصيغة التالية $(ZnO)_x(Al_2O_3)_{1-x}$ تمت دراسة اثر تغير تركيز التطعيم على كل من الخصائص الكهربائية والخصائص التركيبية تم تحضير ZnO المطعم بالـ ALO على شكل أفلام رقيقة عن طريق الطريقة الجلاتينية على ركائز من الزجاج درست الخصائص الضوئية للعينات بواسطة مطيافية الأشعة البنفسجية والأشعة المرئية في المدى من $(200 - 800)nm$ ، أما الخصائص التركيبية تم التحقق منها بواسطة جهاز حيود الأشعة السينية وأستخدمت النتائج الضوئية لحساب الخصائص الكهربائية وجد أن الأفلام الرقيقة المحضرة لها خاصية الإنتقالات المباشرة للإلكترونات وجد ان فجوة الطاقة الضوئية لعينة ZnO تساوي $3.615 eV$ بينما فجوة الطاقة لعينة ALO تساوي $3.511 eV$ وجد ان قيمة فجوة الطاقة تناقصت من $3.615 eV$ إلى $3.511 eV$ ، هذا التناقص يعزى لتناقص ALO الموجود في العينات.

وجد أن أعظم قيمة لمعامل الإنكسار لجميع العينات هي 2.13 عند أطوال موجية مختلفة تتوافق والإزاحة نحو الأحمر بزيادة أكسيد الألمونيوم، كما وجد ان كثافة العينات تتناقص مع زيادة عدد الوحدات في التركيب البلوري، أما الحجم البلوري تحدث فيه زيادة بزيادة ALO وعليه تحدث زيادة المسافة ما بين الوحدات بزيادة ZnO في العينات.

أكبر قيمة للموصلية كانت $10 \times 1.3 \Omega^{-1} CM^{-1}$ وهذا يتوافق مع الحساسية العالية للتوليد الضوئي مقابل الإمتصاص كل النتائج السابقة هي مؤشر إلى أن الأفلام الرقيقة هي أشباه الموصلات الجيدة للتطبيقات الكهروضوئية.

Table of Content

No.	Subject	Page No.
	الآية	I
	Dedication	Ii
	Acknowledgment	Iii
	Abstract	Iv
	المستخلص	Vi
	Table of Content	Vii
	List of Tables	X
	List of Figures	Xi
Chapter One		
Introduction		
1.1	Introduction	1
1.2	Research Problem	3
1.3	Significance	3
1.4	Layout of study	3
Chapter Two		
Theoretical Background		
2.1	Introduction	4
2.2	Crystals	6
2.2.1	Crystallization	7
2.2.2	Nano layer	8
2.3	Zinc Properties and Application	9
2.3.1	Occurrence	11
2.3.2	Applications	12
2.4	Optical Prorates	27
2.4.1	Absorption coefficients	27
2.4.2	Determination of Band Gaps	28
2.4.3	Refractive index	29
2.4.4	Reflection	30
2.4.5	Absorption	31
2.4.6	Transmission	31

Chapter Three Literature Review		
3.1	Introduction	32
3.2	Synthesis and Characterization of Aluminum Oxide (Al ₂ O ₃) Nanoparticles and its Application in Azodye Decolourisation	32
3.3	Trapping Iron Oxide into Hollow Gold Nanoparticles	33
3.4	Reduced Graphene Oxide and Its Natural Counterpart Shungite Carbon	34
3.5	Response of wheat to foliar application of zinc	35
3.6	Sulfidization flotation of a low grade oxide Pb-Zn ore	36
3.7	Convenient Preparation of Graphene Oxide from Expandable Graphite and Its Characterization by Positron Annihilation Lifetime Spectroscopy	37
3.8	Zinc and zinc nanoparticles: biological role and application in biomedicine	38
3.9	Zinc in Human Health	39
3.10	Electronic structure of aluminum oxide: ab initio simulations of α and γ phases and comparison with experiment for amorphous films	40
3.11	Biomedical applications of aluminum oxide nanoparticles	42
3.12	Physical and Chemical Properties of Zinc Cyanoferrates(II)	43
3.13	Optical properties of semiconductor nanocrystals: A symmetry-based tight-binding approach	44
3.14	Paper modified with ZnO nanorods – antimicrobial studies	45
3.15	Photocatalytic paper using zinc oxide nanorods	46
3.16	Preparation of Zinc Oxide Nanoparticles and its Characterization Using Scanning Electron Microscopy (SEM) and X-Ray Diffraction(XRD)	47
3.17	Influence of zinc acetate concentration in the preparation of ZnO nanoparticles via chemical bath deposition	48
Chapter Four Experimental Details		
4.1	Introduction	49
4.2	Materials	49
4.2.1	Aluminum Nitrate+	49
4.2.2	Zinc Acetate	49
4.2.3	Distilled Water	50

4.2.4	Hydrochloric Acid	50
4.2.5	Methanol	51
4.3	Equipment's	51
4.3.1	Ultraviolet – visible spectrometer	51
4.3.2	Shimadzu X-ray Diffractometer XRD-7000	53
Chapter Five		
Results, discussions, Conclusion and Recommendation		
5.1	Introduction	55
5.2	Results	55
5.2.1	Absorbance's	66
5.2.2	Transmittance	66
5.2.3	Reflectance	66
5.2.4	Absorption coefficient (α)	67
5.2.5	Extinction coefficient (K)	67
5.2.6	The optical energy gap (Eg)	68
5.2.7	The refractive index (n)	68
5.2.8	Real Dielectric Constant (ϵ_1)	69
5.2.9	The imaginary dielectric constant (ϵ_2)	69
5.2.10	Electrical and Optical Conductivity	70
5.3	The XRD charts Discussion	86
	References	88

List of Tables

Table caption	Page No.
Table (5.1) some crystallite lattice parameter (size , Miller indices and d-spacing) of the $(\text{ZnO})_{0.9}(\text{Al}_2\text{O}_3)_{0.1}$ sample	71
Table (5.2) some crystallite lattice parameter (size , Miller indices and d-spacing) of the $(\text{ZnO})_{0.8}(\text{Al}_2\text{O}_3)_{0.2}$ sample	73
Table (5.3) some crystallite lattice parameter (size , Miller indices and d-spacing) of the $(\text{ZnO})_{0.7}(\text{Al}_2\text{O}_3)_{0.3}$ sample	74
Table (5.4) some crystallite lattice parameter (size , Miller indices and d-spacing) of the $(\text{ZnO})_{0.6}(\text{Al}_2\text{O}_3)_{0.4}$ sample	75
Table (5.5) some crystallite lattice parameter (size , Miller indices and d-spacing) of the $(\text{ZnO})_{0.5}(\text{Al}_2\text{O}_3)_{0.5}$ sample	76
Table (5.6) some crystallite lattice parameter (size , Miller indices and d-spacing) of the $(\text{ZnO})_{0.4}(\text{Al}_2\text{O}_3)_{0.6}$ sample	77
Table (5.7) some crystallite lattice parameter (size , Miller indices and d-spacing) of the $(\text{ZnO})_{0.3}(\text{Al}_2\text{O}_3)_{0.7}$ sample	78
Table (5.8) some crystallite lattice parameter (size , Miller indices and d-spacing) of the $(\text{ZnO})_{0.2}(\text{Al}_2\text{O}_3)_{0.8}$ sample	79
Table (5.9) some crystallite lattice parameter (size , Miller indices and d-spacing) of the $(\text{ZnO})_{0.1}(\text{Al}_2\text{O}_3)_{0.9}$ sample	80
Table (5.10) some crystallite lattice parameter (size , Miller indices and d-spacing) of the $(\text{ZnO})_{0.0}(\text{Al}_2\text{O}_3)_{1.0}$ sample	81
Table (5.11) some crystallite lattice parameter (size , Miller indices and d-spacing) of the $(\text{ZnO})_{1.0}(\text{Al}_2\text{O}_3)_{0.0}$ sample	82
Table (5.12) some crystallite lattice parameter (c- form , a,b,c, β, α, γ , density , Xs(nm) and d-spacing) of all samples that made by $(\text{ZnO})_x(\text{Al}_2\text{O}_3)_{1-x}$	83

List of Figures

Name of Figure	Page No.
Fig (4.1) UV/V is spectrophotometer	52
Fig(4.2) X-ray diffracted measured	54
Fig(4.3) the sample that preparing	54
Fig(5.1) The relation between absorbance and wavelngths of elevant $(\text{ZnO})_x (\text{Al}_2\text{O}_3)_{1-x}$ samples	55
Fig (5.2)The relation between transission and wavelngths ofelevant $(\text{ZnO})_x (\text{Al}_2\text{O}_3)_{1-x}$ samples	56
Fig (5.3)The relation between reflection and wavelngths ofelevant $(\text{ZnO})_x (\text{Al}_2\text{O}_3)_{1-x}$ samples	57
Fig (5.4)The relation between absorption coefficient (α) and wavelngths ofelevant $(\text{ZnO})_x (\text{Al}_2\text{O}_3)_{1-x}$ samples	58
Fig (5.5)The relation between extencion coefficient (α) and wavelngths ofelevant $(\text{ZnO})_x (\text{Al}_2\text{O}_3)_{1-x}$ samples	59
Fig(5.6)The optical energy band gab ofelevant $(\text{ZnO})_x (\text{Al}_2\text{O}_3)_{1-x}$ samples	60
Fig (5.7)The relation between refractivie index and wavelngths ofelevant $(\text{ZnO})_x (\text{Al}_2\text{O}_3)_{1-x}$ samples	61
Fig (5.8)The relation between reail dielectric constant and wavelngths ofelevant $(\text{ZnO})_x (\text{Al}_2\text{O}_3)_{1-x}$ samples	62
Fig (5.9)The relation between imaganry dielectric constant and wavelngths ofelevant $(\text{ZnO})_x (\text{Al}_2\text{O}_3)_{1-x}$ samples	63
Fig (5.10)The relation between optical conductivity and wavelngths ofelevant $(\text{ZnO})_x (\text{Al}_2\text{O}_3)_{1-x}$ samples	64
Fig (5.11)The relation between electrical conductivity and wavelngths ofelevant $(\text{ZnO})_x (\text{Al}_2\text{O}_3)_{1-x}$ samples	65
Fig(5.12) the XRD charts of the $(\text{ZnO})_{0.9} (\text{Al}_2\text{O}_3)_{0.1}$ sample	71
Fig(5.13) the XRD charts of the $(\text{ZnO})_{0.8} (\text{Al}_2\text{O}_3)_{0.2}$ sample	72
Fig(5.14) the XRD charts of the $(\text{ZnO})_{0.7} (\text{Al}_2\text{O}_3)_{0.3}$ sample	73
Fig(5.15) the XRD charts of the $(\text{ZnO})_{0.6} (\text{Al}_2\text{O}_3)_{0.4}$ sample	74
Fig(5.16) the XRD charts of the $(\text{ZnO})_{0.5} (\text{Al}_2\text{O}_3)_{0.5}$ sample	75

Fig(5.17) the XRD charts of the $(\text{ZnO})_{0.4} (\text{Al}_2\text{O}_3)_{0.6}$ sample	76
Fig(5.18) the XRD charts of the $(\text{ZnO})_{0.3} (\text{Al}_2\text{O}_3)_{0.7}$ sample	77
Fig(5.19) the XRD charts of the $(\text{ZnO})_{0.2} (\text{Al}_2\text{O}_3)_{0.8}$ sample	78
Fig(5.20) the XRD charts of the $(\text{ZnO})_{0.1} (\text{Al}_2\text{O}_3)_{0.9}$ sample	79
Fig(5.21) the XRD charts of the $(\text{ZnO})_{0.0} (\text{Al}_2\text{O}_3)_{1.0}$ sample	80
Fig(5.22) the XRD charts of the $(\text{ZnO})_{1.0} (\text{Al}_2\text{O}_3)_{0.0}$ sample	81
Fig(5.23)Dependence of the crystallites size on the $(\text{ZnO})_x (\text{Al}_2\text{O}_3)_{1-x}$ Concentration(x) = ZnO concentration	84
Fig(5.24)Dependence of the d- spesing on the $(\text{ZnO})_x (\text{Al}_2\text{O}_3)_{1-x}$ Concentration(x) = ZnO concentration	84
Fig(5.25)Dependence of the density on the $(\text{ZnO})_x (\text{Al}_2\text{O}_3)_{1-x}$ Concentration(x) = ZnO concentration	85

Chapter One

Introduction

1.1 Introduction

In recent years, the use of nanotechnology has gained significant attention in environmental applications for wastewater treatment [1]. Nanoparticles in water treatment have been effectively utilized due to their unique characteristics such as high surface area to volume ratio, small size, availability of large number of reactive sites, and high capacity for regeneration [2]. The current water pollution problems, including water quality, can be improved using Nano adsorbents, Nano catalysts, nanostructured catalytic membranes, and many other products and processes resulting from the advancement of nanotechnology [3]. During the last few years a large number of Nano materials have been synthesized and used as adsorbents to remove the pollutants from the wastewater [4]. Inorganic Nano materials such as iron and aluminum based Nano adsorbents were firstly investigated which may be due to low manufacturing cost and high decontamination efficiency . Nano crystals are a material particles having at more complex , melting behavior than conventional solids. And may form the basis of special glass of solids. Solids occur in the crystalline solids about 10^{28} atom/m³ are arranged in three dimension in regular manners . This structure maybe obtain by repeating in three dimensions and elementary arrangement of some atoms or building blocks called unit cells consider the internal Structure of crystals in more detail for its description , its convent the to use the notion of a crystals lattice[5] .A comprehensive theoretical analysis of a monolayer consisting of metal or metalloid electric Nano particles with the dipole and quadruple single- particle resonances has been done[6] . a Nano crystal is a material particle having at least one dimension smaller than 100 Nano meters, based on quantum dots (a nanoparticle) and composed of atoms in either a single- or poly-crystalline arrangement. The size of nanocrystals distinguishes them from larger crystals. For example, silicon nanocrystals can provide efficient light emission while bulk silicon does not] and may be used for memory components. When embedded in solids, nanocrystals may exhibit much more complex melting be heavier than

conventional solid and may form the basis of a special class of solids. They can behave as single-domain systems (a volume within the system having the same atomic or molecular arrangement throughout) that can help explain the behavior of macroscopic samples of a similar material without the complicating presence of grain boundaries and other defects.[citation needed] Semiconductor nanocrystals having dimensions smaller than 10 nm are also described as quantum dots. Nanocrystals made with zeolite are used to filter crude oil into diesel fuel at an ExxonMobil oil refinery in Louisiana at a cost less than conventional methods.[7]The demands made on the substrates of thin films follow from their purpose: the substrate serves as mechanical support for the film and in electronic applications it usually serves also as an insulator. The need for long-term stability in thin film substrates makes it imperative that no chemical reactions occur which could change the properties of thin film. The substrate must therefore fulfill certain requirements as to mechanical strength and there must be adequate adhesion of the film substrate, not only at normal temperature but also during relatively large temperature changes. Thickness is one of the most important thin-film parameters since it largely determines the properties of a film. On the other hand, almost all properties on thin film depends on thickness depends on the method measurement selected or, more accurately, different method of measurement may yield different results i.e [8]. The thin film technology strategic research program (or thin film SRP) was officially launched in April 2001 to keep pace with the technological advancement in thin film related application areas. These areas include substrate patterning, bump metallurgy, thin film filters and coating for fiber optic telecommunication systems. Medical implants and wear protection, etc. Thin film technology is also closely linked with nanotechnology, which is becoming one of the main areas in the new-generation manufacturing and precision engineering industries. With decreasing thickness the surface structure of a coating gain more and more importance in the extreme case of ultrathin films the surface roughness may be in the order of the film thickness and can influence all film properties such as mechanical, electrical, magnetically or optical properties. Also film morphology, inner structure texture and crystalline are strongly connected to roughness evolution. This section shall briefly discuss basic roughness types, the mechanism of their origin, roughness measurement and roughness quantification .[8]Zinc is the heaviest member of the first row transition series of elements, consisting of SC , Ti, V, Cr, MN, Fe, Co, Ni, Cu and Zn, and belongs to group 12

of the periodic table, along with Cd and Hg. The element has an atomic number of 30, an atomic mass of 65, one main oxidation state (+2) and five naturally occurring isotopes (^{64}Zn , ^{66}Zn , ^{67}Zn , ^{68}Zn and ^{70}Zn), of which ^{64}Zn , ^{66}Zn and ^{68}Zn are the most abundant at 48.6%, 27.9% and 18.8% respectively of the total mass. The chemistry of Zn is most similar to that of Cd. Zinc is a halophile metallic element and forms several minerals, including the commonest Zn mineral, ZnCO_3 and zincite ZnO , but is also widely dispersed as a trace element in pyroxene, amphibole, mica, garnet and magnetite. During magmatic processes, Zn, like most other first-row transition metals, shows compatibility during early fractionation and thus becomes enriched in mafic relative to felsic rocks. The principal Zn carrier in mafic rocks is magnetite, while biotite is generally the most important in granite [9]

1.2 Research Problem

The zinc plays an important role in fabrication of solar cells. The efficiency ZnO solar cells is low. The chemical treatment of Zn does not till now lead to find suitable doping material that enhance Zn solar cells efficiency.

1.3 Significance

ZnO are used in fabrication of solar cells and light sensors. Thus the doping of Zn with other compounds to improve its optical properties helps in improving the performance of solar cells and optical sensors.

1.4 Layout of study

The research consist of five chapter as follows: Chapter one is the introduction and proposal, Chapter two consist of the theoretical background Chapter three is the literature review, and then Chapter four is devote for the practical and methodology. Then is the last chapter concert analysis, discussion and conclusion.

Chapter Two

Theoretical Background

2.1 Introduction

Nanotechnology is the science of controlling matter at the atomic or molecular scale. In the past decade major advances have been made in the synthesis of nanoparticles (NPs) of various size, shape and composition with high degree of monodispersity. However applications in imaging, plasmonics and metamaterials¹[4] require a substantial progress in engineering multifunctional NP surfaces as well as assembly of individual nanoparticles into complex 3D geometries. The optical and magnetic responses of an ensemble of NPs are dramatically different compared to the individual NPs due to collective resonance of electrons on the surface. Hence a very high degree of control over spatial organization is required to assemble and arrange the nanoparticles into various configurations to achieve desired optical response from the material. Functionalizing NP surfaces with various biomolecules, polymers and surfactants is a key step towards tuning free electrons on the surface. Hence a very high degree of control over spatial organization is required to assemble and arrange the nanoparticles into various configurations to achieve desired optical response from the material. Functionalizing NP surfaces with various biomolecules, polymers and surfactants is a key step towards tuning free electrons on the surface. Hence a very high degree of control over spatial organization is required to assemble and arrange the nanoparticles into various configurations to achieve desired optical response from the material. Functionalizing NP surfaces with various biomolecules, polymers and surfactants is a key step towards tuning various forces acting upon the NPs that eventually lead to organized superstructures. This dissertation reports novel developments in engineering functional metallic

nanoparticles and their application in molecular imaging, diagnostics and optical met materials .The emergence of "molecular imaging" as an integrated discipline in medicine has set the stage for an evolutionary leap in diagnostic imaging and therapeutic monitoring. Molecular imaging makes molecular processes visible, quant able, and tractable electrons on the surface. Hence a very high degree of control over spatial organization is required to assemble and arrange the nanoparticles into various conjurations to achieve desired optical response from the material. Functionalizing NP surfaces with various biomolecules, polymers and surfactants is a key step towards ne tuning various forces acting upon the NPs that eventually lead to organized superstructures. This dissertation reports novel developments in engineering functional metallic nanoparticles and their application in molecular imaging, diagnostics and optical meta materials. The emergence of "molecular imaging" as an integrated discipline in medicine has set the stage for an evolutionary leap in diagnostic imaging and therapeutic monitoring. Molecular imaging makes molecular processes visible, quant able, and tractable over time in a live animal or human, in physiologically authentic environments. In the preclinical stages, molecular imaging reduces the number of experimental animals that need to be ascribed because data is generated noninvasively. In clinical practice, molecular imaging may help with the decision to take, or not take, a drug candidate into clinical trials and will ore another way to monitor each once a drug is in trials. Molecular imaging involves integrating new imaging technology with new imaging agents. The coincident expansion of nanotechnology, which can sig accelerate the development of new imaging agents, has already played a fundamental role not only in molecular imaging, but also in biosensors, biomarkers, and drug delivery.⁵This area of research is anticipated to lead to the development of novel, sophisticated, multifunctional applications which can recognize specie receptors, deliver drugs to targeted tissue, aid in reporting

outcome of therapy, provide real-time assessment of therapeutic each, and most importantly, monitor intracellular changes to help understand pathological mechanisms.

2.2 Crystals

The scientific definition of a "crystal" is based on the microscopic arrangement of atoms inside it, called the crystal structure. A crystal is a solid where the atoms form a periodic arrangement. (Quasi crystals are an exception, see below.) Not all solids are crystals. For example, when liquid water starts freezing, the phase change begins with small ice crystals that grow until they fuse, forming a polycrystalline structure. In the final block of ice, each of the small crystals (called "crystallites" or "grains") is a true crystal with a periodic arrangement of atoms, but the whole polycrystalline does not have a periodic arrangement of atoms, because the periodic pattern is broken at the grain boundaries. Most macroscopic inorganic solids are polycrystalline, including almost all metals, ceramics, ice, rocks, etc. Solids that are neither crystalline nor poly crystalline, such as glass, are called amorphous solids, also called glassy, vitreous, or non crystalline. These have no periodic order, even microscopically. There are distinct differences between crystalline solids and amorphous solids: most notably, the process of forming a glass does not release the latent heat of fusion, but forming a crystal does. A crystal structure (an arrangement of atoms in a crystal) is characterized by its unit cell, a small imaginary box containing one or more atoms in a specific spatial arrangement. The unit cells are stacked in three-dimensional space to form the crystal. The symmetry of a crystal is constrained by the requirement that the unit cells stack perfectly with no gaps. There are 219 possible crystal symmetries, called crystallographic space groups. These are grouped into 7 crystal systems, such as cubic crystal system (where the crystals may form cubes or rectangular boxes, such

as halite shown at right) or hexagonal crystal system (where the crystals may form hexagons, such as ordinary water ice)[10] . Crystal face and shapes

2.2.1 Crystallization

Crystallization is the process of forming a crystalline structure from a fluid or from materials dissolved in a fluid. (More Crystallization is the process of forming a crystalline structure from a fluid or from materials dissolved in a fluid. (More rarely, crystals may be deposited directly from gas; see thin-film deposition and epitaxial.)Crystallization is a complex and extensively-studied field, because depending on the conditions, a single fluid can solidify into many different possible forms. It can form a single crystal, perhaps with various possible phases, stoichiometry's, impurities, defects, and habits. Or, it can form a polycrystalline, with various possibilities for the size, arrangement, orientation, and phase of its grains. The final form of the solid is determined by the conditions under which the fluid is being solidified, such as the chemistry of the fluid, the ambient pressure, the temperature, and the speed with which all these parameters are changing. Specific industrial techniques to produce large single crystals (called boules) include the process and the Bridgman technique. Other less exotic methods of crystallization may be used ,depending on the physical properties of the substance, including hydrothermal synthesis, sublimation, or simply solvent synthesis, sublimation, or simply solvent based crystallization. Large single crystals can be created by geological processes. For example, selenite crystals in excess of 10 meters are found in the Cave of the Crystals in Nazca, Mexico [11] . Occurrence in nature ROCKS By volume and weight, the largest concentrations of crystals in the Earth are part of its solid bedrock. Crystals found in rocks typically range in size from a fraction of a millimeter to several centimeters across, although

exceptionally large crystals are occasionally found. As of 1999, the world's largest[12]

2.2.2 Nanolayer

Today new packaging development has been emerging in the market and a big chunk of this new market trend goes to multilayer barrier films. It has been proven that increasing the number of layers is among the most significant factor that affects mechanical properties of film, in Addition improved barriers properties, and the ability to manufacture many different film structures, especially when comes to barrier film products flexible packaging converters are always looking for innovations, to create new structures to innovations, the shelf life of products and provide new substances for use in packaging. they are working to develop ways to enhance packing efficiency and the possibility of reducing the thickness of film without sacrificing the quality. The current advancement in Nano layer offers flexibility in the film Structure and leads to a greater choice for products in terms of mechanical propriety, optical properties and quality, Latest Nano layer technology was a result of development in Nano layer offers flexibility in the film structure and leads to a greater choice for products in terms of mechanical, optical properties and quality. Latest Nano layer technology related to the modular disk die, alpha Marathon has expanded its collaboration with BBS Corporation and developed high output blown film systems for these application, using its proprietary alpha plus double bubble technology. Today, rapidly developing market forum for shrinkable barrier film, involving the design and fabrication of ultra thin and highly constrain barrier polymer layers, Drives the need for a fundamental understanding of micro –and Nano-layer technology. In combination, Nano-layer technology with double bubble technology reduced the capital and facility costs to establish production, reduce Operating costs and significantly

increase production output. Consequent improve mints in the physical properties enable a reduction in the film thickness without compromising packaging performance, resulting in lower resin input cost per package ,further improving profitability with the added benefit of lower shipping costs per un packaging fresh meat. Shrink film /bags are convenient since standard sized bags adapt themselves to the individual sizes of each portion . They provide clarity and enhance the appearance of the packaged meat .They are temper evident and maintain product quality. Alpha marathons offers double bubble lines with co-extrusion or Nano-layer which produce highest quality shrink barrier films for superior packaging needs .standard sized bags adapt themselves to the individual sizes of each portion . They provide clarity and enhance the appearance of the packaged meat .They are temper evident and maintain product quality. Alpha marathons offers double bubble lines with co-extrusion or Nano-layer which produce highest quality shrink barrier films for superior packaging needs[13].

2.3 Zinc Properties and Application

ZIN Zinc is a chemical element with symbol Zn and atomic number 30. It is the first element in group 12 of the periodic table .In some respects zinc is chemically similar to magnesium: both elements exhibit only one normal oxidation state(+2),and the Zn^{2+} and Mg^{2+} ions are of similar size. Zinc is the 24th most abundant element in Earth's crust and has five stable isotopes. The most common zinc ore is sphalerite (zinc blende), a zinc sulfide mineral. The largest workable lodes are in Australia ,Asia, and the United States. Zinc I refined by froth flotation of the ore ,roasting, and final extraction using electricity (electro winning). Zinc, $30Zn$ Appearance silver-gray . Standard atomic 65.38(2)[1]weight (AR, standard) ,Zinc in the periodic table , Atomic number (Z) 30 Group 12 Period period4 ,Element category post-transition metal, Alternatively considered a transition ,

metal Block d-block, Electron configuration [AR] $3d^{10}4s^2$, Electrons per shell 2, 8, 18, 2. Physical properties: Phase at STP solid Melting point 692.68 K (419.53 °C, 787.15 °F) Boiling point 1180 K (907 °C, 1665 °F) Density (near r.t.) 7.14 g/cm³ when liquid (at m.p.) 6.57 g/cm³ Heat of fusion 7.32 kJ/mole Heat of vaporization 115 kJ/mole Molar heat capacity 25.470 J/(mole · K). Atomic properties Oxidation states (-2, 0, +1, +2) (an amphoteric oxide) Electronegativity Pauling scale: 1.65, Ionization energies 1st: 906.4 kJ/mole 2nd: 1733.3 kJ/mole 3rd: 3833 kJ/mole (more) Atomic radius empirical: 134 pm Covalent radius 122±4 pm Van der Waals radius 139 pm Other properties Crystal structure hexagonal close packed (hcp) Speed of sound 3850 m/s (at r.t.) thin rod (rolled) Thermal expansion 30.2 μm/(m·K) (at 25 °C) Thermal conductivity 116 W/(m·K) Electrical resistivity 59.0 nΩ·m (at 20 °C) Magnetic ordering diamagnetic Magnetic susceptibility (298 K) $-11.4 \cdot 10^{-6}$ cm³/mole [2] Young's modulus 108 GP a Shear modulus 43 GP a Bulk modulus 70 GPa Poisson ratio 0.25 Mohs hardness 2.5 Brinell hardness 327–412 MPa CAS Number 7440-66-6 Characteristics Physical properties Zinc is a bluish-white, lustrous, diamagnetic metal, [12] though most common commercial grades of the metal have a dull finish. [13] It is somewhat less dense than iron and has a hexagonal crystal structure, with a distorted form of hexagonal close packing, in which each atom has six nearest neighbors (at 265.9 pm) in its own plane and six others at a greater distance of 290.6 pm. [14] The metal is hard and brittle at most temperatures but becomes malleable between 100 and 150 °C. [12][13] Above 210 °C, the metal becomes brittle again and can be pulverized by beating. [15] Zinc is a fair conductor of electricity. [12] For a metal, zinc has relatively low melting (419.5 °C) and boiling points (907 °C). [16] The melting point is the lowest of all the d-block metals aside from mercury and cadmium; for this, among other reasons, zinc, cadmium, hexagonal close packing, in which each atom has six nearest neighbors (at 265.9 pm) in its own plane and six others at a greater distance of 290.6 pm. [14]

The metal is hard and brittle at most temperatures but becomes malleable between 100 and 150 °C.[12][13] Above 210 °C, the metal becomes brittle again and can be pulverized by beating.[15] Zinc is a fair conductor of electricity.[12] For a metal, zinc has relatively low melting (419.5 °C) and boiling points (907 °C).[16] The melting point is the lowest of all the d-block metals aside from mercury and cadmium; for this, among other reasons, zinc, cadmium, and mercury are often not considered to be transition metals like the rest of the d-block metals are.[16] Many alloys contain zinc, including brass. Other metals long known to form binary alloys with zinc are aluminum, antimony, bismuth, gold, iron, lead, mercury, silver, tin, magnesium, cobalt, nickel, tellurium and sodium.[17] Although neither zinc nor zirconium are ferromagnetic, their alloy ZrZn₂ exhibits ferromagnetism below 35 K.[12] A bar of zinc generates a characteristic sound when bent, similar to tin cry.

2.3.1 Occurrence:

Zinc makes up about 75 ppm (0.0075%) of Earth's crust, making it the 24th most abundant element. Soil contains zinc in 5–770 ppm with an average 64 ppm. Seawater has only 30 ppb and the atmosphere, 0.1–4 µg/m³. [18] The element is normally found in association with other base metals such as copper and lead in ores.[19] Zinc is a halophile, meaning the element is more likely to be found in minerals together with sulfur and other heavy halogens, rather than with the light chalcogen oxygen or with non-chalcogen electronegative elements such as the halogens. Sulfides formed as the crust solidified under the reducing conditions of the early Earth's atmosphere.[20] Sphalerite, which is a form of zinc sulfide, is the most heavily mined zinc-containing ore because its concentrate contains 60–62% zinc.[19] Other source minerals for zinc include Smithsonite (zinc carbonate), hemimorphite (zinc silicate), quartzite (another zinc sulfide), and sometimes hydrozincate (basic zinc carbonate).[21] With the exception of quartzite, all the soother

minerals were formed by weathering of the primordial zinc sulfides.[20] Identified world zinc resources total about 1.9–2.8 billion to nine billion tonnes.[22][23] Large deposits are in Australia, Canada and the United States, with the largest reserves in Iran.[20][24][25] The most recent estimate of reserve base for zinc (meets specified minimum physical criteria related to current mining and production practices) was made in 2009 and calculated to be roughly 480 Mt.[26] Zinc reserves, on the other hand, are geologically identified ore bodies whose suitability for recovery is quality, and quantity) at the time of determination. Since exploration and mine development is an on going process, the amount of zinc reserves is not a fixed number and sustainability of zinc ore supplies cannot be judged by simply extrapolating the combined mine life of today's zinc mines. This concept is well supported by data from the United States Geological Survey (USGS), which illustrates that although refined zinc production increased 80% between 1990 and 2010, the reserve lifetime for zinc has remained unchanged. About 346 million tonnes have been extracted throughout history to 2002, and scholars have estimated that about 109–305 million tonnes are in use.[27][28][29].

2.3.2 Applications:

Major applications of zinc include (numbers are given for the US)[30] , Galvanizing (55%) , Brass and bronze (16%) , Other alloys (21%) and Miscellaneous (8%) .

2.3.2.1 Anti-corrosion and batteries:

Zinc is more reactive than iron or steel and thus will attract almost all local oxidation until it completely corrodes away.[31] A protective surface layer of oxide and carbonate ($Zn_5(OH)_6(CO_3)_2$) forms as the zinc corrodes.[32] This protection lasts even after the zinc layer is scratched but degrades through times

the zinc corrodes away.[32] The zinc is applied electrochemically or as molten zinc by hot-dip galvanizing or spraying. Galvanization is used on chain-link fencing, guard rails, suspension bridges, light posts, metal roofs, heat exchangers, and car bodies.[18] The relative reactivity of zinc and its stability to attract oxidation to itself makes it an efficient sacrificial anode in cathodic protection (CP). For example, cathodic protection of a buried pipeline can be achieved by connecting anodes made from zinc to the pipe.[32] Zinc acts as the anode (negative terminus) by slowly corroding away as it passes current to the steel pipeline.[106][note 2] Zinc is also used to cathodically protect metals that are exposed to sea water.[33] A zinc disc attached to a ship's iron rudder will slowly corrode while the rudder stays intact.[31] Similarly, a zinc plug attached to a propeller or the metal protective guard for the keel of the ship provides temporary protection. With a standard electrode potential (SEP) of -0.76 volts, zinc is used as an anode. Zinc was used to produce 13.6 billion pennies in the United States.[34] Alloys of zinc with small amounts of copper, aluminum, and magnesium are useful in die casting as well as spin casting, especially in the automotive, electrical, and hardware industries.[12] These alloys are marketed under the name Zamak.[35] An example of this is zinc aluminum. The low melting point together with the low viscosity of the alloy makes possible the production of small anode material for batteries. (More reactive lithium (SEP -3.04 V) is used for anode in lithium batteries). Powdered zinc is used in this way in alkaline batteries and the case (which also serves as the anode) of zinc-carbon batteries formed from sheet zinc.[36][37] Zinc is used as the anode or fuel of the zinc-air battery/fuel cell.[110][111][112] The zinc cerium redox flow battery also relies on a zinc-based negative half-cell.[38].

2.3.2.2 Alloys :

A widely used zinc alloy is brass, in which copper is alloyed with anywhere from 3% to 45% zinc, depending. Other widely used zinc alloys include nickel silver, typewriter metal, soft and aluminum solder, and commercial bronze.[12] Zinc is also used in contemporary pipe organs as a substitute for the traditional lead/tin alloy in pipes.[39] Alloys of 85–88% zinc, 4–10% copper, and 2–8% aluminum find limited use in certain types of machine bearings. Zinc is the primary metal in American one cent coins (pennies) since 1982.[40] The zinc core is coated with a thin layer of copper to give the appearance of a copper coin. In 1994, 33,200 tones (36,600 short tons) of zinc were used to produce 13.6 billion pennies in the United States.[35] Alloys of zinc with small amounts of copper, aluminum, and magnesium are useful in die casting as well as spin casting, especially in the automotive, electrical, and hardware industries.[12] These alloys are marketed under the name Zamak.[39] An example of this is zinc aluminum. The low melting point together with the low viscosity of the alloy makes possible the production of small and intricate shapes. The low working temperature leads to rapid cooling of the cast products and fast production for assembly.[12][38] Another alloy, marketed under the brand name Prestel, contains 78% zinc and 22% aluminum, and is reported to be nearly as strong as steel but as malleable as plastic.[12][39] This super plasticity of the alloy allows it to be molded using die casts made of ceramics and cement.[12] Similar alloys with the addition of a small amount of lead can be cold-rolled into sheets. An alloy of 96% zinc and 4% aluminum is used to make stamping dies for low production run applications for which ferrous metal dies would be too expensive.[41] For building facades, roofing, and other applications for sheet metal formed by deep drawing, rollforming, or bending, zinc alloys with titanium and copper are used.[42] Unalloyed zinc is too brittle for these

manufacturing processes.[42] As a dense, inexpensive, easily worked material, zinc is used as a lead replacement. In the wake of lead concerns, zinc appears in weights for various applications ranging from fishing[43] to tire balances and flywheels [43]. Cadmium zinc telluride (CZT) is a semi conductive alloy that can be divided into an array of small sensing devices.[44] These devices are similar to an integrated circuit and can detect the energy of incoming gamma ray photons.[44] When behind an absorbing mask, the CZT sensor array can determine the direction of the rays.[44].

2.3.2.3 Other industrial uses:

Roughly one quarter of all zinc output in the United States in 2009 was consumed in zinc compounds,[36] a variety of which are used industrially. Zinc oxide is widely used as a white pigment in paints and as a catalyst in the manufacture of rubber to disburse heat. Zinc oxide is used to protect rubber polymers and plastics from ultraviolet radiation (UV).[18] The semiconductor properties of zinc oxide make it useful in visitors and photocopying products.[45] The zinc zinc-oxide cycle is a two step thermochemical process based on zinc and zinc oxide for hydrogen production.[46]methyl (Zn(CH₃)₂) is used in a number of organic syntheses.[47] Zinc sulfide (ZnS)is used in luminescent pigments such as on the hands of clocks, X-ray and television screens, and luminous paints.[48] Crystals of ZnS are used in lasers that operate in the mid-infrared part of the spectrum.[49] Zinc sulfate is a chemical in dyes and pigments.[46] Zinc pyrithione is used in antifouling paints.[50] . Zinc powder is sometimes used as a propellant in model rockets.[51] When a compressed mixture of 70% zinc and 30% sulfur powder is ignited there is a violent chemical reaction.[51] This produces zinc sulfide, together with large amounts of hot gas, heat, and light.[51]Zinc sheet metal is used to make zinc bars.[52]. ⁶⁴zn, the most abundant isotope of zinc, is very susceptible

to neutron activation, being transmuted into the highly radioactive ^{65}Zn , which has a half-life of 244 days and produces intense gamma radiation. Because of this, zinc oxide used in nuclear reactors as an anticorrosion agent is depleted of ^{64}Zn before use, this is called depleted zinc oxide. For the same reasons, zinc has been proposed as a salting material for nuclear weapons (cobalt is another better-known salting material) (135) jacket of isotopically enriched ^{64}Zn would be irradiated by the intense high energy neutron flux from an exploding thermonuclear weapon, forming a large amount of ^{65}Zn significantly increasing the radioactivity of the weapon's fallout.[135] Such a weapon is not known to have ever been built, tested, or used.[53] ^{65}Zn is used as a tracer to study how alloys that contain zinc wear out, or the path and the role of zinc in organisms.[54] Zinc includes Zinc, Mentram, Propineb and Ziram.[55] Zinc naphthylate is used as wood preservative.[55] Zinc in the form of ZDDP, is used as an anti-wear additive for metal parts in engine oil.[56] thiocarbamate complexes are used as agricultural fungicides; these. Organozinc chemistry is the science of compounds that contain carbon-zinc reacts with alkene(or alkyne) and converts them to cyclopropane The Addition reaction of organozinc compounds to form carbonyl compounds The Barbier reaction (1899), which is the zinc equivalent of the magnesium Grignard reaction and is the better of the two. In presence of water, formation of the organomagnesium halide will fail, whereas the Barbier reaction can take place in water. On the downside, organozincs are much less nucleophilic than Grignard's, and they are expensive and difficult to handle. Commercially available organozinc compounds are dimethyl zinc, diethyl zinc and biphenyl zinc. In one study,[57][58] the active organozinc compound is obtained from much cheaper organobromine precursors The Negishi coupling is also important reaction for the formation of new carbon-carbon bonds between unsaturated carbon atoms in alkenes, arenes and alkynes. The catalysts are nickel and palladium.. A key step in the catalytic cycle is a transmetalation in which a

zinc halide exchanges its organic substituent for another halogen with the palladium (nickel)metal center. The Fukuyama coupling is another coupling reaction, but it uses a $\text{C}=\text{O}$ as reactant and produces acetone. Zinc has found many applications as catalyst in organic synthesis include in asymmetric synthesis, being cheap and easily available alternative to precious metal complexes. The results (yield and) obtained with chiral zinc catalysts are comparable to those achieved with palladium, ruthenium, iridium and others, and zinc becomes metal catalyst of choice.[58] Dietary supplement. In most single-tablet, over-the-counter, daily vitamin and mineral supplements, zinc is included in such forms as zinc oxide, zinc acetate, or zinc gluconate.[59]Zinc is generally considered to be an antioxidant. However, it is redox inert and thus can serve such a function on its own directly.[59] Generally, zinc supplement is recommended where there is high risk of zinc deficiency (such as low and middle income countries) as a preventive measure.[60]Zinc deficiency has been associated with major depressive disorder (MDD), and zinc supplements may be an effective treatment.[61]Zinc serves as a simple, inexpensive, and critical tool for treating diarrhea. A Cochrane review stated that people taking zinc supplement may be less likely to progress to age-related macular degeneration [62]. Zinc supplement is an effective treatment for acrodermatitis enteropathica, a genetic disorder affecting zinc absorption that was previously fatal to affected infants.[57]Gastroenteritis is strongly attenuated by ingestion of zinc, possibly by direct antimicrobial action of the ions in the gastrointestinal tract, or by the absorption of the zinc and re-release from immune cells (all granulocytes secrete zinc), or both.[44][63]In 2011, researchers reported that adding large amounts of zinc to a urine sample masked detection of drugs. The researchers did not test whether orally consuming a zinc dietary supplement could have the same effect [64]. Zinc is a negative allosteric modulator of the GABA_A receptor [59].

Common cold: Zinc supplements (frequently zinc acetate or zinc gluconate lozenges) are a group of dietary supplements that are commonly used for the treatment of the common cold.[158] The use of zinc supplements at doses in excess of 75 mg/day within 24 hours of the onset of symptoms has been shown to reduce the duration of cold symptoms by about 1 day.[47][53] Due to a lack of data, there is insufficient evidence to determine whether the preventative use of zinc supplements reduces the likelihood of contracting a cold.[59] Adverse effects with zinc supplements by mouth include bad taste and nausea.[58][59] The intranasal use of zinc-containing nasal sprays has been associated with the loss of the sense of smell;[158] consequently, in June 2009, the United States Food and Drug Administration (USFDA) warned consumers to stop using intranasal zinc products.[58] The human rhinovirus – the most common viral pathogen in humans – is the predominant cause of the common cold.[60] The hypothesized mechanism of action by which zinc reduces the severity and/or duration of cold symptoms is the suppression of nasal inflammation and the direct inhibition of rhinoviral receptor binding and rhinoviral replication in the nasal mucosa.[58].

Topical use : Topical preparations of zinc include those used on the skin, often in the form of zinc oxide. Zinc preparations can protect against sunburn in the summer and windburn in the winter.[57] Applied thinly to a baby's diaper area (perineum) with each diaper change, it can protect against diaper rash.[57] Chelated zinc is used in toothpastes and mouthwashes to prevent bad breath.[161] Zinc pyrithione is widely included in shampoos to prevent dandruff.[62] Zinc is an essential trace element for humans[63][64][65] and other animals,[66] for plants[68] and for microorganisms.[67] Zinc is required for the function of over 300 enzymes and 1000 transcription factors,[65] and is stored and transferred in metallothioneins.[68][69] It is the second most abundant trace metal in humans .

Biological role: after iron and it is the only metal which appears in all enzyme classes.[68][65] In proteins, zinc ions are often coordinated to the amino acid side chains of aspartic acid, glutamic acid, cysteine and histidine. The theoretical and computational description of this zinc binding in proteins (as well as that of other transition metals) is difficult.[70] Roughly 2–4 grams of zinc[71] are distributed throughout the human body. Most zinc is in the brain, muscle, bones, kidney, and liver, with the highest concentrations in the prostate and parts of the eye.[72] Semen is particularly rich in zinc, a key factor in prostate gland function and reproductive organ growth.[73] In humans, the biological roles of zinc are ubiquitous.[9][64] It interacts with "a wide range of organic ligands", [9] and has roles in the metabolism of RNA and DNA, signal transduction, and gene expression. It also regulates apoptosis. A 2006 study estimated that about 10% of human proteins (2800) potentially bind zinc, in addition to hundreds more that transport and traffic zinc; a similar in silico study in the plant *Arabidopsis thaliana* found 2367 zinc-related proteins.[68] In the brain, zinc is stored in specific synaptic vesicles by glutamatergic neurons and can modulate neuronal excitability.[64][65][74] It plays a key role in synaptic plasticity and so in learning.[64][75] Zinc homeostasis also plays a critical role in the functional regulation of the central nervous system.[64][74][65] Dysregulation of zinc homeostasis in the central nervous system that results in excessive synaptic zinc concentrations is believed to induce neurotoxicity through mitochondrial oxidative stress (e.g., by disrupting certain enzymes involved in the electron transport chain, including complex I, complex III, and α -ketoglutarate dehydrogenase), the dysregulation of calcium homeostasis, glutamatergic neuronal excitotoxicity, and interference with intraneuronal signal transduction.[64][76] L- and D-histidine facilitate brain zinc uptake.[77] SLC30A3 is the primary zinc transporter involved in cerebral zinc homeostasis.[64].

Enzymes: Ribbon diagram of human carbonic anhydrase II, with zinc atom visible in the center. Zinc is an efficient Lewis acid, making it a useful catalytic agent in hydroxylation and other enzymatic reactions.[78] The metal also has a flexible coordination geometry, which allows proteins using it to rapidly shift conformations to perform biological reactions.[79] Two examples of zinc-containing enzymes are carbonic anhydrase and carboxypeptidase, which are vital to the processes of carbon dioxide (CO₂) regulation and digestion of proteins, respectively.[80] In vertebrate blood, carbonic anhydrase converts (CO₂) into bicarbonate and the same enzyme transforms the bicarbonate back into CO₂ for exhalation through the lungs.[81] Without this enzyme, this conversion would occur about one million times slower[82] at the normal blood pH of 7 or would require a pH of 10 or more.[83] The non-related β -carbonic anhydrase is required in plants for leaf formation, the synthesis of indoleacetic acid (auxin) and alcoholic fermentation.[84] Carboxypeptidase cleaves peptide linkages during digestion of proteins. A coordinate covalent bond is formed between the terminal peptide and a C=O group attached to zinc, which gives the carbon a positive charge. This helps to create a hydrophobic pocket on the enzyme near the zinc, which attracts the non-polar part of the protein being digested.[80].

Signalling: Zinc has been recognized as a messenger, able to activate signaling pathways. Many of these pathways provide the driving force in aberrant cancer growth. They can be targeted through ZIP transporters.[85] .

Other proteins: Zinc serves a purely structural role in zinc fingers, twists and clusters.[86] Zinc fingers form parts of some transcription factors, which are proteins that recognize DNA base sequences during the replication and transcription of DNA. Each of the nine or ten Zn²⁺ ions in a zinc finger helps

maintain the finger's structure by coordinately binding to four amino acids in the transcription factor.[82] The transcription factor wraps around the DNA helix and uses its fingers to accurately bind to the DNA sequence. In blood plasma, zinc is bound to and transported by albumin (60%, lowaffinity) and transferrin (10%).[71] Because transferrin also transports iron, excessive iron reduces zinc absorption, and vice versa. A similar antagonism exists with copper.[87] The concentration of zinc in blood plasma stays relatively constant regardless of zinc intake.[188] Cells in the salivary gland, prostate, immune system, and intestine use zinc signaling to communicate with other cells.[89] Zinc may be held in metallothioneinreserves within microorganisms or in the intestines or liver of animals.[90] Metallothionein in intestinal cells is capable of adjusting absorption of zinc by 15–40%.[91] However, inadequate or excessive zinc intake can be harmful; excess zinc particularly impairs copper absorption because metallothioneinabsorbs both metals.[92]. The human dopamine transporter contains a high affinity extracellular zinc binding site which, upon zinc binding, nhibitsdopamine reuptake and amplifies amphetamine-induced dopamine efflux in vitro.[93][94][95] The human serotonin transporter and norepinephrine transporter do not contain zinc binding sites.[95].

Dietary recommendations : The U.S. Institute of Medicine (IOM) updated Estimated Average Requirements (EARs) and Recommended Dietary Allowances (RDAs) for zinc in 2001. The current EARs for zinc for women and men ages 14 and up is 6.8 and 9.4 mg/day, respectively. The RDAs are 8 and 11 mg/day. RDAs are higher than EARs so as to identify amounts that will cover people with higher than average requirements. RDA for pregnancy is 11 mg/day. RDA for lactation is 12 mg/day. For infants up to 12 months the RDA is 3 mg/day. For children ages 1–13 years the RDA increases with age from 3 to 8 mg/day. As for safety, the IOM

sets Tolerable upper intake levels (ULs) for vitamins and minerals when evidence is sufficient. In the case of zinc the adult UL is 40 mg/day (lower for children). Collectively the EARs, RDAs, AIs and ULs are referred to as Dietary Reference Intakes (DRIs).[96] The European Food Safety Authority (EFSA) refers to the collective set of information as Dietary Reference Values, with Population Reference Intake (PRI) instead of RDA, and Average Requirement instead of EAR. AI and UL are defined the same as in United States. For people ages 18 and older the PRI calculations are complex, as the EFSA has set higher and higher values as the phytate content of the diet increases. For women, PRIs increase from 7.5 to 12.7 mg/day as phytate intake increases from 300 to 1200 mg/day; for men the range is 9.4 to 16.3 mg/day. These PRIs are higher than the U.S. RDAs.[97] The EFSA reviewed the same safety question and set its UL at 25 mg/day, which is much lower than the U.S. value.[98] For U.S. food and dietary supplement labeling purposes the amount in a serving is expressed as a percent of Daily Value (%DV). For zinc labeling purposes 100% of the Daily Value was 15 mg, but as of May 27, 2016 it has been revised to 11 mg.[99] A table of the old and new adult Daily Values is provided at Reference Daily Intake. Food and supplement companies have until January 1, 2020 to comply with the change.[100] .

Dietary intake : Animal products such as meat, fish, shellfish, fowl, eggs, and dairy contain zinc. The concentration of zinc in plants varies with the level in the soil. With adequate zinc in the soil, the food plants that contain the most zinc are wheat (germ and bran) and various seeds, including sesame, poppy, alfalfa, celery, and mustard.[101] Zinc is also found in beans, nuts, almonds, whole grains, Foods and spices containing zinc pumpkin seeds, sunflower seeds, and blackcurrant.[102] Plant phytates are particularly found in pulses and cereals and interfere with zinc absorption. Other sources include fortified food and dietary supplements in various

forms. A 1998 review concluded that zinc oxide, one of the most common supplements in the United States, and zinc carbonate are nearly insoluble and poorly absorbed in the body.[103] This review cited studies that found lower plasma zinc concentrations in the subjects who consumed zinc oxide and zinc carbonate than in those who took zinc acetate and sulfate salts.[203] For fortification, however, a 2003 review recommended cereals (containing zinc oxide) as a cheap, stable source that is as easily absorbed as the more expensive forms.[104] A 2005 study found that various compounds of zinc, including oxide and sulfate, did not show statistically significant differences in absorption when added as fortificants to maize tortillas.[105].

Deficiency :

Zinc deficiency is usually due to insufficient dietary intake, but can be associated with malabsorption, acrodermatitis enteropathica, chronic liver disease, chronic renal disease, sickle cell disease, diabetes, malignancy, and other chronic illnesses.[10] Groups at risk of zinc deficiency include the elderly, children in developing countries, and those with renal dysfunction. In the United States, a federal survey of food consumption determined that for women and men over the age of 19, average consumption was 9.7 and 14.2 mg/day, respectively. For women, 17% consumed less than the EAR, for men 11%. The percentages below EAR increased with age.[106] The most recent published update of the survey (NHANES 2013–2014) reported lower averages – 9.3 and 13.2 mg/day – again with intake decreasing with age.[207] Symptoms of mild zinc deficiency are diverse.[108] Clinical outcomes include depressed growth, diarrhea, impotence and delayed sexual maturation, alopecia, eye and skin lesions, impaired appetite, altered cognition, impaired host defense properties, defects in carbohydrate utilization, and reproductive teratogenesis.[88] Mild zinc deficiency depresses

immunity,[109] although excessive zinc does also.[71] Animals with a zinc deficiency require twice as much food to attain the same weight gain as animals with sufficient zinc.[30] Despite some concerns,[110] western vegetarians and vegans do not suffer any more from overt zinc deficiency than meat-eaters.[111] Major plant sources of zinc include cooked dried beans, sea vegetables, fortified cereals, soy foods, nuts, peas, and seeds.[110] However, phytates in many whole-grains and fibers may interfere with zinc absorption and marginal zinc intake has poorly understood effects. The zinc chelator phytate, found in seeds and cereal bran, can contribute to zinc malabsorption.[10] Some evidence suggests that more than the US RDA (15 mg) of zinc daily may be needed in those whose diet is high in phytates, such as some vegetarians.[110] These considerations must be balanced against the paucity of adequate zinc biomarkers, and the most widely used indicator, plasma zinc, has poor sensitivity and specificity.[112] Diagnosing zinc deficiency is a persistent challenge.[9] Nearly two billion people in the developing world are deficient in zinc.[10] In children, it causes an increase in infection and diarrhea and contributes to the death of about 800,000 children worldwide per year.[9] The World Health Organization advocates zinc supplementation for severe malnutrition and diarrhea.[113] Zinc supplements help prevent disease and reduce mortality, especially among children with low birth weight or stunted growth.[113] However, zinc supplements should not be administered alone, because many in the developing world have several deficiencies, and zinc interacts with other micronutrients.[114]

Soil remediation :

Species of *Calluna*, *Erica* and *Vaccinium* can grow in zinc metalliferous soils, because translocation of toxic ions is prevented by the action of ericoid mycorrhizal fungi.[115]

Agriculture:

Zinc deficiency appears to be the most common micronutrient deficiency in crop plants; it is particularly common in highpHsoils.[116] Zinc-deficient soil is cultivated in the cropland of about half of Turkey and India, a third of China, and most of Western Australia. Substantial responses to zinc fertilization have been reported in these areas.[98] Plants that grow in soils that are zinc-deficient are more susceptible to disease. Zinc is added to the soil primarily through the weathering of rocks, but humans have added zinc through fossil fuel combustion, mine waste, phosphate fertilizers, pesticide (zinc phosphide), limestone, manure, sewage sludge, and particles from galvanized surfaces. Excess zinc is toxic to plants, although zinc toxicity is far less widespread.[98]

Precautions :

Toxicity . Although zinc is an essential requirement for good health, excess zinc can be harmful. Excessive absorption of zinc suppresses copper and iron absorption.[92] The free zinc ion in solution is highly toxic to plants, invertebrates, and even vertebrate Precautions fish.[117] The Free Ion Activity Model is well-established in the literature, and shows that just micromolar amounts of the free ion kills some organisms. A recent example showed 6 micromolar killing 93% of all Daphnia in water.[118] The free zinc ion is a powerful Lewis acid up to the point of being corrosive. Stomach acid contains hydrochloric acid, in which metallic zinc dissolves readily to give corrosive zinc chloride. Swallowing a post-1982 American one cent piece (97.5% zinc) can cause damage to the stomach lining through the high solubility of the zinc ion in the acidic stomach.[119] Evidence shows that people taking 100– 300 mg of zinc daily may suffer induced copper deficiency. A 2007 trial observed that elderly men taking 80 mg daily were

hospitalized for urinary complications more often than those taking a placebo.[120] Levels of 100–300 mg interfere with the utilization of copper and iron or adversely affect cholesterol.[92] Zinc in excess of 500 ppm in soil interferes with the plant absorption of other essential metals, such as iron and manganese.[99] A condition called the zinc shakes or "zinc chills" can be induced by inhalation of zinc fumes while brazing or welding galvanized materials.[30] Zinc is a common ingredient of denture cream which may contain between 17 and 38 mg of zinc per gram. Disability and even deaths from excessive use of these products have been claimed.[121] The U.S. Food and Drug Administration (FDA) states that zinc damages nerve receptors in the nose, causing anosmia. Reports of anosmia were also observed in the 1930s when zinc preparations were used in a failed attempt to prevent polio infections.[122] On June 16, 2009, the FDA ordered removal of zinc-based intranasal cold products from store shelves. The FDA said the loss of smell can be life-threatening because people with impaired smell cannot detect leaking gas or smoke, and cannot tell if food has spoiled before they eat it.[123] Recent research suggests that the topical antimicrobial zinc pyrithione is a potent heat shock response inducer that may impair genomic integrity with induction of PARP-dependent energy crisis in cultured human keratinocytes and melanocytes.[124] .

Poisoning:

In 1982, the US Mint began minting pennies coated in copper but containing primarily zinc. Zinc pennies pose a risk of zinc toxicosis, which can be fatal. One reported case of chronic ingestion of 425 pennies (over 1 kg of zinc) resulted in death due to gastrointestinal bacterial and fungal sepsis. Another patient who ingested 12 grams of zinc showed only lethargy and ataxia (gross lack of coordination of muscle movements).[125] Several other cases have been reported

of humans suffering zinc intoxication by the ingestion of zinc coins.[126][127] Pennies and other small coins are sometimes ingested by dogs, requiring veterinary removal of the foreign objects. The zinc content of some coins can cause zinc toxicity, commonly fatal in dogs through severe hemolytic anemia and liver or kidney damage; vomiting and diarrhea are possible symptoms.[128] Zinc is highly toxic in parrots and poisoning can often be fatal.[129] The consumption of fruit juices stored in galvanized cans has resulted in mass parrot poisonings with zinc.[57] List of countries by zinc production Spelter Wet storage stain Zinc alloy electroplating See also Notes (An East India Company ship carrying a cargo of nearly pure zinc metal from the Orient sank off the coast Sweden in 1745 (Emsley 2001, p. 502) . And electric current will naturally flow between zinc and steel but in some circumstances inert anodes are used with an external DC source.

2.4 Optical Prorates

2.4.1 Absorption coefficients

Much of the information about the properties of materials is obtained when they interact with electromagnetic radiation. When a beam of light (photons) is incident on a material, the intensity is expressed by the Lambert-Beer-Bouguer law:

$$I = I_0 \exp(-\alpha d) \quad (2-1)$$

If this condition for absorption is met, it appears that the optical intensity of the light wave, (I), is exponentially reduced while traveling through the film. If the power that is coupled into the film is denoted by I_0 , gives the transmitted intensity that leaves the film of thickness d .

(α) Is called “absorption coefficient”. From (1) it follows that

$$\alpha = -\frac{1}{d} \text{Lin}\left(\frac{I}{I_0}\right) \quad (2-2)$$

It is clear that α must be a strong function of the energy $h\nu$ of the photons. For $h\nu < E_g$ (direct), no electron hole pairs can be created, the material is transparent and α is small. For $h\nu \geq E_g$ (direct), absorption should be strong. All mechanisms other than the fundamental absorption may add complications (e.g. "sub band gap absorption" through excitons), but usually are not very pronounced.

Optical transmission measurements were carried out to determine the film thickness, the wavelength dependence of the refractive index and optical absorption coefficient. The optical constants were determined from the optical transmission measurements using the method described by Swanepoel [130].

The transparent substrate has a thickness several orders of magnitude larger than (d) and has index of refraction (n) and absorption coefficient ($\alpha = 0$). The index of refraction for air is taken to be $n_0 = 1$. In the transparent region ($\alpha = 0$) the transmission is determined by n and s through multiple reflections. In the region of weak absorption α is small and the transmission begins to decrease. In the medium absorption region α is large and the transmission decreases mainly due to the effect of α . In the region of strong absorption the transmission decreases drastically due almost exclusively to the influence of α . If the thickness d is uniform, interference effects give rise to the spectrum.

2.4.2 Determination of Band Gaps

The fundamental absorption is related to band-to-band or to exaction transition, which are subjected to certain selection rules [17]. The transitions are classified into several types, according to the band structure of a material. The relation between absorption coefficient and optic band gap for direct transition ($k=0$) is given by Tauc equation [129]:

$$\sqrt{\alpha h\nu} = B(h\nu - E_g^{\text{opt}}) \quad (2-3)$$

And for indirect transition ($k \neq 0$) the relation becomes

$$\alpha(h\nu) \propto \frac{(\hbar\omega - E_{\text{gap}})^2}{\hbar\omega} \quad (2-4)$$

From the $\alpha h\nu$ versus $h\nu$ one obtains E_g and B parameters. B is also a useful diagnostic of the material since it is inversely proportional to the extent of the tail state (ΔE) at conduction and valance band edges[130].

2.4.3 Refractive index

Light that is transmitted into the interior of transparent materials experiences a decrease in velocity, and, as a result, is bent at the interface; this phenomenon is termed refraction. The index of refraction n of a material is defined as the ratio of the velocity in a vacuum c to the velocity in the medium or

$$n = \frac{c}{v} \quad (2.5)$$

The magnitude of n (or the degree of bending) will depend on the wavelength of the light. This effect is graphically demonstrated by the familiar dispersion or separation of a beam of white light into its component colors by a glass prism. Each color is deflected by a different amount as it passes into and out of the glass, which results in the separation of the colors. Not only does the index of refraction affect the optical path of light, but also, as explained shortly, it influences the fraction of incident light that is reflected at the surface. Just as Equation (2.5) defines the magnitude of c , an equivalent expression gives the velocity of light in a medium as

$$v = \frac{1}{\sqrt{\epsilon\mu}} \quad (2.6)$$

Where v and are, respectively, the permittivity and permeability of the particular substance. From Equation (2.5), we have

$$n = \frac{c}{v} = \frac{\sqrt{\epsilon_0\mu_0}}{\sqrt{\epsilon_r\mu_r}} = \sqrt{\epsilon_r\mu_r} \quad (2.7)$$

Where ϵ_r and μ_r are the dielectric constant and the relative magnetic permeability, respectively. Because most substances are only slightly magnetic, and

$$n \cong \sqrt{\epsilon_r} \quad (2.8)$$

Thus, for transparent materials, there is a relation between the index of refraction and the dielectric constant[130].

2.4.4 Reflection

When light radiation passes from one medium into another having a different index of refraction, some of the light is scattered at the interface between the two media even if both are transparent. The reflectivity R represents the fraction of the incident light that is reflected at the interface, or

$$R = \frac{I_R}{I_0} \quad (2.9)$$

Where I_0 and I_R are the intensities of the incident and reflected beams, respectively. If the light is normal (or perpendicular) to the interface, then

$$R = \left(\frac{n_2 - n_1}{n_2 + n_1} \right)^2 \quad (2.10)$$

Where n_1 and n_2 are the indices of refraction of the two media. If the incident light is not normal to the interface, R will depend on the angle of incidence. When light is transmitted from a vacuum or air into a solid s , then

$$R = \left(\frac{n_s - 1}{n_s + 1} \right)^2 \quad (2.11)$$

because the index of refraction of air is very nearly unity. Thus, the higher the index of refraction of the solid, the greater the reflectivity[131].

2.4.5 Absorption

The intensity of the net absorbed radiation is dependent on the character of the medium as well as the path length within. The intensity of transmitted or non-absorbed radiation continuously decreases with distance x that the light traverses:

$$I_T = I_0 e^{-\beta x} \quad (2.12)$$

Where I_0 is the intensity of the non-reflected incident radiation and β the absorption Coefficient (in mm^{-1}), is characteristic of the particular material; furthermore, varies with wavelength of the incident radiation. The distance parameter x is measured from the incident surface into the material. Materials that have large values are considered highly absorptive[130].

2.4.6 Transmission

The phenomena of absorption, reflection, and transmission may be applied to the passage of light through a transparent solid. For an incident beam of intensity I_0 that impinges on the front surface of a specimen of thickness l and absorption coefficient, the transmitted intensity at the back face I_T is

$$I_T = I_0 (1 - R)^2 e^{-\beta l} \quad (2.13)$$

Where R is the reflectance; for this expression, it is assumed that the same medium exists outside both front and back faces. The derivation of Equation (2.11) is left as a homework problem. Thus, the fraction of incident light that is transmitted through a transparent material depends on the losses that are incurred by absorption and reflection. Again, the sum of the reflectivity R , absorptivity A , and transmissivity T , is unity according to Equation (2.12). Also, each of the variables R , A , and T depends on light wavelength. This is demonstrated the transmission[132].

Chapter Three

Literature Review

3.1 Introduction

Many attempts were made to use metal oxide in fabrication of solar cells. The physical characteristics of these metal oxide like conductivity absorption coefficient are important parameters that play an important role in solar cells performance. In this chapter different attempts made will be exhibited here.

3.2 Synthesis and Characterization of Aluminum Oxide (Al_2O_3) Nanoparticles and its Application in Azodye Decolourisation:

This work done by Vijay a Pandering Dawdle. Come from India Post Graduate Department of Physics, New Arts Commerce and Science College, Parmer, Ahmednagar, India. The adsorption behavior of an Azodye Methylene Blue (MB) over aluminum oxide Nano particles (AONP) generated by sol-gel method has been studied to investigate the physicochemical process involved and explore the potential use of AONP in wastewater treatment. The variables incorporated in the present study are concentration of dye, dosage of adsorbent and contact time. The characterizations of AONPs were carried out using X-ray diffractometer (XRD), Scanning Electron Microscopy (SEM), Fourier Transform Infrared Spectroscopy (FTIR), Energy Dispersive Analysis of X-rays (EDAX) and Raman spectroscopy. SEM image showed the distribution pattern of nanoparticles. FTIR spectra revealed that functional groups (O-Al-O) are present. Raman spectra showed the crystalline nature of nanoparticles. Average size of Al_2O_3 nanoparticle from XRD peak was found to be 25 nm having rhombohedra structure. Chemical composition of AONPs was confirmed from EDAX spectroscopy measurement. The smaller dosage of AONP was tested for the photo catalytic degradation. To conclusions

this study for Aluminum oxide nanoparticles (Al_2O_3) were successfully synthesized via sol gel technique and the average particle size was found to be 25 nm having rhombohedra structure. FTIR spectra of aluminum oxide nanoparticles indicated the formation of aluminum oxide nanoparticles (Al_2O_3). X-Ray diffraction patterns confirm the formation of aluminum oxide (Al_2O_3) nanoparticles. The formation of aluminum oxide (Al_2O_3) nanoparticles was validated from Raman spectra, XRD, SEM and EDAX analysis. Maximum Decolourisation was found to be 36% for 25mg methylene blue (MB) dye concentration and 30 mg dose of aluminum oxide (AONP) nanoparticles. The average amount of dye adsorbed in the batch experiment was 23.9 mg/g. Thus, the above results support the recommendation that aluminum oxide nanoparticles offer new dimension towards reliable and economically affordable water treatment of clouded industrial effluents. The nanomaterial is very promising and can be effectively used for the removal of Azodye from the aqueous solutions [134]

3.3 Trapping Iron Oxide into Hollow Gold Nanoparticles

Work by Chienwen Huang . In this study Synthesis of the core/shell-structured $\text{Fe}_3\text{O}_4/\text{Au}$ nanoparticles by trapping Fe_3O_4 inside hollow Au nanoparticles is described. The produced composite nanoparticles are strongly magnetic with their surface plasmon resonance peaks in the near infrared region (wavelength from 700 to 800 nm), combining desirable magnetic and plasmonic properties into one nanoparticle. They are particularly suitable for in vivo diagnostic and therapeutic applications. The intact Au surface provides convenient anchorage sites for attachment of targeting molecules, and the particles can be activated by both near infrared lights and magnetic fields. As more and more hollow nanoparticles become available, this synthetic method would find general applications in the fabrication of core-shell multifunctional nanostructures. In Conclusion we have

shown that the core/shell-structured Fe₃O₄/Au nanoparticles can be synthesized by trapping Fe₃O₄ nanoparticles inside hollow Au nanoparticles. Because the resulted composite nanoparticles combine the desirable magnetic and plasmonic properties into one nanoentity, they are particularly suitable for in vivo diagnostic and therapeutic applications, where the Au surface provides anchorage sites for attachment of functional molecules and the particles can be activated by both NIR light and magnetic field. As more and more hollow nanoparticles become available, we believe that this synthetic method would find general applications in the fabrication of core-shell multifunctional nanostructures[135]

3.4 Reduced Graphene Oxide and Its Natural Counterpart Shungite Carbon

This study by Elena F. Sheka *Russian Peoples' Friendship University of Russia Moscow, 117198 Russia* Large variety of structure and chemical-composition of reduced graphene oxide (RGO) is explained from a quantum-chemical standpoint. The related molecular theory of graphene oxide, supported by large experience gained by the modern graphene science, has led the foundation of the concept of a multi-stage graphene oxide reduction. This microscopic approach has found a definite confirmation when analyzing the available empirical data concerning both synthetic and natural RGO products, the latter in view of shungite carbon, suggesting the atomic-microscopic model for its structure. The understanding of the discussed peculiarities of the GO reduction allowed throwing light on the formation of RGOs under natural conditions. It was shown that RGOs of shungite carbon were formed in the course of oxidation/reduction/hydrogenation reactions that govern chemical modification of the pristine graphene lamellae. The first two reactions work simultaneously but serving different purposes: oxidation terminates the growth of pristine graphene lamellae thus determining their size, while

reduction strengthens the tendency and consequently releases the oxygenated nanosheets from OCGs located through over basal plane and at the sheets perimeter. The emptied sites in the circumference are filled with hydrogen atoms thus inhibiting high reactivity of edge atoms and finally stabilizing shungite RGO as final product. This conclusion is well consistent with shungite carbon empirical data, the main of which are related to exhibiting (1) ~1 nm planar-like RGO sheets as basic structural elements of the macroscopic shungite structure; and (2) low contents of remaining oxygen and hydrogen in the most carbon-pure shungite samples. The existence of this natural product opens up large prospects of low-performance applications based on using technical grapheme [136].

3.5 Response of wheat to foliar application of zinc

This work done by Tiago Zozi , Wheat is grown in Brazil, mostly in no-till, a system in which the zinc can become potentially deficient, due to excessive application of acidity corrective and phosphate fertilizers in surface and, or at shallow depths. This study aimed to evaluate the effect of foliar application of zinc in agronomic characteristics and yield of wheat. The experimental design was randomized blocks with five replications. Treatments consisted of four doses of zinc (0, 54, 108 and 216g ha⁻¹ Zn), divided into two foliar applications, the first at tillering (18 days after plant emergence) and the second at the boot stage (65 days after emergence). Foliar application of zinc increased the number of fertile tillers and yield of wheat, however, have little effect on the agronomic characteristics of no-tilled crop with high nutrient content in soil. Significant increases in wheat grains yield to foliar Zn application were reported in other countries including Egypt (SEADH et al., 2009; ZEIDAN et al.,2010) and China (ZHAO et al., 2011) corroborating data obtained in this study to the Brazilian conditions. Such effects of foliar Zn application may be due to its role in crop growth (CAKMAK, 2008),

involving processes of photosynthesis, nitrogen assimilation, respiration and activation of other biochemical and physiological processes and hence their importance in obtaining greater yields. It is noteworthy also that Zn translocation applied to leaves depends on the plantnutritional status (MARTINEZ et al., 2005). Thus, it can be inferred that due to the high micronutrient availability in the soil, there was greater use and Zn translocation applied to wheat leaves. Zinc application to leaves increased the number of fertile tillers and wheat yield; however, it had no effect on the agronomic characteristics of crop in no-till system with high nutrient content in soil [137] .

3.6 Sulfidization flotation of a low grade oxide Pb-Zn ore

This work by Osman Sivrikaya - Adana Science and Technology University. In this study, a low grade Pb-Zn oxide ore from a complex ore deposit located at central Anatolia-Turkey was concentrated with sulfidization flotation. Chemical analysis results indicated that the studied sample contained 3.95% Pb and 7.40% Zn. The main objective of the research was to produce separate lead and zinc concentrates with acceptable grade and recovery. The previous studies showed that the floatability of some zinc oxide minerals was difficult. In this study, the production of zinc oxide mineral concentrate with sulfidization flotation experiments was aimed. A series of laboratory flotation tests were performed using a self-aerated flotation machine. The investigated operational parameters of the flotation tests were pH of the medium, type and dosage of sulfidizer- of sulphydryl collectors (KEX and KAX)- of frothers (pine oil, MIBC)- of depressant ($ZnSO_4$ and Na_2SiO_3). The grades of the concentrates were determined and then recoveries of Pb and Zn concentrates were calculated. Pb oxide minerals were recovered with sufficient recovery (84.43%) and grade (50.38%) through multistage sulfidization flotation while Zn oxide minerals cannot be recovered by

sulfidization flotation due to their mineralogical and structural complexity. The conclusion flotation tests of studied oxide complex ore showed that the flotation of Zn oxide minerals is impossible with sulfhydryl type collectors after sulfidization process. Zn activation and re-grinding did not work to recover Zn oxide minerals as well. The reason of un-flotability of Zn oxide minerals is their mineralogical and structural complexity. The optimal pH for sulfidization flotation to produce Pb concentrate from this oxide Pb-Zn complex ore was found around 9. The degree of sulfidization before flotation affects the recovery of Pb concentrate and increasing Na₂S dosage from 1000 g/ton to 4000 g/ton increased the recovery of Pb. Considering only the recovery of Pb oxide minerals from the ore, the use of KAX and KEX collectors has indicated the best flotation performance at a pH about 9 after sulfidization process of finely ground ore. A multi-stage flotation flowsheet was suggested to produce Pb concentrate with sufficient recovery and grade (84.43% recovery with 50.38% Pb grade). This flowsheet can be used to evaluate this complex ore to get a Pb concentrate from the bulk of the ore. Almost all of the Zn was remained in the tailing of multi-stage flotation. The extraction of Zn found in the tailing can be done by metallurgical processing [138].

3.7 Convenient Preparation of Graphene Oxide from Expandable Graphite and Its Characterization by Positron Annihilation Lifetime Spectroscopy

Guido Panzarasa Department of Polymer Engineering and Science, Montanuniversität, Otto-Glöckel Straße 2, 8700 Leoben, Austria that who dony this work. Graphene oxide (GO) is conveniently prepared from expandable graphite using a simplified Hummers' method. The product is thoroughly characterized by usual techniques (UV-vis, Fourier-transform infrared (FTIR) and Raman

spectroscopies, zeta potential, electron microscopy, X-ray diffraction, nitrogen adsorption) to confirm the success of synthesis. Positron annihilation lifetime spectroscopy (PALS) is then used to extract information on the microenvironment in between the layers of graphene oxide.

Conclusions in the present work, we demonstrated that graphene oxide can be conveniently prepared from expandable graphite through a simplified Hummers' method. The characterization techniques implemented allowed us to follow the different stages of the synthesis and to demonstrate the quality of the obtained product, which is comparable to that obtained by other state-of-the-art methods.

Furthermore, positron annihilation lifetime spectroscopy (PALS) was used to probe the interlayer space of graphene oxide. The difference observed for the values of the interlayer distance as obtained with X-ray diffraction and with PALS has been explained by the steric hindrance originated by the oxygen-based functional groups (such as hydroxyl, epoxy and carboxylic acid) decorating both sides of the graphene oxide layers as well as by the entrapped water molecules. These groups may also be responsible for the reduced positronium formation due to Ps quenching. In conclusion, we are confident that the application of positron annihilation lifetime spectroscopy will be helpful to provide a better understanding of the micro- and nanostructure of graphene-based materials[139] .

3.8 Zinc and zinc nanoparticles: biological role and application in biomedicine

K.I. Bogutska from Taras Shevchenko National University of Kyiv done this study . Due to nanodimension of functional components of living cells, the application of nanotechnologies in biomedical purposes is an important problem for today. One of the most promising directions is to use zinc nanoparticles for

molecular diagnostics, target delivery of drugs, developing new pharmaceutical preparations. The paper presents the data on biological properties of zinc and its compounds, their location in the organism and role in important biological processes, which show the ways of possible practical applications of zinc nanoparticles in biomedicine. Particular attention is paid to the role of zinc ion's zinc in muscle functioning. Conclusions current nanotechnologies make it possible to design nanoparticles with desired physicochemical and biological properties. Zinc and its compounds can open wide possibilities of biomedical applications due to nanosize, optical, chemical, biological and pharmaceutical properties. The researches in this field also have practical importance due to possibility to regulate functional activity of muscles using zinc ions both in normal and pathological states[140].

3.9 Zinc in Human Health

This work done by Ch.Bimola Devi. Zinc is an essential micronutrient for human health. In spite of the proven benefits of adequate zinc nutrition, approximately 2 billion people still remain at risk of zinc deficiency. Zinc is found as component of more than 300 enzymes and hormones and plays a crucial part in the health of our skin, teeth, bones, hair, nails, muscles, nerves and brain function as well as it is essential for growth. Zinc controls the enzymes that operate and renew the cells in our bodies. The formation of DNA, the basis of all life on our planet, would not be possible without zinc. Zinc deficiency is an important public health problem, affecting large number of women and children in India and worldwide. Zinc deficiency is the fifth leading risk factor for disease in the developing world. In a recent survey by WHO, zinc deficiency is found in most of the Indian population and zinc supplement is used commonly to enhance wound healing and treatment of pneumonia. The element is important in maintaining the healthy growth of the

human body, especially for infants and young children. The conclusion of this work was Zinc is an essential trace element which is involved in many fundamental activities of cellular metabolism that accounts for its essentiality to all life forms. A large number of studies have elucidated the significant role of zinc as an intracellular signalling molecule playing very important role in cell-mediated immune functions and oxidative stress with very wide clinical ramifications. Concurrent zinc deficiency present in many chronic disorders needs correction to obviate complications and increased morbidity. Mild to moderate zinc deficiency may be common in the developing countries but the public health importance of this degree of zinc deficiency is not well defined. It is therefore suggested that status of zinc should be assessed in relevant clinical situations. There are still avenues for further research particularly controlled clinical trials to establish the potential use of zinc as a preventive and therapeutic agent for a wide range of diseases in human [141].

3.10 Electronic structure of aluminum oxide: ab initio simulations of α and γ phases and comparison with experiment for amorphous films

T.V. Perevalov who do this work . The electronic structure of γ -Al₂O₃ and α -Al₂O₃ has been investigated by means of the density functional theory. A comparison of the calculation results with experimental data for amorphous alumina films is also presented. The electronic structure is described in terms of band structure and density of states. It has been found that γ -Al₂O₃ have similar electronic structure with α -Al₂O₃ and amorphous Al₂O₃. Effective electron masses in γ -Al₂O₃ as well as in α -Al₂O₃ equal to $m^*e \approx 0.4m_0$ that is in a good

Agreement with the experimentally found tunnel electron mass in amorphous Al₂O₃. The heavy holes in both alumina crystals are explained by the valence band top forming by O $2p\pi$ nonbonding orbitals. Conclusion γ -Al₂O₃ has considerable technological importance for modern microelectronics. We have presented a comparative study of the electronic properties of γ -Al₂O₃ with α -Al₂O₃ and amorphous Al₂O₃. The comparisons with experimental results for α - and amorphous alumina shows that our calculation technique and crystal structures provide correct description of the electronic structure and interatomic interaction of both Al₂O₃ modifications. We have shown that γ -Al₂O₃ and α -Al₂O₃ have similar electronic structure. It can be concluded that the electronic properties of Al₂O₃ are determined by the short-range atomic order. For both crystals the electron effective mass are isotropic and equal to $0.4m_0$. This value comparable to most semiconductors and is smaller than the hole effective mass. This indicates that the electronic conduction in these crystals is possible, if somehow the electrons can be promoted to CB by overcoming the large bandgap. The top of the highest VB for both α - and γ -Al₂O₃ is formed by the nonbonding O $2p\pi$ orbitals preferentially. In all probability, it explains the presence of the heavy effective hole masses in α - and γ -Al₂O₃. The light holes are explained by the admixture of bonding O $2p$ and Al $3s, 3p$ orbitals. The calculated values of the plasmon energy for both α - and γ -Al₂O₃ are equal to 26.5 eV which is in a good agreement with previous calculated values and experimental data for α -Al₂O₃. The work was partly supported by Siberian Branch Russian Academy of Science through the Integration project No. 70. The computations have been partially performed at the Siberian Supercomputer Center SB RAS NKS-160. The authors are grateful to A.V. Shaposhnikov and B.Z. Olshanetsky for helpful discussions and A.E. Dolbak for EELS measurements [142].

3.11 Biomedical applications of aluminum oxide nanoparticles

This work done by Peyman Hassanpour. Aluminium oxide (Al_2O_3) nanoparticles (AlNPs) are class of metal oxide nanoparticles that have diverse biomedical applications owing to their exceptional physicochemical and structural features such as resistance towards wear, chemicals, mechanical stresses as well as their favourable optical properties and a porous vast surface area. Other reasons for widespread applications of AlNPs are their low cost of preparation and easy handling. Therefore, owing to the economic importance, the recent achievements and possible health risks associated with the biomedical applications of AlNPs are overviewed in this work . Conclusion and future perspectives: Considering the needs of rapidly growing biomedical science for using new class of materials, AlNPs have been considered as suitable nanomaterials which have been found to be applicable in different aspects of biomedical science and biotechnology. Nonetheless, some observed biotoxicity may hinder the rapid advancement of AlNPs towards more applications, for instance their use as vehicles for intracellular delivery of therapeutic nucleic acids and proteins. Therefore, it seems that using some surface engineering strategies is inevitable strategy to produce completely biocompatible AlNPs towards producing a next-generation bionanomaterial with wider biomedical uses. Therefore, due to attractive features, the future research of AlNPs would be exciting as other areas of biomedical science are being developed. In other words, these nanomaterials can be applied in other less-investigated areas such as in vivo imaging, nucleic acid delivery, targeted therapy and tissue engineering. Synthesis of different forms of AlNPs, e.g. other shapes, would expedite the future research on their application. Also, with the help of other disciplines such as nanoscale surface chemistry, AlNPs can be used as artificial enzymes for developing novel diagnostic assays [143]

3.12 Physical and Chemical Properties of Zinc Cyanoferrates(II)

T. A. Denisova who to do this work . Neutral zinc cyanoferrate(II) $Zn_2Fe(CN)_6 \cdot 2.5H_2O$ and its hydrogen form $HZn_{1.5}Fe(CN)_6 \cdot 4.5H_2O$ were synthesized and studied. X-ray diffraction, vibrational spectroscopy, and 1H NMR showed that $Zn_2Fe(CN)_6 \cdot 2.5H_2O$ in aqueous solutions undergoes reversible hydrolysis. The hydrogen form of zinc cyanoferrate (II) is stable up to $\approx 200^\circ C$. The conductivity of $HZn_{1.5}Fe(CN)_6 \cdot 4.5H_2O$ in the temperature range $90-120^\circ C$ is $\sigma = 10^{-3.3}$ S/cm, which is about three orders of magnitude higher than the conductivity of the neutral salt. Thus, X-ray diffraction, IR spectroscopy and 1H NMR show that neutral zinc cyanoferrate $Zn_2Fe(CN)_6 \cdot 2.5H_2O$ undergoes hydrolysis in the course of synthesis from a solution of $H_4Fe(CN)_6$. The hydrolytic interaction with water molecules caused by the high charge of the cyanoferrate anion is reversible due to the presence of bulky channels in the crystal lattice, through which ionic forms of hydrolysis products can move rather easily. The synthesized hydrogen form of zinc cyanoferrate $\zeta Zn_{1.5}Fe(CN)_6 \cdot 4.5H_2O$ has an individual crystal structure, which persists upon thermal removal of water molecules up to $150-200^\circ C$. Annealing at higher temperatures leads to removal of acid protons and is accompanied by the destruction of the compound. The presence of acid protons in $\zeta Zn_{1.5}Fe(CN)_6 \cdot 4.5H_2O$ results in a higher hydrate composition of the compound as compared to the normal cyanoferrate, which leads to the formation of a continuous hydrogen bond network in structure channels and an increase in the conductivity of the compound by several orders of magnitude [144].

3.13 Optical properties of semiconductor nanocrystals: A symmetry-based tight-binding approach

This work done by A.K. Bhattacharjee . We present a review of our symmetry-based tight-binding (TB) approach for calculating the electronic structure and optical transitions in semiconductor quantum dots (QD's) and quantum dot quantum wells (QDQW's). It is based on the semi-empirical sp^3s^{ζ} model, including the spin-orbit interaction, which accounts for the main features of the bulk semiconductor band structure. Exact diagonalization of the oneelectron TB Hamiltonian by using group-theoretical methods yields the full single-particle spectrum including the symmetry classification of the eigenstates. We next deduce the low-energy exciton spectrum in the configuration-interaction approach and thus obtain the optical gap and the photoluminescence Stokes shifts. The high-energy absorption spectra are also computed. Our method has so far been applied to CdTe and CdSe QD's and CdS/HgS/CdS QDQW's of overall diameter up to 6 nm. The results show satisfactory agreement with the available experimental data, providing a unified picture of the optical properties. To conclude, we have developed a symmetry-based TB approach which provides a unified picture of the optical properties of spherical semiconductor nanocrystals and nanoheterostructures, covering a wide range of energies. The low-energy exciton fine structure provides a satisfactory description of the size-dependent optical absorption gap and PL Stokes shifts. In the zincblende CdTe QD's, the resonant Stokes shift is shown to originate from the electron-hole exchange interaction, but in the wurtzite-structure CdSe QD's the crystal-field term plays a major role. The TB approach is particularly appropriate for QDQW's involving thin well layers [145] .

3.14 Paper modified with ZnO nanorods – antimicrobial studies

Mayuree Jaisai done this study . Paper with antimicrobial properties was developed through in situ growth of ZnO nanorods. The targeted application for this type of paper is in health centers as wallpaper, writing paper, facemasks, tissue paper, etc. The paper was tested on three model microbes, Gram-positive bacteria *Staphylococcus aureus*, Gram-negative bacteria *Escherichia coli* and common airborne fungus *Aspergillus niger*. No viable bacterial colonies or fungal spores could be detected in the bacteria *Escherichia coli* areas surrounding test samples of the antimicrobial paper. Gram-negative *coli* were found to be inhibited in an area that is 239% and 163% the area of the paper sample under different room lighting conditions, i.e., halogen and fluorescent lamp illumination, respectively. For Gram-positive bacteria *Staphylococcus aureus* the zones of inhibition surrounding the paper samples are 102% and 70%, and for *Aspergillus niger*, 224% and 183% of the sample area, under similar lighting conditions. The conclusion Antimicrobial paper has been successfully prepared by growing ZnO nanorods on paper prepared from bleached soft wood kraft pulp by using a simple hydrothermal process at low temperature. The antimicrobial paper inhibits the growth of harmful microbes due to a slow release of zinc ions and the inhibition is further enhanced through photocatalysis under room lighting conditions. The antimicrobial paper was successfully used to immobilize two common bacteria, *E. coli* and *S. aureus*, in their immediate vicinity of the paper. The photocatalytic effect of the paper containing ZnO nanorods on the Gram-negative bacterium *E. coli* is more pronounced, with inhibition zones of 2.8 cm under halogen lighting and 2.4 cm under fluorescent lighting around the square samples of edge 1.5 cm after 72 h of incubation. The growth of the Gram-positive bacterium *S. aureus* could be inhibited in a zone of 2.1 cm under halogen lighting and 1.9 cm under fluorescent

lighting. The antimicrobial paper was also observed to inhibit the growth of the fungus *A. niger* with an inhibition zone of 2.6 cm. Antimicrobial papers based on ZnO nanorods can find wide applications as wallpaper, cleaning tissue, writing paper and as a facemask material [146] .

3.15 Photocatalytic paper using zinc oxide nanorods

Sunandan Baruah, Mayuree Jaisai, Reza Imani done this work . Zinc oxide (ZnO) nanorods were grown on a paper support prepared from soft wood pulp. The photocatalytic activity of a sheet of paper with ZnO nanorods embedded in its porous matrix has been studied. ZnO nanorods were firmly attached to cellulose fibers and the photocatalytic paper samples were reused several times with nominal decrease in efficiency. Photodegradation of up to 93% was observed for methylene blue in the presence of paper filled with ZnO nanorods upon irradiation with visible light at 963Wm^{-2} for 120 min. Under similar conditions, photodegradation of approximately 35% was observed for methyl orange. Antibacterial tests revealed that the photocatalytic paper inhibits the growth of *Escherichia coli* under room lighting conditions. Conclusions ZnO nanorods have been successfully grown in paper supports and their photocatalytic activity was determined. The efficient photodegradation of organic dyes (methylene blue and methyl orange) and the photocatalytic immobilization of common bacterium, *E. coli*, were studied under visible-light irradiation. A 93% photodegradation was observed for methylene blue and a 35% photodegradation was observed for methyl orange in the presence of the photocatalyst paper upon white-light irradiation at 963Wm^{-2} . Repeatability tests showed that the photocatalytic paper could be reused several times with a nominal decrease in efficiency. Antibacterial tests revealed that the photocatalytic paper is capable of completely eliminating *E. coli* in its vicinity even under room lighting condition [147] .

3.16 Preparation of Zinc Oxide Nanoparticles and its Characterization Using Scanning Electron Microscopy (SEM) and X-Ray Diffraction(XRD)

This work done by Ananthu C Mohan. Zinc oxide can be called a multifunctional material thanks to its unique physical and chemical properties. The main objective of this paper is the preparation of zinc oxide nanoparticles using conventional methods and the preparation using surfactant. The first part of this paper presents the different methods of preparation of Zinc oxide nanoparticles using different precursors and its surface modification using Poly Vinyl Alcohol (PVA). The next part of this paper deals with characterization of the prepared zinc oxide using Scanning Electron Microscopy (SEM) and X-Ray Diffraction in order to determine which method is more feasible in terms of particle agglomeration, particle size, particle separation. Conclusions Zinc oxide nanoparticles were successfully prepared with and without using surfactant. Poly Vinyl Alcohol (PVA) was used as the surfactant and the prepared Nano powder was characterized using Scanning Electron Microscopy (SEM) And X-Ray Diffraction (XRD). According to the characterization results it's clear that the conventional method of preparation i.e. without any surfactant highly affected by particle agglomeration and also the particle separation is not good enough. But when prepared using a surfactant the particle agglomeration is very less and also the particle separation is good. And the most important thing is that the particle size of zinc oxide prepared using PVA is in the nanometre range whereas in conventional method of preparation particle size in the micron range. According to the XRD characterization the average particle size of zinc oxide prepared using PVA as surfactant has been determined using scherrer's equation. The average particle size of zinc oxide nanoparticles has been found to be 25nm [148] .

3.17 Influence of zinc acetate concentration in the preparation of ZnO nanoparticles via chemical bath deposition

This study by F V Molefe. Zinc acetate (ZnAc) concentration was varied to prepare ZnO using the chemical bath deposition method (CBD). X-ray diffraction (XRD), scanning electron microscopy (SEM), ultraviolet visible (UV-vis) and photoluminescence (PL) systems were employed to investigate the influence of ZnAc on the structural, morphological, optical and photoluminescence properties. The obtained crystal structure from XRD analysis was the hexagonal wurtzite structure. It was observed that at higher molar concentration of ZnAc the structure changed to mixture of ZnO and ZnAc. The estimated average crystallite size was 23 nm. There was no effect on the crystallite size as ZnAc concentration was varied. SEM images shows non-uniform agglomerated flower like structures at lower concentrations, at the highest ZnAc concentration flowerlike structures are observed to grow into platelets-like structure. There was no effect on the absorption edges and the energy band gap as ZnAc concentration increases in the UV-vis measurements. PL measurements revealed a slight red-shift in the visible region with an increase in ZnAc concentration. Conclusion ZnO nanoparticles were successfully prepared using CBD method by varying molar concentrations of the ZnAc. There was no change in the crystallite size when increasing ZnAc concentration. Not uniform flower-like structure indicated that the morphology is independent from the ZnAc concentration. UV-vis spectroscopy shows no appreciable change in band gap energy of the flowerlike structure when the ZnAc concentration increases. PL showed that the emission of the ZnO nanoparticles also depends on the ZnAc concentration [149].

Chapter Four

Experimental Details

4.1 Introduction

The optical and electrical properties of Zinc oxide was sanded by UV spectrometer beside XRD technique . The optical properties include absorption coefficient, refractive index ,while the electrical properties includes conductivity and electrical permittivity .

4.2 Materials

The materials used in this work are Zinc oxide (ZnO)_x beside Aluminum oxide (Al_2O_3)_{1-x} . Some chemical catalysts were also used .

4.2.1 Aluminum Nitrate+

Aluminum nitrate is an important salting agent in the nuclear solvent extraction. It is not extracted by TBP used as solvent in in PUREX, THOREX or interim-23 processes. For effective computer simulation, contribution of its density to the aqueous sub-system is required. Information on the thermodynamic parameters for aqueous solutions of aluminum nitrate is severely limited. In this paper, coefficients of density equation and apparent molal volume of aqueous solutions of aluminum nitrate at 298.15 K and 0.1 MPa will be reported.

4.2.2 Zinc Acetate

Zinc acetate as the dehydrate is a salt of zinc used to inhibit the absorption of copper in patients with Wilson's disease. Its structural formula is: Zinc acetate occurs as white crystals or granules, freely soluble in water and in boiling alcohol, and slightly soluble in alcohol (Zinc Acetate) Capsules contain the equivalent of 25

or 50 mg of zinc, in addition to corn starch and magnesium stearate in gelatin capsules. The 25 mg capsule shells contain titanium dioxide and the 50 mg capsule shells contain titanium dioxide, methylparaben and propylparaben.

4.2.3 Distilled Water

Water is indispensable for all forms of life. Experts agree that we need six to eight glasses of water per day to maintain optimum health. The daily cleansing of wastes from each cell, the flushing of the alimentary canal and the purifying of the blood are all dependent on our drinking water. Our bodies lose water by various means – through the kidneys, through breathing and through perspiration. Without sufficient water, food cannot be properly digested, absorbed and carried to all parts of the blood stream. Waste-bearing water (urine) is necessary to flush away the end products of metabolism. Without water to moisten the surface of the lungs, there can be no intake of oxygen or expulsion of carbon dioxide. Distilled water is water which has been heated to the boiling point so that impurities are separated from the water which itself becomes vapor or steam. It is then condensed back into pure liquid form. The impurities remain in the residue, which is simply thrown away. Distilled water contains no solids, minerals or trace elements and has no taste. Distillation removes the debris, bacteria and other contaminants.

4.2.4 Hydrochloric Acid

Hydrochloric acid has many uses. It is used in the production of chlorides, fertilizers, and dyes, in electroplating, and in the photographic, textile, and rubber industries. Hydrochloric acid is corrosive to the eyes, skin, and mucous membranes. Acute (short-term) inhalation exposure may cause eye, nose, and respiratory tract irritation and inflammation and pulmonary edema in humans. Acute oral exposure may cause corrosion of the mucous membranes, esophagus,

and stomach and dermal contact may produce severe burns, ulceration, and scarring in humans. Chronic (long-term) occupational exposure to hydrochloric acid has been reported to cause gastritis, chronic bronchitis, dermatitis, and photosensitization in workers. Prolonged exposure to low concentrations may also cause dental discoloration and erosion. EPA has not classified hydrochloric acid for carcinogenicity.

4.2.5 Methanol

General Properties: Methanol is colorless hygroscopic liquid usually containing 0.01 - 0.04 percent water. It is highly inflammable and toxic. Physical Properties: Molecular weight: 32.04 Freezing point (°C): -97.7 Boiling point (°C): 64.7 Flash point (°C): 11 Min. ignition temp. (°C): 455 Density (g/cm³): 0.796115 0.791320 0.786625 Refractive Index: 1.328420 1.326525 Viscosity (cPoise): 0.550625 0.544535 Dielectric constant: 32.7 Ionization potential (eV): 10.84 Solubility: water, organic solvents Optical properties: Wavelength (nm) 200 210 220 230 240 250 260 Transmission (%) 2 20 50 75 85 95 98 . Application: Methanol is a polar, protic solvent frequently used to dissolve laser dyes like Coumadin's, Rhoda mines, and Cyanines. Its excellent optical transparency makes it the ideal solvent for UV-pumped dye lasers.

4.3 Equipments

Many equipment's were used in this work .Here we exhibit them

4.3.1 Ultraviolet – visible spectrometer

The visible spectra obtained in shimadzo mini 1240 spectrophotometer scanning between 200 -1200 nm. The spectrophotometer measures how much of the light is absorbed by the sample .the intensity of light before e going into a certain sample

is symbolized by I_0 . The intensity of light remaining after it had gone through the sample is symbolized by I . the fraction of light transmitted is (I_0/I) which is usually expressed as percent transmittance (%T) from this information, the absorbance of the sample is determined for that wavelength or as function for range of wavelength. sophisticated UV/visible spectrophotometers often do this automatically. Although the sample could be solid (or even gaseous, they are usually liquid).

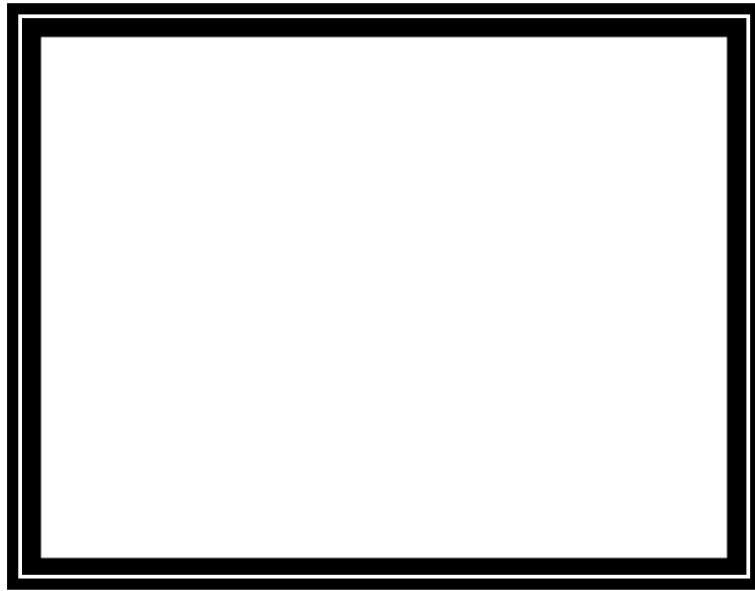
A transparent cell, often called cavetti. It used to hold a liquid sample in spectrophotometer. The path length L through the sample is then the width of the cell through which the light passes through. Simple (economic) spectrophotometer may use cavetti shape like cylindrical test tubes, but more sophisticated one use rectangular cavity common 1cm in width for just visible spectroscopy, ordinary glass cavity may be used, but ultraviolet spectroscopy requires special cavities made of UV transparent materials such as quartz. An ultraviolet visible spectrum is essentially a graph of light absorbance vs. Wave length in arrange of ultraviolet or visible regions.



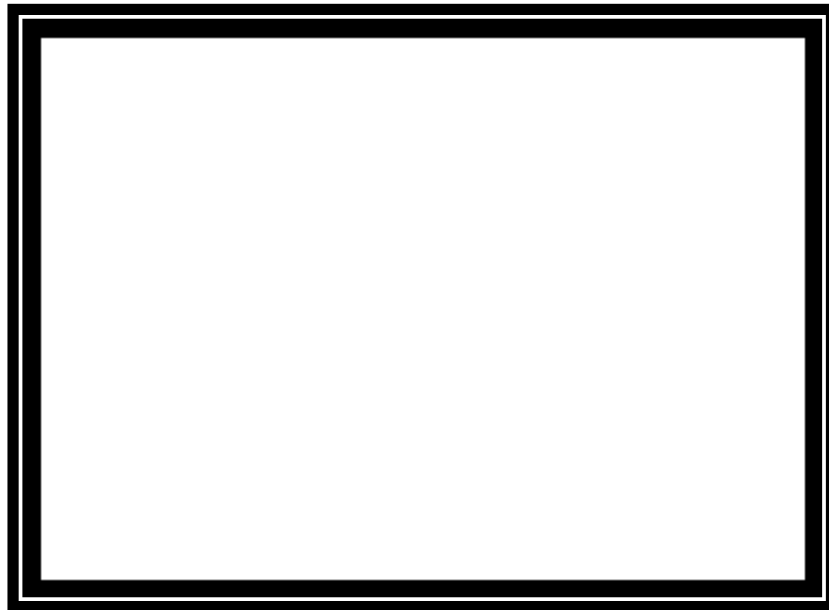
Fig (4.1) UV/V is spectrophotometer

4.3.2 Shimadzu X-ray Diffractometer XRD-7000

The new XRD-7000 Series X-ray diffractometer feature a high-precision vertical goniometer and are able to handle huge samples than conventional instruments - up to $W400 \times D550 \times H400$ mm. In addition to basic qualitative and quantitative analysis, the XRD-7000 Series handles residual austenite quantitation, environmental quantitative analysis, precise lattice constant determination, degree of crystalline calculations, crystallite size and crystal strain calculations, crystal system determination, as well as Riveted analysis and other software-based crystal structure analysis. The addition of attachments permits stress measurements, measurements on non-ambient condition, and the measurement of thin-film samples. The newly developed large R- stage permits automatic stress mapping of an entire sample up to 350 mm diameter. The strong parallel beam optical system with built-in polycarpellary unit is available to further expand the range of application .Principle of operation: The XRD-7000, an X-ray diffractometer analyze crystalline states under normal atmospheric conditions. This method is nondestructive. X-rays focused on a sample fixed on the axis of the spectrometer (goniometer) are diffracted by the sample. The changes in the diffracted X-ray intensities are measured, recorded and plotted against the rotation angles of the sample. The result is referred to as the X-ray diffraction pattern of the sample. Computer analysis of the peak positions and intensities associated with this pattern enables qualitative analysis, lattice constant determination and/or stress determination of the sample. Qualitative analysis may be conducted on the basis of peak height or peak area. The peak angles and profiles may be used to determine particle diameters and degree of crystallization, and are useful in conducting precise X-ray structural analysis.



Fig(4.2) X-ray diffracted measured



Fig(4.3) the sample that preparing

Chapter Five

Results, discussions, Conclusion and

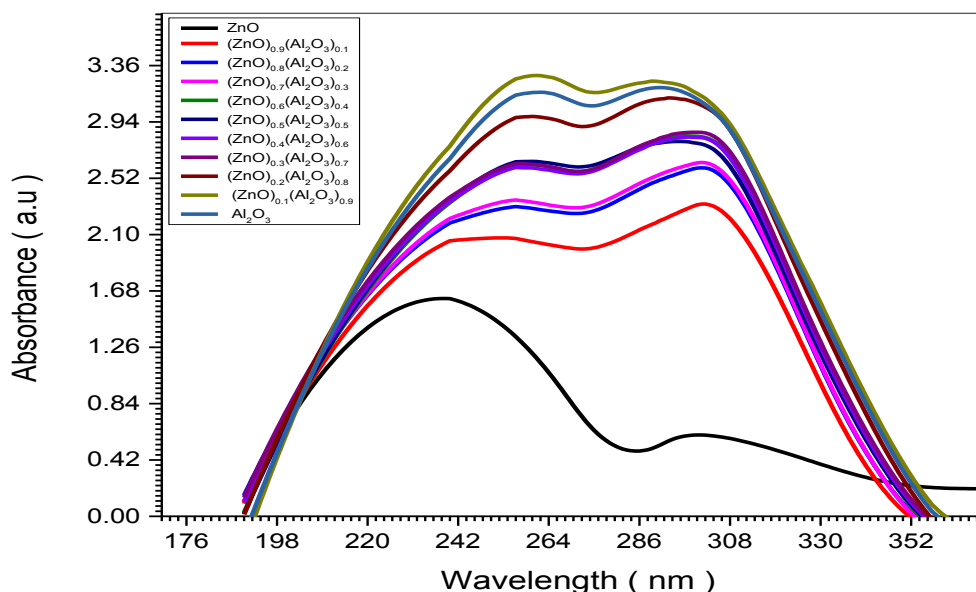
Recommendation

5.1 Introduction

After preparing eleven samples of Zinc oxide doping by Aluminum oxide . The optical and electrical properties of Zinc oxide was sanded by UV spectrometer beside XRD technique .

5.2 Results

The absorption ,transmission m , absorption permittivity and conductivity Spectra are exhibited in this section . The XRD diffraction patterred for all samples beside



.The cores ponding tables showing the crystal parameters are also presented .

Fig(5.1) The relation between absorbance and wavelngths of eleven $(\text{ZnO})_x(\text{Al}_2\text{O}_3)_{1-x}$ samples

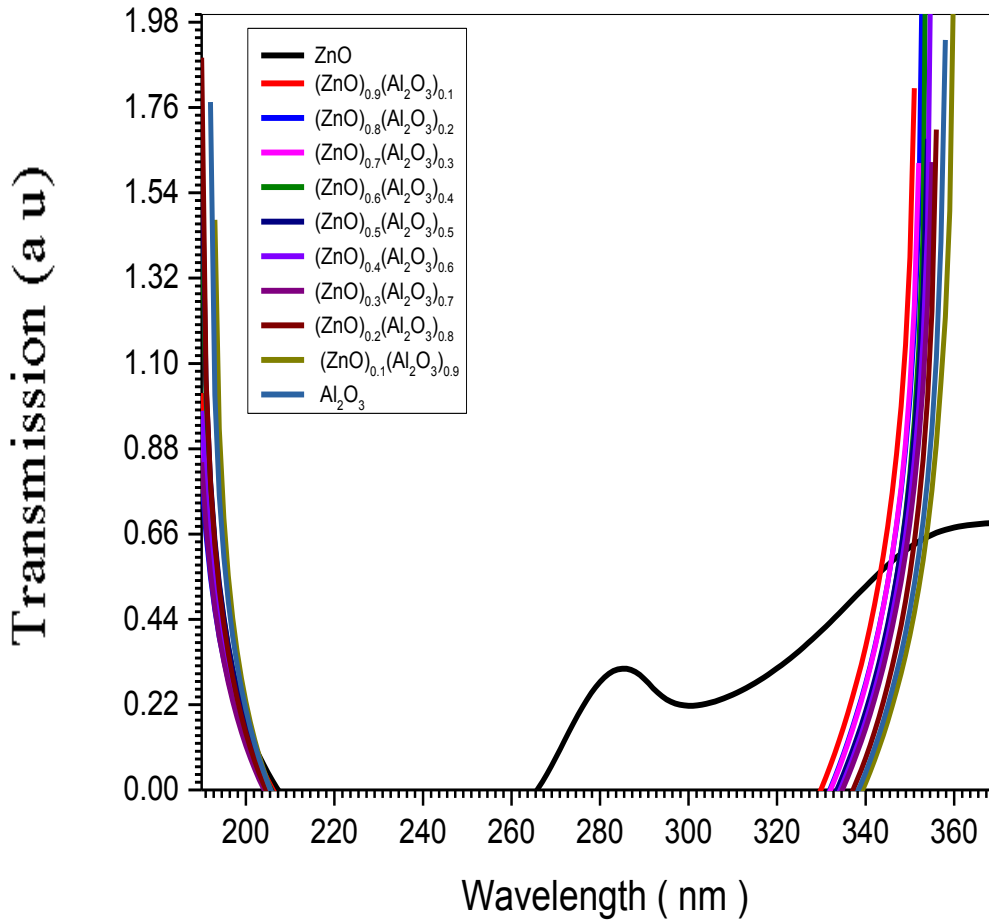


Fig (5.2)The relation between transmission and wavelngths of eleven $(\text{ZnO})_x(\text{Al}_2\text{O}_3)_{1-x}$ samples

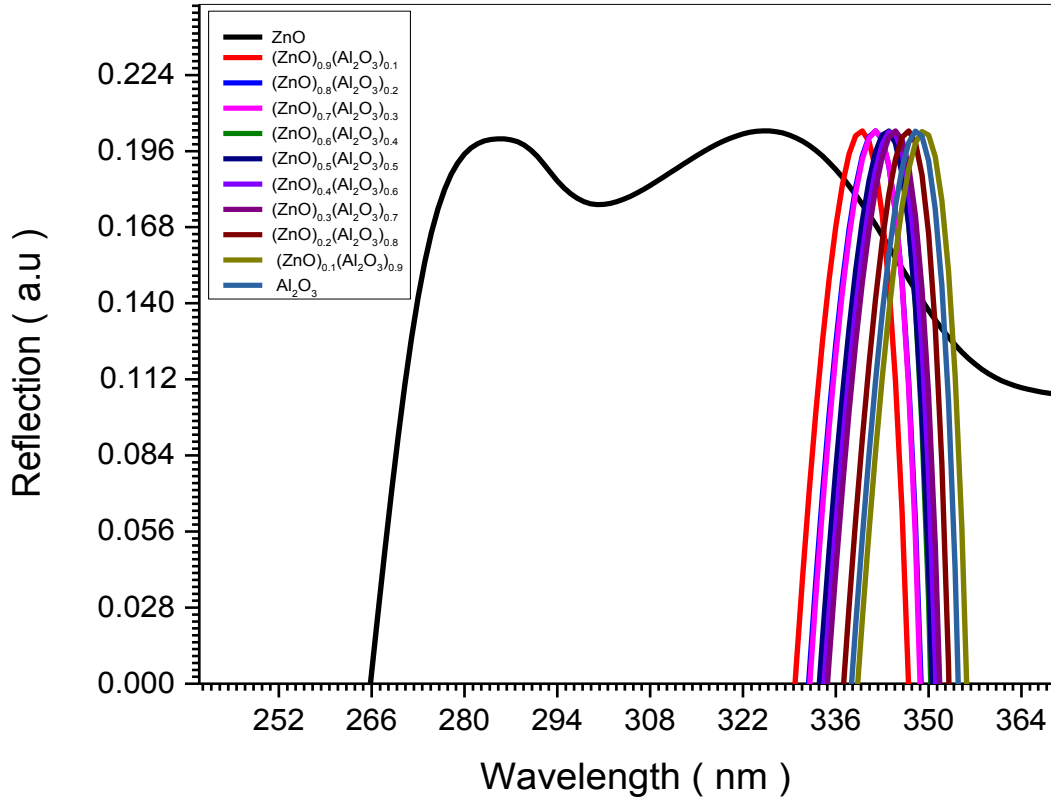


Fig (5.3)The relation between reflection and wavelengths of eleven $(\text{ZnO})_x(\text{Al}_2\text{O}_3)_{1-x}$ samples

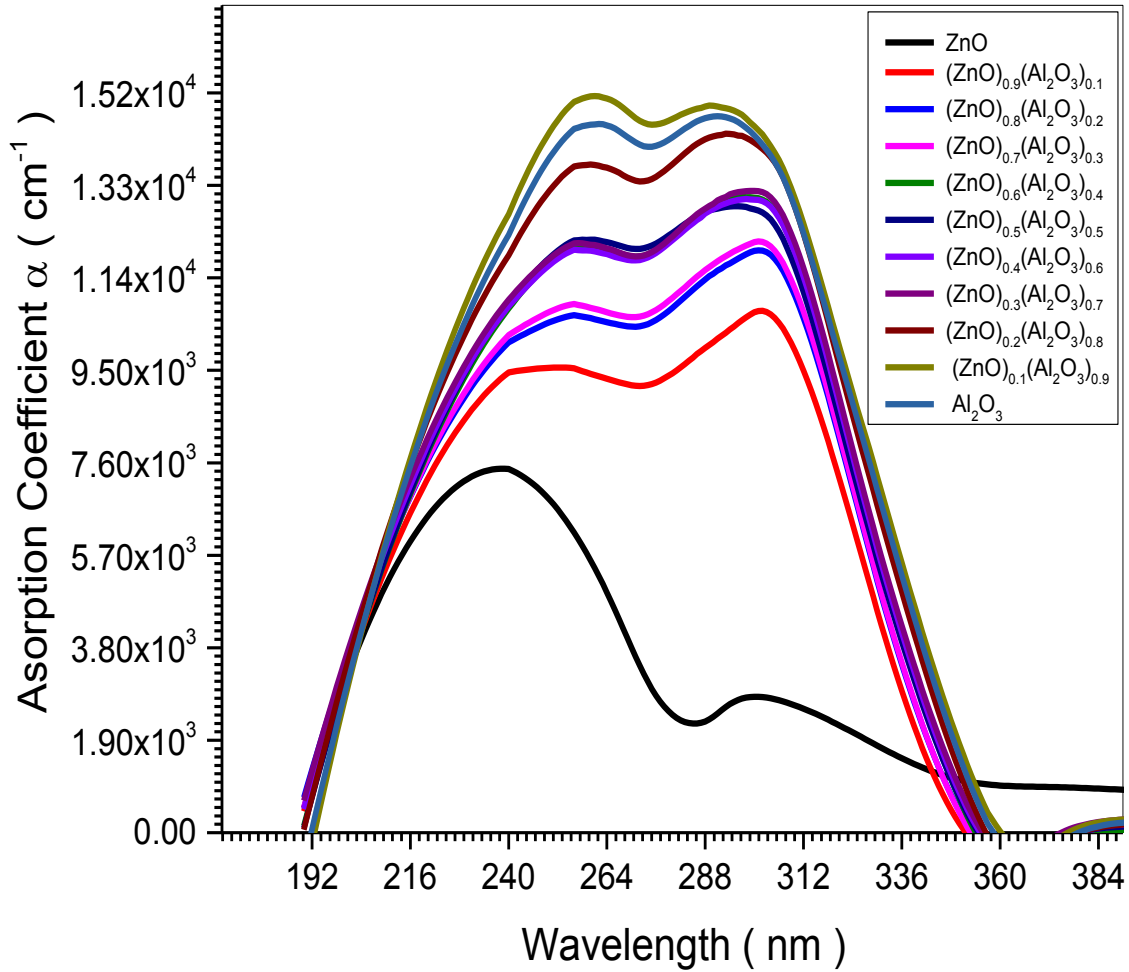


Fig (5.4)The relation between absorption coefficient (α) and wavelengths of eleven $(\text{ZnO})_x (\text{Al}_2\text{O}_3)_{1-x}$ samples

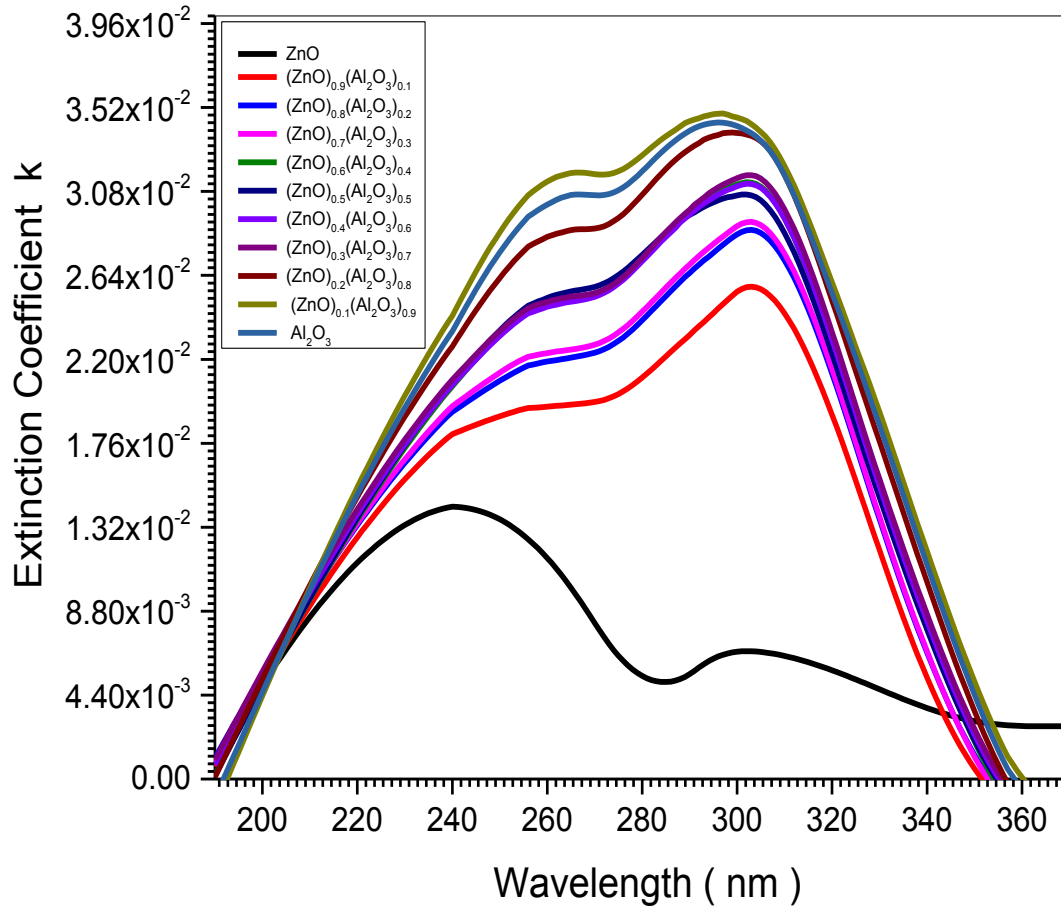
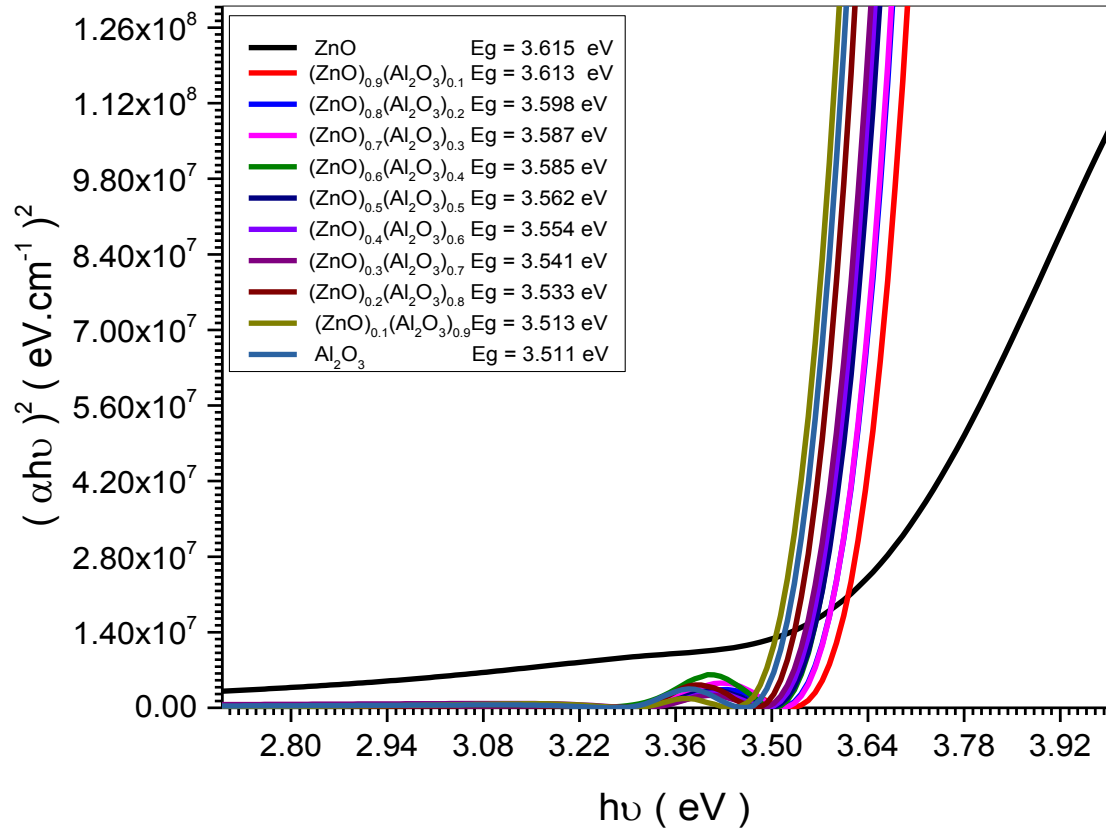


Fig (5.5)The relation between extention coefficient (α) and wavelenghts of eleven $(\text{ZnO})_x(\text{Al}_2\text{O}_3)_{1-x}$ samples



Fig(5.6)The optical energy band gab of eleven $(\text{ZnO})_x(\text{Al}_2\text{O}_3)_{1-x}$ samples

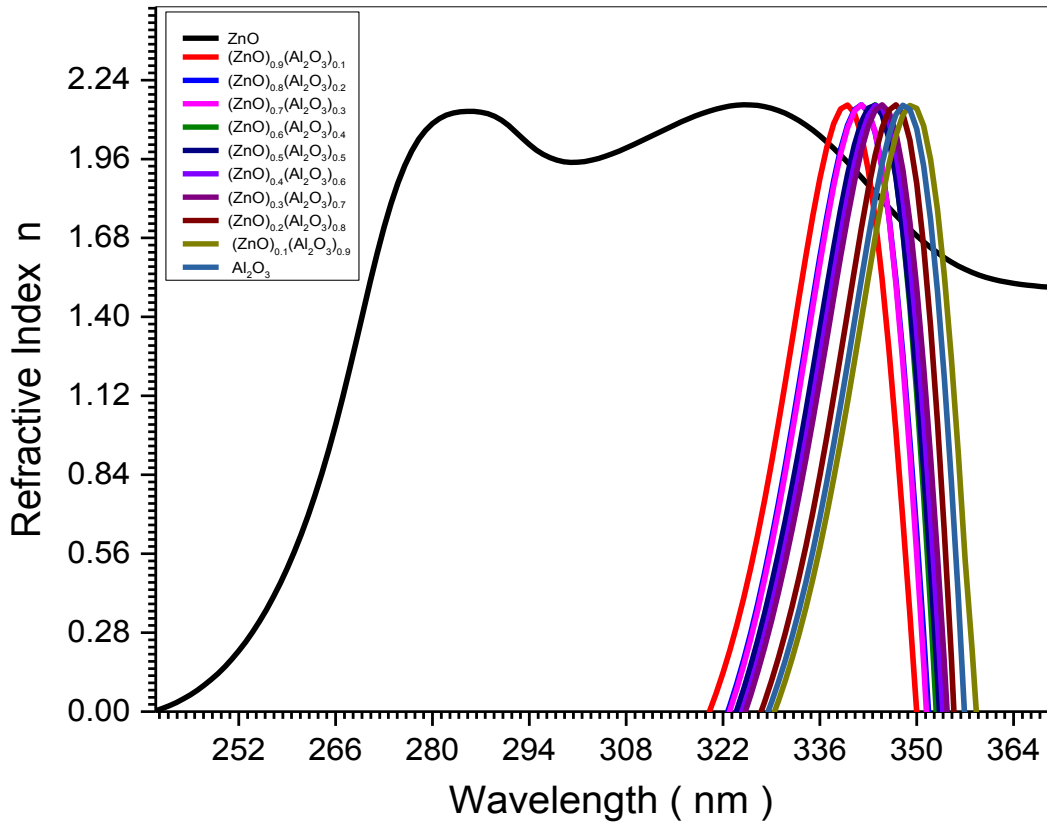


Fig (5.7)The relation between refractive index and wavelengths of eleven $(\text{ZnO})_x(\text{Al}_2\text{O}_3)_{1-x}$ samples

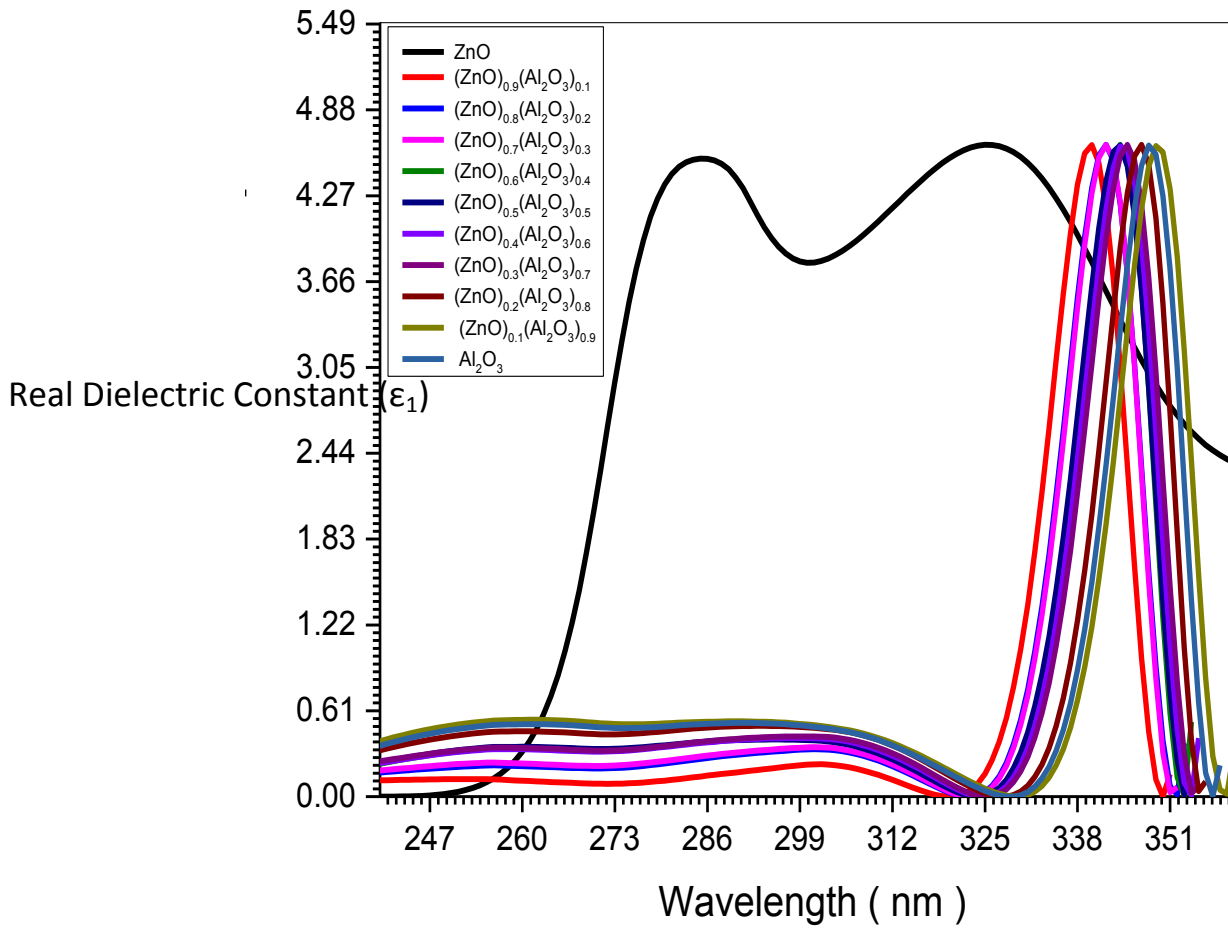


Fig (5.8) The relation between real dielectric constant and wavelengths of eleven $(\text{ZnO})_x(\text{Al}_2\text{O}_3)_{1-x}$ samples

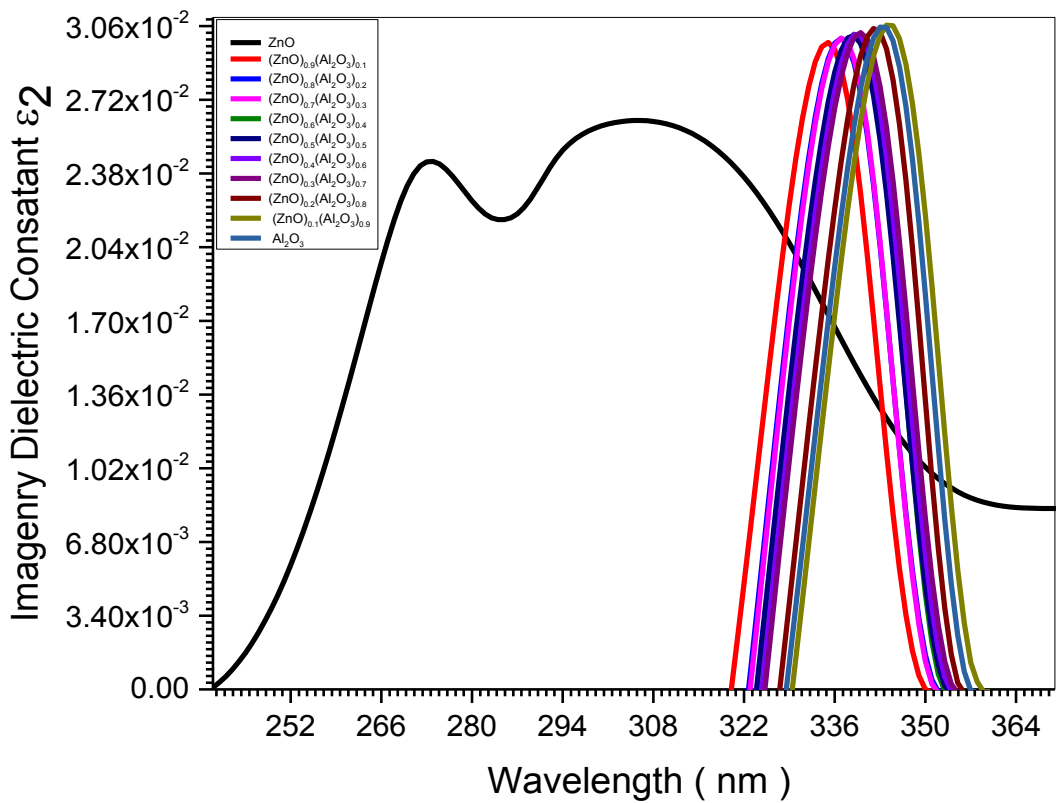


Fig (5.9)The relation between imaginary dielectric constant and wavelengths of eleven $(\text{ZnO})_x(\text{Al}_2\text{O}_3)_{1-x}$ samples

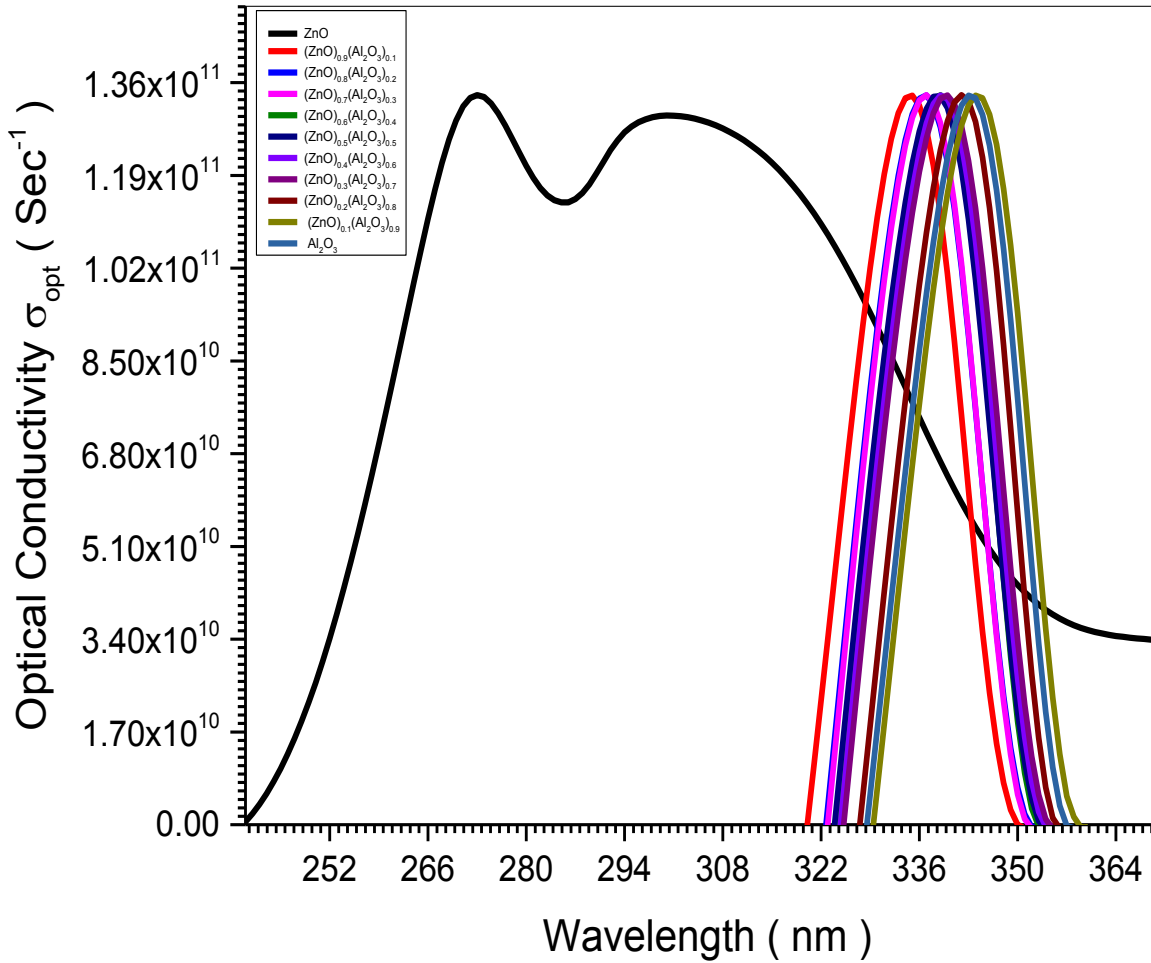


Fig (5.10)The relation between optical conductivity and wavelengths of eleven $(\text{ZnO})_x (\text{Al}_2\text{O}_3)_{1-x}$ samples

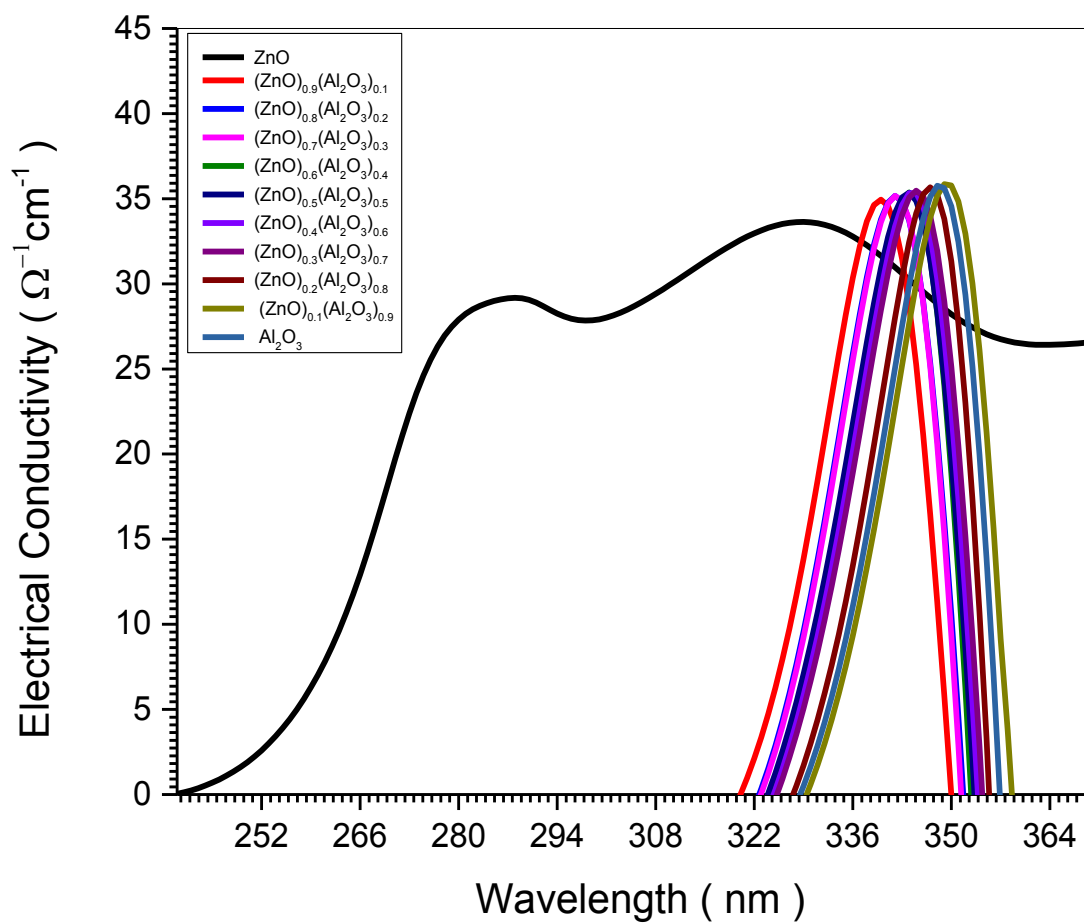


Fig (5.11)The relation between electrical conductivity and wavelengths of eleven $(\text{ZnO})_x(\text{Al}_2\text{O}_3)_{1-x}$ samples

5.2.1 Absorbance's

The absorbance we found the behavior of curves is the same for eleven samples of $(\text{ZnO})_x (\text{Al}_2\text{O}_3)_{1-x}$ studied using UV-VS min 1240 spectrophotometer. Show all resolute of absorbance in fig(5.1). In fig. (5.1) shows the relation between absorbance and wavelengths for eleven samples of $(\text{ZnO})_x (\text{Al}_2\text{O}_3)_{1-x}$, the rapid increase of the absorption at wavelengths ranged (250 -300 nm). The effects of Aluminum Oxide index (Al_2O_3)_{1-x} in the absorbance value, when the Aluminum Oxide index (Al_2O_3)_{1-x} increased the absorbance value increase.

5.2.2 Transmittance

In fig(5.2) shows the transimission for eleven samples of $(\text{ZnO})_x (\text{Al}_2\text{O}_3)_{1-x}$ and we have dissicused in this seccation from the renged (190 to 370nm). From fig.(5.2), the transmittance spectra value curves reach's saturation above 266 nm for the first sample (ZnO) and the average transmittance of the samples is >0.31(a.u) . And in fig.(5.2), the transmittance spectra value well be (red sheft) of other samples of $(\text{ZnO})_x (\text{Al}_2\text{O}_3)_{1-x}$ when the Alminum Oxied index for (Al_2O_3)_{1-x} increased , reach's the sheft above 330 nm and the average transmittance of the other samples is > 1.54(a.u).

5.2.3 Reflectance

Shows the results of reflectance spectra of the eleven sample was tretednent by $(\text{ZnO})_x (\text{Al}_2\text{O}_3)_{1-x}$ infig (5.3). In fig. (5.3) show the reflectance spectra of the eleven it has a maximum value at (283 nm) for the first sample (ZnO) and it increased in the wavelength (red sheft) when the Aluminum Oxied index for (Al_2O_3)_{1-x} increased for all samples of $(\text{ZnO})_x (\text{Al}_2\text{O}_3)_{1-x}$.

5.2.4 Absorption coefficient (α)

The absorption coefficient (α) of the eleven prepared sample was by $(\text{ZnO})_x(\text{Al}_2\text{O}_3)_{1-x}$ were found from the following relation

$$\alpha = \frac{2.303 A}{d} \quad (5.1)$$

where (A) is the absorbance and (d) is the optical length in the samples. In fig (5.4) shows the plot of (α) with wavelength (λ) of eleven sample was treated by $(\text{ZnO})_x(\text{Al}_2\text{O}_3)_{1-x}$, which obtained that the value of $\alpha > 2.37 \times 10^3 \text{ cm}^{-1}$ for all samples in the U.V region (240 nm), this means that the transition must corresponding to a direct electronic transition, and the properties of this state are important since they are responsible for electrical conduction. Also, fig.(5.4) shows that the value of (α) for the eleven samples of $(\text{ZnO})_x(\text{Al}_2\text{O}_3)_{1-x}$ increase while the Aluminium Oxide index for $(\text{Al}_2\text{O}_3)_{1-x}$ increased.

5.2.5 Extinction coefficient (K)

Extinction coefficient (K) was calculated using the related

$$k = \frac{\alpha \lambda}{4\pi} \quad (5.2)$$

The variation at the (K) values as a function of (λ) are shown in fig. (5.5) for relevant samples of $(\text{ZnO})_x(\text{Al}_2\text{O}_3)_{1-x}$ and it is observed that the spectrum shape of (K) as the same shape of (α). The Extinction coefficient (K) for eleven samples of $(\text{ZnO})_x(\text{Al}_2\text{O}_3)_{1-x}$ in fig.(4.5) obtained the value of (K) at the (190-370 nm) region was depend on the samples treatment method, where the value of (K) at 295 nm for untreated sample (ZnO) is 6.5×10^{-3} while for other untreated sample (Al_2O_3) at the same wavelength equal 3.5×10^{-2} . The effects of Aluminum Oxide index ($\text{Al}_2\text{O}_3)_{1-x}$ in the Extinction coefficient (K) value is increased when the

Aluminium Oxide index (Al_2O_3)_{1-x} increased, and value decrease when the Zinc Oxide index (ZnO)_x increased .

5.2.6 The optical energy gap (E_g)

The optical energy gap (E_g) has been calculated by the relation

$$(\alpha h\nu)^2 = C(h\nu - E_g) \quad (5.3)$$

where (C) is constant. By plotting $(\alpha h\nu)^2$ vs photon energy (hν) as shown in fig.(4.6) for the relevant prepared sample was by (ZnO)_x (Al_2O_3)_{1-x}. And by extrapolating the straight thin portion of the curve to intercept the energy axis , the value of the energy gap has been calculated .In fig (5.6) the value of (E_g) of untreated sample (ZnO) obtained was (3.615) eV while for other untreated sample (Al_2O_3) obtained was (3.511) eV. The value of (E_g) was decreased from (3.615) eV to (3.511) eV. The decreasing of (E_g) related to Aluminum Oxide index for (Al_2O_3)_{1-x} on the samples. It was observed that the different Aluminum Oxide index for (ZnO)_x (Al_2O_3)_{1-x} confirmed the reason for the band gap shifts .

5.2.7 The refractive index (n)

The refractive index (n) is the relative between speed of light in vacuum to its speed in material which does not absorb this light. The value of n was calculated from the equation

$$n = \left[\left(\frac{(1+R)}{(1-R)} \right)^2 - (1 + k^2) \right]^{\frac{1}{2}} + \frac{(1+R)}{(1-R)} \quad (5.4)$$

Where (R) is the reflectivity. The variation of (n) vs (λ) for relevant samples was treatment by (ZnO)_x (Al_2O_3)_{1-x} is shown in fig.(4.7). Fig (5.7) Show that relationship of relevant prepared sample by (ZnO)_x (Al_2O_3)_{1-x} refractive index (n) spectra, which shows that the maximum value of (n) is (2.13) for all samples at

the differences wavelength which is agreement with (red sheft when the Alminum Oxied index for $(Al_2O_3)_{1-x}$ increased for all samples of $(ZnO)_x (Al_2O_3)_{1-x}$. Also we can show that the value of (n) begin to decrease befor 280 nm and after 350 nm of region of spectrum .

5.2.8 Real Dielectric Constant (ϵ_1)

Fig(5.8) shows the variation of the realdielectric constant (ϵ_1) with wavelengthof elevant samples prepared by $(ZnO)_x (Al_2O_3)_{1-x}$ form, which calculatedfrom the relation

$$\epsilon_1 = n^2 - k^2 \quad (5.5)$$

Where the real the dielectric (ϵ_1) is thenormal dielectric constant .From fig (5.8)the variation of (ϵ_1) is follow therefractive index, where increased in theregion that $\lambda > 247$ nm for untreated sample (ZnO) and $\lambda > 325$ nm for the other sample that tretednent by $(Al_2O_3)_{1-x}$ form , where theabsorption of the samples for thesewavelength is small, but the polarizationwas increase. The maximum value of (ϵ_1)equal to (5.5) for all samples at wavelengthnear (284) nm for untreated sample (ZnO) and near (340) nmfor tretednent by $(Al_2O_3)_{1-x}$. The effect of treetetment by $(Al_2O_3)_{1-x}$ of samples increased (ϵ_1)in the region (340 to 350 nm) nm wavelength .

5.2.9The imaginary dielectric constant (ϵ_2)

The imaginary dielectric constant (ϵ_2)vs(λ) was shown in fig(5.9) this valuecalculated from the relation

$$\epsilon_2 = 2nK \quad (5.6)$$

(ϵ_2) represent the absorptionassociated with free carriers.As shown in fig(4.9) the shape of (ϵ_2)is thesame as (ϵ_1), this means that therefractive index was dominated

in these behavior . The maximum values of (ϵ_2) are different according to the treatment operation , so The maximum value of (ϵ_1) equal to (5.5) for all samples at wavelength near (284) nm for untreated sample (ZnO) and near (340) nm for treated by (Al₂O₃)_{1-x}, while the maximum value of (ϵ_2) equal to (2.5x10⁻²) for all samples at wavelength near (284) nm for untreated sample (ZnO) and near (340) nm for treated by (Al₂O₃)_{1-x}, these behavior may be related to the different absorption mechanism for free carriers.

5.2.10 Electrical and Optical Conductivity

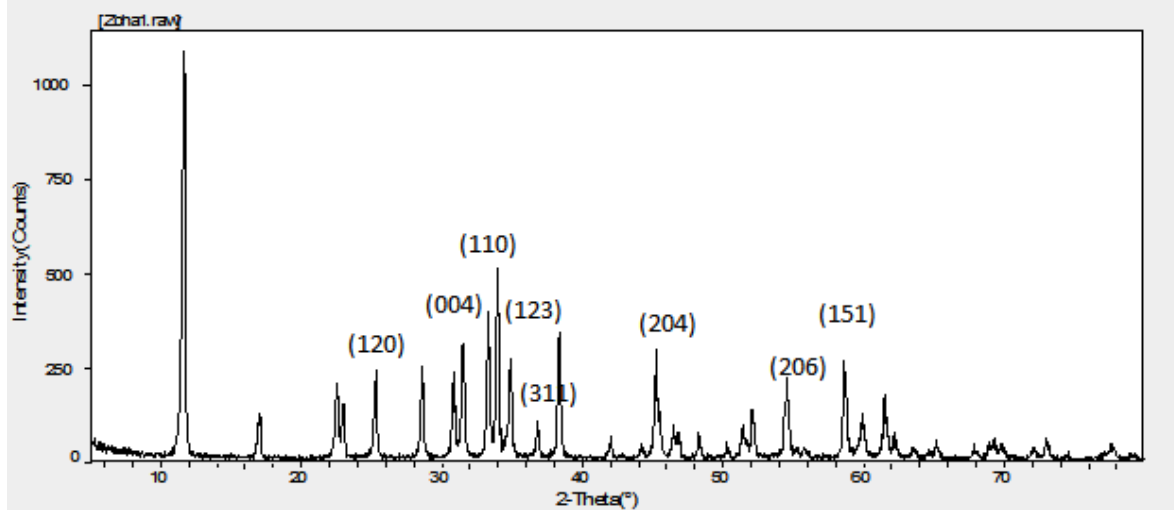
The optical conductivity is a measure of frequency response of material when irradiated with light which is determined using the following relation,

$$\delta_{opt} = \frac{\alpha n c}{4\pi} \quad (5.7)$$

Where (c) is the light velocity. The electrical conductivity can be estimated using the following relation.

$$\delta_{ele} = \frac{2\lambda\delta_{opt}}{\alpha} \quad (5.8)$$

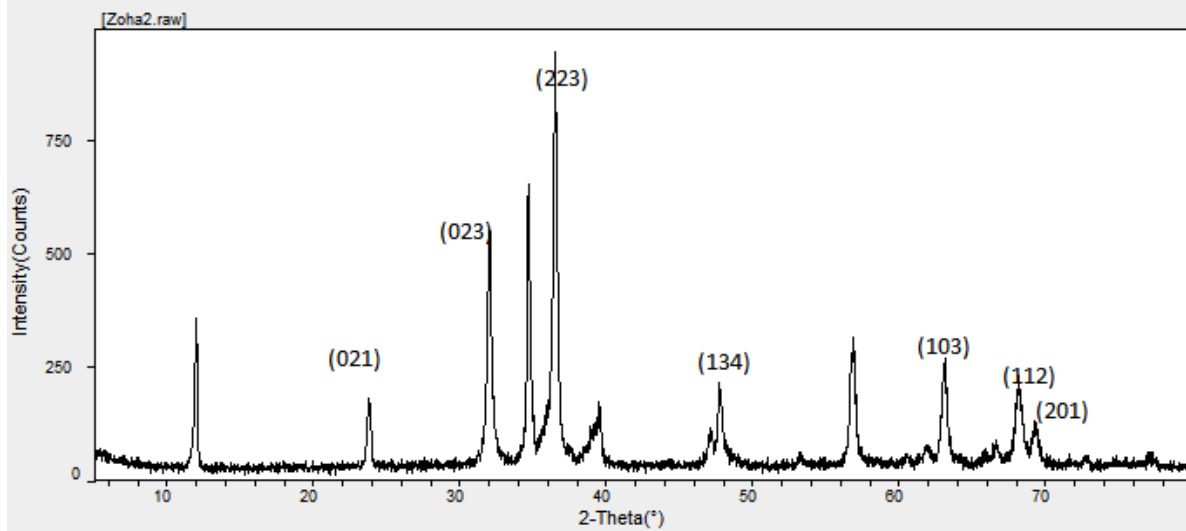
The high magnitude of optical conductivity (1.3x10¹¹ sec⁻¹) confirms the presence of very high photo-response of the relevant samples prepared by (ZnO)_x (Al₂O₃)_{1-x} form . The increased of optical conductivity at high photon energies is due to the high absorbance of relevant samples prepared by (ZnO)_x (Al₂O₃)_{1-x} form and may be due to electron excitation by photon energy as it is shown in Figs (5.10) and (5.11) .



Fig(5.12) the XRD charts of the $(\text{ZnO})_{0.9}(\text{Al}_2\text{O}_3)_{0.1}$ sample

Table (5.1) some crystallite lattice parameter (size , Miller indices and d – spacing) of the $(\text{ZnO})_{0.9}(\text{Al}_2\text{O}_3)_{0.1}$ sample

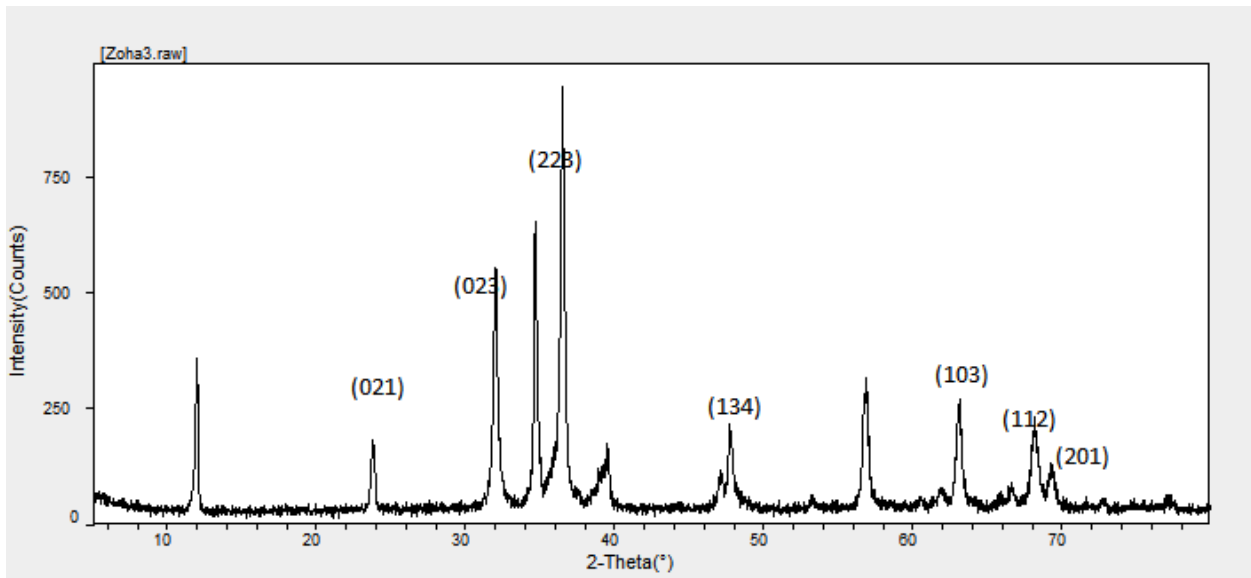
2-Theta	Xs (nm)	d(nm)	H	k	L
25.309	42.1	0.35000	1	2	0
30.830	33.4	0.29200	0	0	4
31.598	31.3	0.28910	1	1	0
33.951	45.7	0.26270	1	2	3
36.773	48.0	0.24383	3	1	1
38.348	42.8	0.23530	0	2	4
45.230	53.5	0.19980	2	0	4
54.550	31.9	0.16740	2	0	6
59.873	36.9	0.15420	1	5	1



Fig(5.13) the XRD charts of the $(\text{ZnO})_{0.8}(\text{Al}_2\text{O}_3)_{0.2}$ sample

Table (5.2) some crystallite lattice parameter (size , Miller indices and d – spacing) of the $(\text{ZnO})_{0.8} (\text{Al}_2\text{O}_3)_{0.2}$ sample

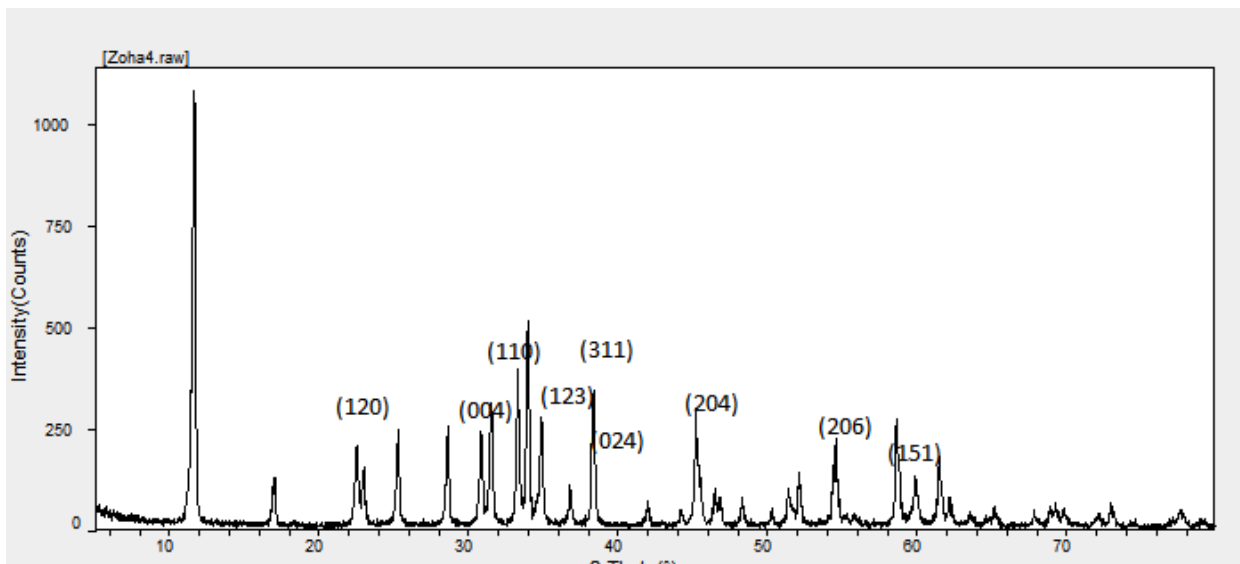
2-Theta	Xs (nm)	d(nm)	H	k	L
23.810	32.7	0.374	0	2	1
32.030	25.6	0.279	0	2	3
39.514	24.3	0.228	2	2	3
47.750	24.8	0.191	1	3	4
63.110	27.5	0.148	1	0	3
68.189	24.5	0.138	1	1	2
69.371	30.7	0.136	2	0	1



Fig(5.14) the XRD charts of the $(\text{ZnO})_{0.7} (\text{Al}_2\text{O}_3)_{0.3}$ sample

Table (5.3) some crystallite lattice parameter (size , Miller indices and d – spacing) of the $(\text{ZnO})_{0.7} (\text{Al}_2\text{O}_3)_{0.3}$ sample

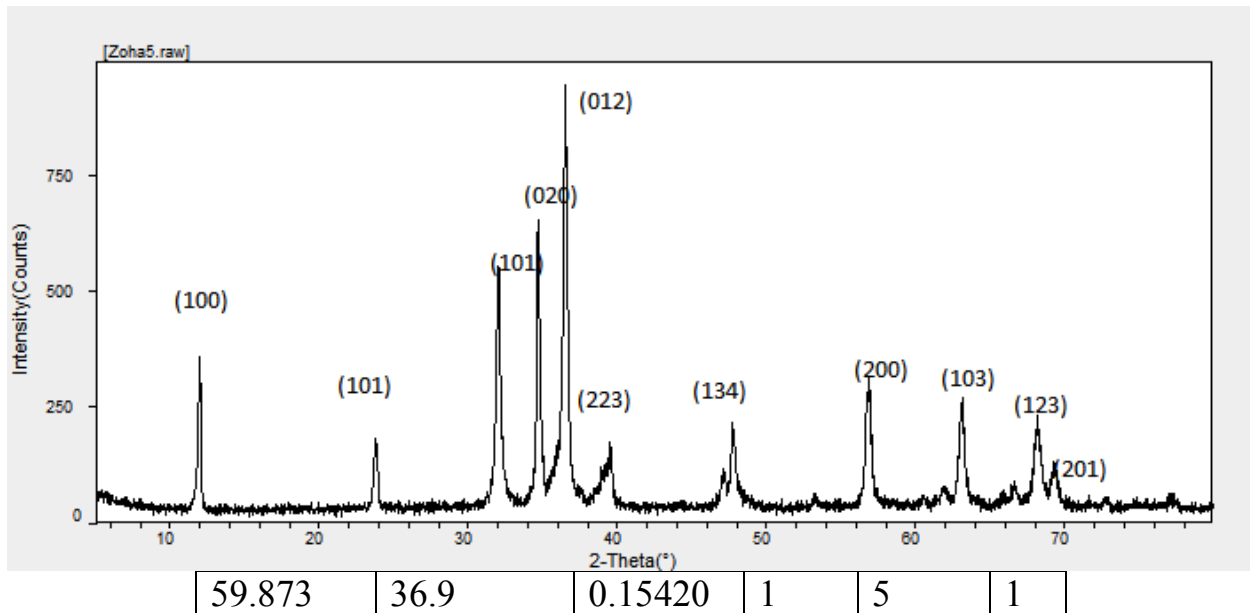
2-Theta	Xs (nm)	d(nm)	H	k	L
23.810	32.7	0.374	0	1	1
32.030	25.6	0.279	0	2	3
39.514	24.3	0.228	2	2	3
47.750	24.8	0.191	1	3	4
63.110	27.5	0.148	1	0	3
68.189	24.5	0.138	1	1	2
69.371	30.7	0.136	2	0	1



Fig(5.15) the XRD charts of the $(\text{ZnO})_{0.6} (\text{Al}_2\text{O}_3)_{0.4}$ sample

Table (5.4) some crystallite lattice parameter (size , Miller indices and d – spacing) of the $(\text{ZnO})_{0.6} (\text{Al}_2\text{O}_3)_{0.4}$ sample

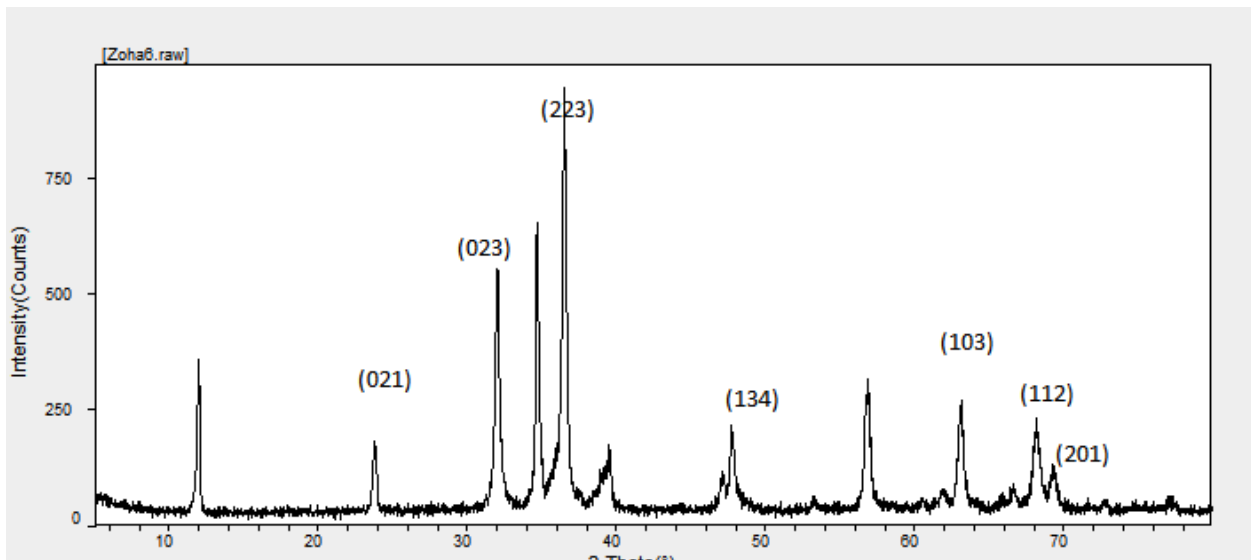
2-Theta	Xs (nm)	d(nm)	H	k	L
25.309	42.1	0.35000	1	2	0
30.830	33.4	0.29200	0	0	4
31.598	31.3	0.28910	1	1	0
33.951	45.7	0.26270	1	2	3
36.773	48.0	0.24383	3	1	1
38.348	42.8	0.23530	0	2	4
45.230	53.5	0.19980	2	0	4
54.550	31.9	0.16740	2	0	6



Fig(5.16) the XRD charts of the $(\text{ZnO})_{0.5} (\text{Al}_2\text{O}_3)_{0.5}$ sample

Table (5.5) some crystallite lattice parameter (size , Miller indices and d – spacing) of the $(\text{ZnO})_{0.5} (\text{Al}_2\text{O}_3)_{0.5}$ sample

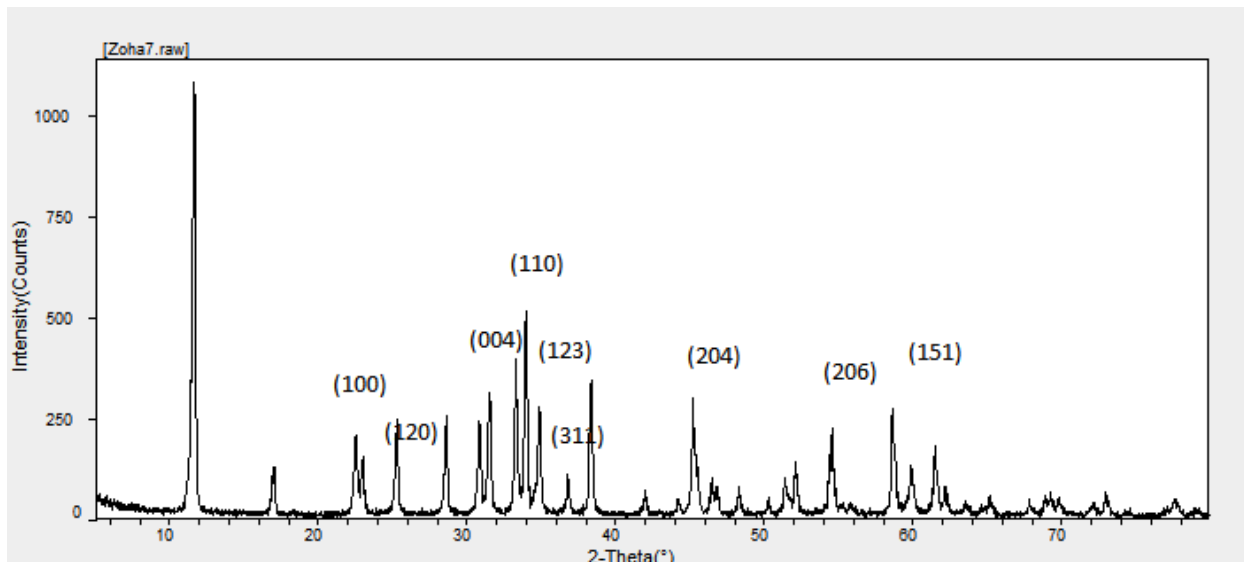
2-Theta	Xs (nm)	d(nm)	H	k	L
17.012	39.7	0.738	1	0	0
22.549	32.7	0.373	0	1	1
32.132	25.6	0.279	1	0	1
33.27	37.9	0.258	1	1	1
35.81	26.6	0.246	0	2	0
37.04	24.3	0.228	0	1	2
39.514	24.3	0.227	2	2	3
47.75	27.2	0.192	1	0	3
56.48	21.4	0.162	2	0	0
63.11	27.5	0.147	1	0	3
68.83	24.5	0.137	1	2	3
69.37	30.7	0.135	2	0	1



Fig(5.17) the XRD charts of the $(\text{ZnO})_{0.4} (\text{Al}_2\text{O}_3)_{0.6}$ sample

Table (5.6) some crystallite lattice parameter (size , Miller indices and d – spacing) of the $(\text{ZnO})_{0.4}(\text{Al}_2\text{O}_3)_{0.6}$ sample

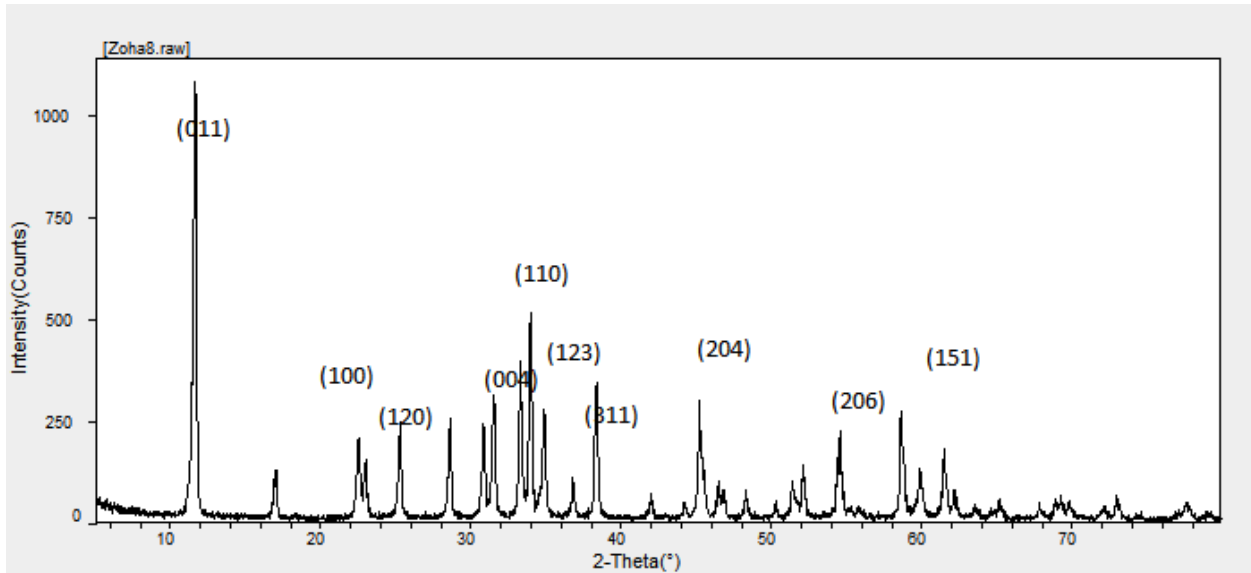
2-Theta	Xs (nm)	d(nm)	H	k	L
23.810	32.7	0.374	0	2	1
32.030	25.6	0.279	0	2	3
39.514	24.3	0.228	2	2	3
47.750	24.8	0.191	1	3	4
63.110	27.5	0.148	1	0	3
68.189	24.5	0.138	1	1	2
69.371	30.7	0.136	2	0	1



Fig(5.18) the XRD charts of the $(\text{ZnO})_{0.3}(\text{Al}_2\text{O}_3)_{0.7}$ sample

Table (5.7) some crystallite lattice parameter (size , Miller indices and d – spacing) of the $(\text{ZnO})_{0.3} (\text{Al}_2\text{O}_3)_{0.7}$ sample

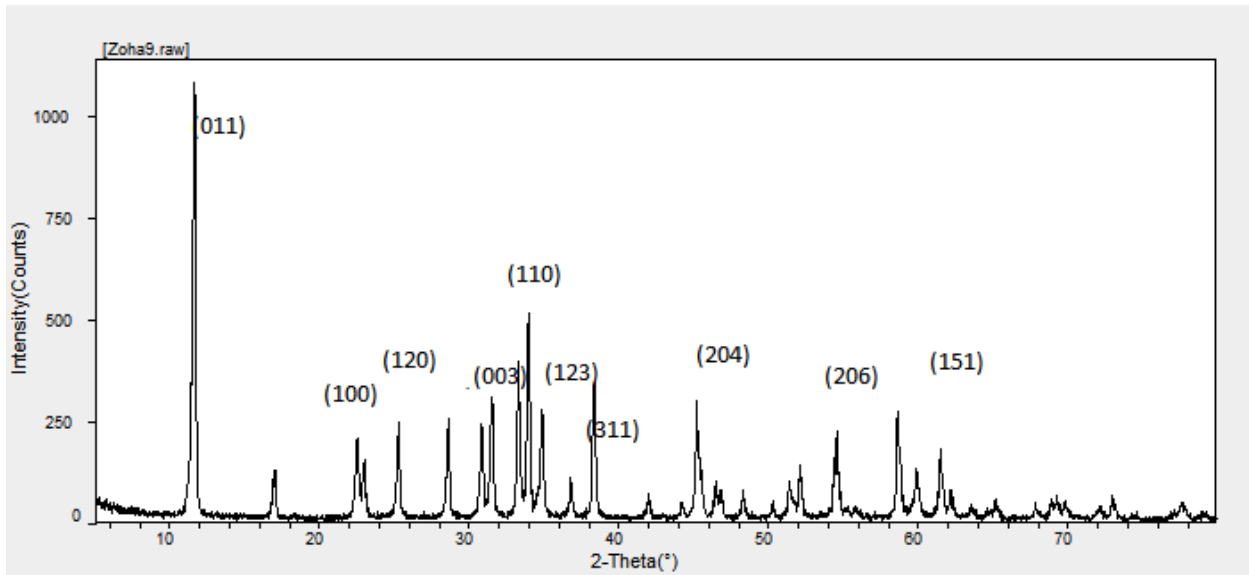
2-Theta	Xs (nm)	d(nm)	H	k	L
22.549	26.8	0.39398	1	0	0
25.309	42.1	0.35000	1	2	0
30.830	33.4	0.29200	0	0	4
31.598	31.3	0.28910	1	1	0
33.951	45.7	0.26270	1	2	3
36.773	48.0	0.24383	3	1	1
38.348	42.8	0.23530	0	2	4
45.230	53.5	0.19980	2	0	4
54.550	31.9	0.16740	2	0	6
59.873	36.9	0.15420	1	5	1



Fig(5.19) the XRD charts of the $(\text{ZnO})_{0.2} (\text{Al}_2\text{O}_3)_{0.8}$ sample

Table (5.8) some crystallite lattice parameter (size , Miller indices and d – spacing) of the $(\text{ZnO})_{0.2} (\text{Al}_2\text{O}_3)_{0.8}$ sample

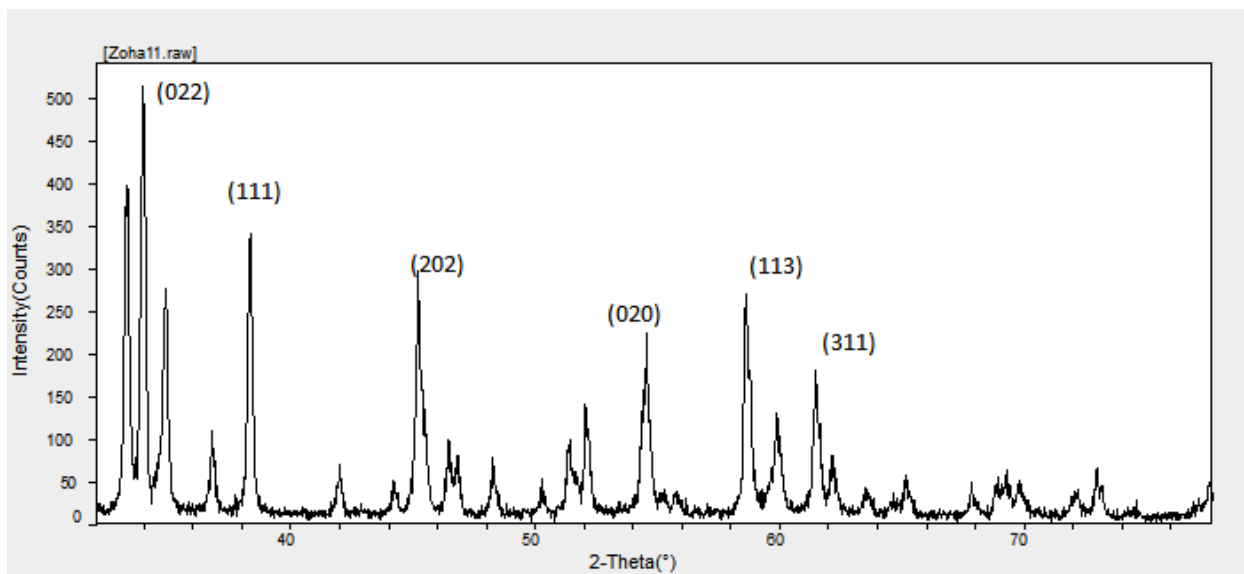
2-Theta	Xs (nm)	d(nm)	H	k	L
11.67	36.3	0.52078	0	1	1
22.549	26.8	0.39398	1	0	0
25.309	42.1	0.35000	1	2	0
30.830	33.4	0.29200	0	0	4
31.598	31.3	0.28910	1	1	0
33.951	45.7	0.26270	1	2	3
36.773	48.0	0.24383	3	1	1
38.348	42.8	0.23530	0	2	4
45.230	53.5	0.19980	2	0	4
54.550	31.9	0.16740	2	0	6
59.873	36.9	0.15420	1	5	1



Fig(5.20) the XRD charts of the $(\text{ZnO})_{0.1} (\text{Al}_2\text{O}_3)_{0.9}$ sample

Table (5.9) some crystallite lattice parameter (size , Miller indices and d – spacing) of the $(\text{ZnO})_{0.1} (\text{Al}_2\text{O}_3)_{0.9}$ sample

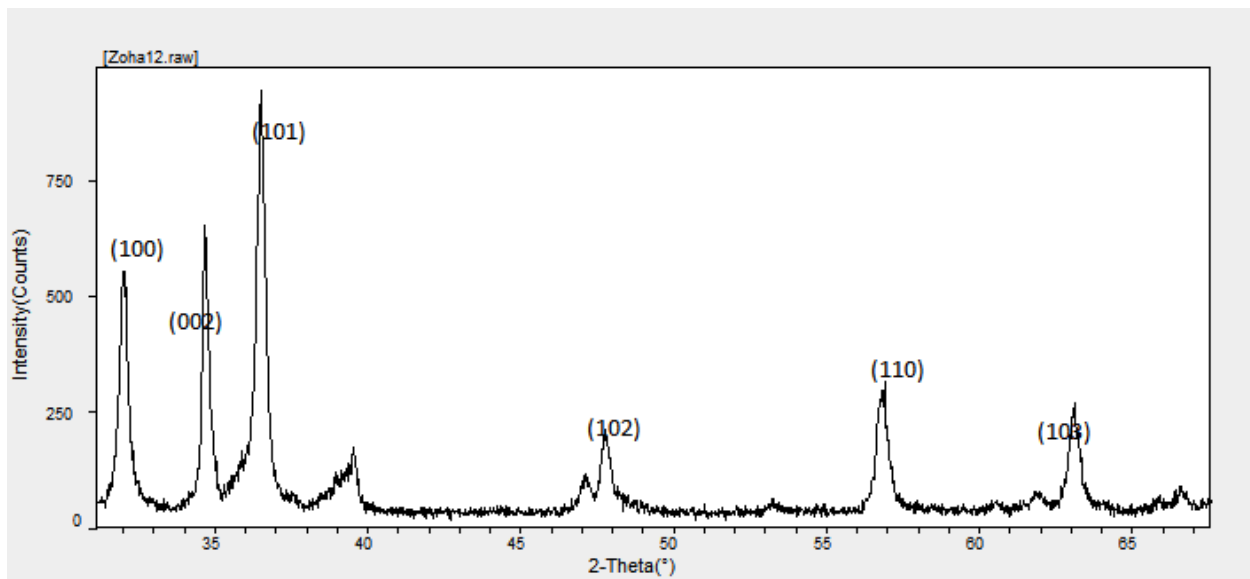
2-Theta	Xs (nm)	d(nm)	H	k	L
11.67	36.3	0.52078	0	1	1
22.549	26.8	0.39398	1	0	0
25.309	42.1	0.35000	1	2	0
30.830	33.4	0.29200	0	0	3
31.598	31.3	0.28910	1	1	0
33.951	45.7	0.26270	1	2	3
36.773	48.0	0.24383	3	1	1
38.348	42.8	0.23530	0	2	4
45.230	53.5	0.19980	2	0	4
54.550	31.9	0.16740	2	0	6
59.873	36.9	0.15420	1	5	1



Fig(5.21) the XRD charts of the $(\text{ZnO})_{0.0}(\text{Al}_2\text{O}_3)_{1.0}$ sample

Table (5.10) some crystallite lattice parameter (size , Miller indices and d – spacing) of the $(\text{ZnO})_{0.0} (\text{Al}_2\text{O}_3)_{1.0}$ sample

2-Theta	Xs (nm)	d(nm)	H	k	L
34.87	32.4	0.257	0	2	2
38.35	42.8	0.235	1	1	1
45.23	33.7	0.200	2	0	2
54.53	31.9	0.168	0	2	0
58.59	33.2	0.157	1	1	3
61.48	38.9	0.151	3	1	1



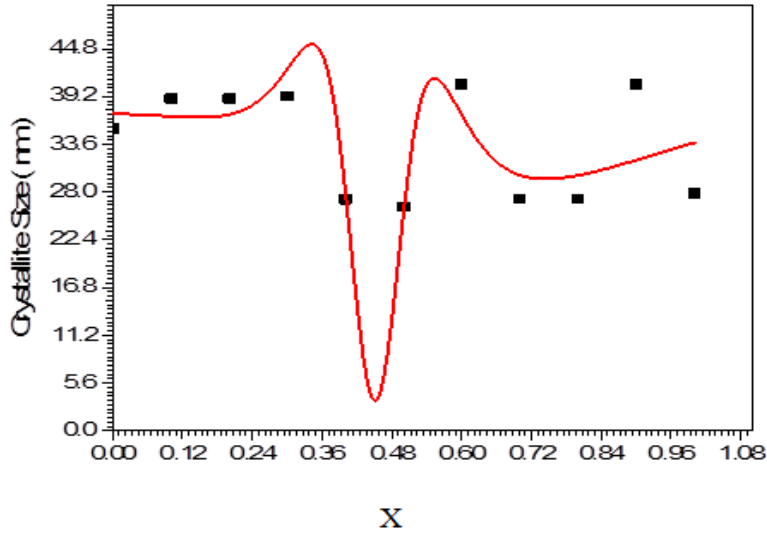
Fig(5.22) the XRD charts of the $(\text{ZnO})_{1.0} (\text{Al}_2\text{O}_3)_{0.0}$ sample

Table (5.11) some crystallite lattice parameter (size , Miller indices and d – spacing) of the $(\text{ZnO})_{1.0} (\text{Al}_2\text{O}_3)_{0.0}$ sample

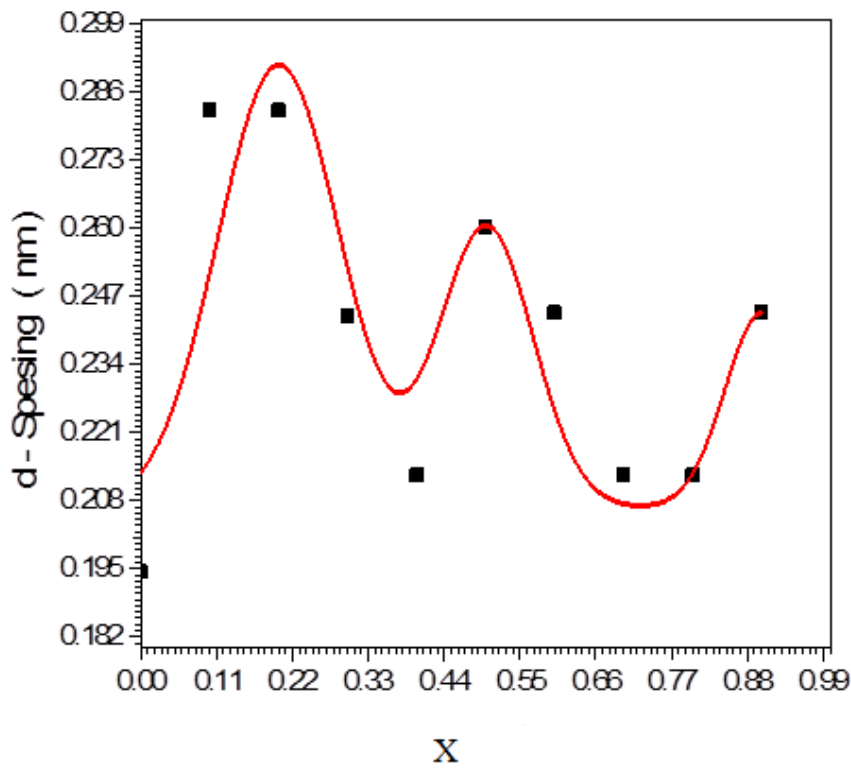
2-Theta	Xs (nm)	d(nm)	H	k	L
32.03	26.6	0.281	1	0	0
34.67	37.9	0.260	0	0	2
36.81	26.6	0.248	1	0	1
47.75	27.2	0.191	1	0	2
56.83	21.4	0.162	1	1	0
63.11	27.5	0.148	1	0	3

Table (5.12) some crystallite lattice parameter (c- form , a,b,c, β, α, γ , density ,Xs(nm) and d – spacing) of all samples that meade by $(\text{ZnO})_x (\text{Al}_2\text{O}_3)_{1-x}$

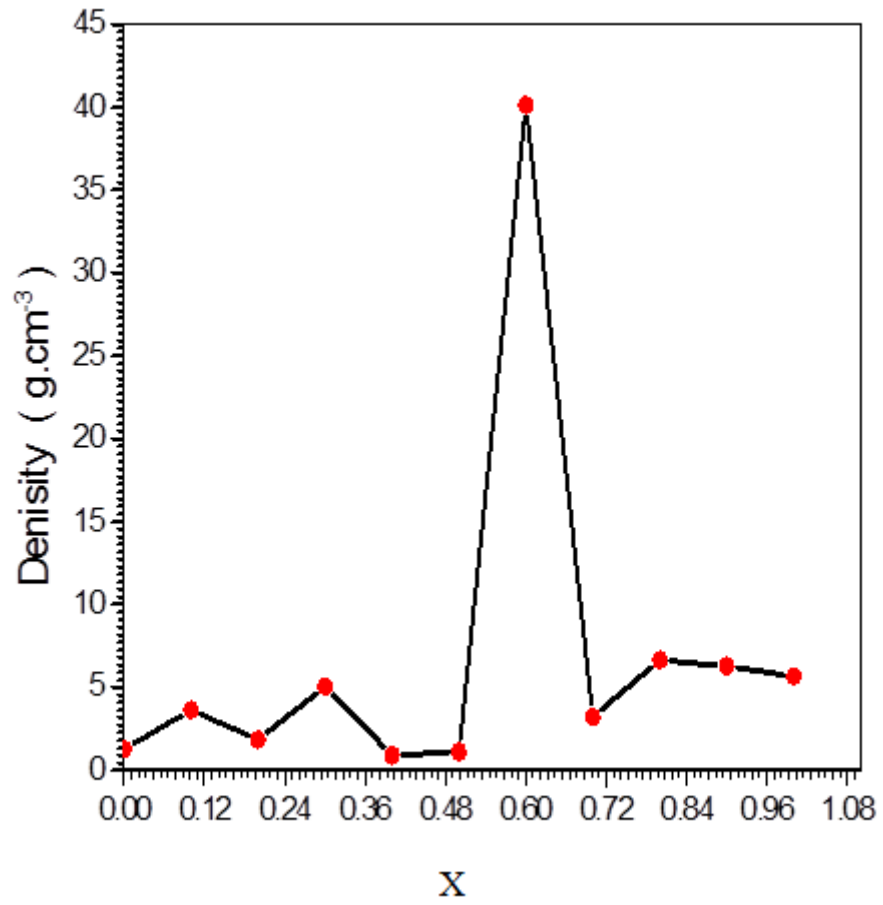
Sample	C-form	A	B	C	α	B	Γ	Density	Xs(nm)	d-spacing
(ZnO) _{0.9} (Al ₂ O ₃) _{0.1}	Hexagonal	5.68	5.68	13.71	90	90	120	6.2756	40.6	0.244
(ZnO) _{0.8} Al ₂ O ₃) _{0.2}	Orthorhombic	7.93	7.96	11.71	90	90	90	6.647	27.2	0.213
(ZnO) _{0.7} (Al ₂ O ₃) _{0.3}	Hexagonal	5.68	5.68	22.52	90	90	120	3.2255	27.2	0.213
(ZnO) _{0.6} (Al ₂ O ₃) _{0.4}	Triclinic	5.00	5.18	4.88	97.5	118.74	184.74	40.15	40.622	0.244
(ZnO) _{0.5} (Al ₂ O ₃) _{0.5}	Hexagonal	3.047	3.037	57.26	90	90	120	1.1069	26.267	0.2602
(ZnO) _{0.4} (Al ₂ O ₃) _{0.6}	Hexagonal	4.83	4.52	7.38	90	90	120	0.9169	27.157	0.213
(ZnO) _{0.3} (Al ₂ O ₃) _{0.7}	Triclinic	2.86	2.85	2.86	59.6	59.9	59.72	5.053	39.24	0.2434
(ZnO) _{0.2} (Al ₂ O ₃) _{0.8}	Monoclinic	5.93	4.77	6.56	90	1172	90	1.8520	38.972	0.2826
(ZnO) _{0.1} (Al ₂ O ₃) _{0.9}	Hexagonal	5.57	5.57	8.64	90	90	120	3.6473	38.973	0.2827
(ZnO) _{0.0} (Al ₂ O ₃) _{1.0}	Monoclinic	9.22	7.54	10.35	90	109.2	90	1.2827	35.483	0.1945
(ZnO) _{1.0} (Al ₂ O ₃) _{0.0}	Hexagonal	3.24	3.24	5.21	90	90	120	5.6779	27.865	0.215



Fig(5.23)Dependence of the crystallites size on the $(\text{ZnO})_x (\text{Al}_2\text{O}_3)_{1-x}$ Concentration(x) = ZnO concentration



Fig(5.24)Dependence of the d- spacing on the $(\text{ZnO})_x (\text{Al}_2\text{O}_3)_{1-x}$ Concentration(x) = ZnO concentration



Fig(5.25)Dependence of the density on the $(\text{ZnO})_x (\text{Al}_2\text{O}_3)_{1-x}$ Concentration(x) = ZnO concentration

(5.3) Discussion

The X-ray diffraction pattern, recorded in table (5.12), is used to determine the distance between two successive planes, the crystal size of the Nano particles X and the density s . The relation, between the ZnO concentration X on one side with the crystal size X , plane spacing d , and matter density s shows that the Nano crystal size [see figures (5.23,5.29)] has maximum values at concentration $X=0.3$, 0.6 and 40.6 nm.

Where as it attains minimum values at $x=0.5$ the plane spacing d variation is not large, where it attains maximum value of 0.1945 nm and minimum value of 0.2827 at concentration $x=0$ and $x=0.1$ respectively.

Figure (4.5) show that the absorption coefficient is smaller when the concentration of ZnO is equal to 0.5 , with small crystal size of about 26 nm. However the absorption coefficient is larger for $(\text{ZnO})_{0.6}$, i.e for the concentration is $x=0.6$,

The crystal size is larger and is about 40 nm. This may be related to the fact that the larger crystal size increases the number of atoms that absorb light which in turn increases of the imaginary dielectric conductivity spectra against the wavelength λ for all samples have been exhibited in figures (5.9) and (5.11)

It is very striking to observe that the imaginary dielectric constant and the electrical conductivity have minimum values for $x=0.5$ and maximum values for $x=0.6$ the crystal size is very small and equal to 26 nm for $x=0.5$ where both χ_2 and σ attains minimum values of about 2.9×10^{-2} and $33 \Omega^{-1} \text{ CM}^{-1}$ respectively.

The crystal size is very large and equals 40 nm for $x=0.6$, when χ_2 and σ have maximum values of about 3.6×10^{-2} and $35 \Omega^{-1} \text{ CM}^{-1}$ respectively.

This may be explain by bearing in maid that when the crystal size is large the space between the become very small .this is since the size of the glass substrate is them
 Of crystal size decreases the electrical resistance and increases electric conductivity

According to on the current density definition

$$J = nev = \frac{d nex}{d t} = \frac{d p}{d t} = x \frac{dE}{dt} = -i\omega(x_1 + i x_2)E =$$

$$\sigma E = (\sigma_1 + i\sigma_2)E$$

$$X_2 = \sigma_1/\omega \tag{5.3.1}$$

The imaginary dielectric constant

$$\varepsilon_2 = \varepsilon_0 x_2 \tag{5.3.2}$$

Increases as .

The large crystal size also increases the internal field E_i also this increases the electrons velocity v , which increase conductivity σ , according to the relation

$$J = \sigma_0(E + E_i) = \sigma_0(E + c_0 E) = \sigma_0(1 + c_0)E = nev \tag{5.3.3}$$

This also increases ε_2 according to equation (5.3.2)

Increases AL_2O_3 cone centration increases the conductivity also .this may be related to the role of it in increasing to table (5.12) the crystal size of AL_2O_3

Only is about 35 nm which is larger that the ZnO crystal size which is about 27 nm

(5.4)conclusion

The absorption coefficient of $(ZnO)_x(AlO)_{1-x}$ thin films decreases as the nano crystal size decreases when ZnO concentration decreases up to 0.3 the electrical conductivity and imaginary electric permittivity are maximum when the crystal size is maximum at $x= 0.6$, while they are minimum when the crystal size in minimum at $x=0.5$.

Also the electric conductivity and imaginary electric permittivity are found to be minimum up on increasing Al_2O_3 concentration .

This may be related to the fact that the size of the crystal form Al_2O_3 alone is larger than that of ZnO crystals .

Generally speaking the conductivity and permittivity increases when the crystal size increases .this result conform with theoretical relation

(5.5) Recommendation

This work can be repeated with ALO instead of ZnO other metal oxide can be also mixed with ZnO electrical and optical properties .

The perform of solar cells formed from ZnO and Al_2O_3 compound can also be tested .

References

- [1] Brame, J., Li, Q., Alvarez, P. J. J., (2011). Nanotechnology enabled water treatment and reuse: emerging opportunities and challenges for developing countries. *Trends Food Sci. Technol.*, 22: 618.
- [2] Ali, I., (2012). New generation adsorbents for water treatment. *Chem. Rev.*, 112: 5073.
- [3] Savage, N., Diallo, M. S., (2005). Nanomaterials and water purification: opportunities and challenges. *Jr. Nanoparticle Res.*, 7: 331.
- [4] Mohmood, I., Lopes, C. B., Lopes, I., Ahmad, I., Duarte, A. C., Pereira, E., (2013). Nanoscale materials and their use in water contaminants removal—a review. *Environ. Sci. Pollut. Res.*, 20: 1239.
- [5] J. Pakarinen (2009). Partial melting mechanism of embedded Nano crystals. *phys. Rev – B* 79-08 54 26. Doi: 10.1103/physrevb.79.085426
- [6] D.V. Talapin (2012). "Nano crystal solids: A modular approach to materials design". *MRS Bulletin* 37. 63. Doi: 10.1557/mrs.2011.337.
- [7] B.N. Khelbtsov, V.A. Khanadeyev, J. Ye, D.W. Mackowski, G. Borghs, and N.G. Khelbtsov, - Coupled plasmon resonances in monolayers of metal nanoparticles and Nano shells," *phys. Rev. B* 77, 035440-1-14 (2008).
- [8] The Institute of Nanotechnology (2006). Road maps for Nanotechnology in Energy. Nanotechnology (NRM) project working paper.
- [9] G. Cressey and I. F. Mercer, (1999) *Crystals*, London, Natural History Museum, page 58

- [10] "Cave of Crystal Giants — National Geographic Magazine" . nationalgeographic.com.
- [11] Meija, J.; et al. (2016). "Atomic weights of the elements 2013 (IUPAC Technical Report)" .Pure and Applied Chemistry. 88(3): 265–91. doi:10.1515/pac-2015-0305 .
- [12] Weast, Robert (1984). CRC, Handbook of Chemistry and Physics. Boca Raton, Florida: Chemical Rubber Company Publishing.pp. E110.ISBN 0-8493-0464-4.
- [13] CRC 2006, p. 4–41 13. Heiserman 1992, p. 123 14. Wells A.F. (1984) Structural Inorganic Chemistry 5th edition p 1277 Oxford Science Publications ISBN 0-19-855370-6
- [14] Scoffern, John (1861). The Useful Metals and Their Alloys .Houlston and Wright. pp. 591–603. Retrieved April 6, 2009.
- [15] "Zinc Metal Properties" . American Galvanizers Association. 2008. Archived from the original on April 7, 2015. Retrieved April 7, 2015.
- [16] Ingalls, Walter Renton (1902). Production and Properties of Zinc: A Treatise on the Occurrence and Distribution of Zinc Ore, the Commercial and Technical Conditions Affecting the Production of the Spelter, Its Chemical and Physical Properties and Uses in the Arts, Together with a Historical and Statistical Review of the Industry . The Engineering and Mining Journal. pp. 142–6.
- [17] Emsley 2001, p. 503
- [18] Lehto 1968, p. 822
- [19] Greenwood 1997, p. 1202

- [20] Emsley 2001, p. 502
- [21] Tolcin, A. C. (2015). "Mineral Commodity Summaries 2015: Zinc" (PDF). United States Geological Survey. Archived (PDF) from the original on May 25, 2015. Retrieved May 27, 2015.
- [22] Erickson, R. L. (1973). "Crustal Abundance of Elements, and Mineral Reserves and Resources". U.S. Geological Survey Professional Paper 820: 21–25.
- [23] Country Partnership Strategy—Iran: 2011–12" . ECO Trade and development bank. Archived from the original on October 26, 2011. Retrieved June 6, 2011.
- [24] "IRAN – a growing market with enormous potential" . IMRG. July 5, 2010. Archived from the original on February 17, 2013. Retrieved March 3, 2010.
- [25] Tolcin, A. C. (2009). "Mineral Commodity Summaries 2009: Zinc" (PDF). United States Geological Survey. Archived (PDF) from the original on July 2, 2016. Retrieved August 4, 2016.
- [26] Gordon, R. B.; Bertram, M.; Graedel, T. E. (2006). "Metal stocks and sustainability" . Proceedings of the National Academy of Sciences. 103 (5): 1209–14. Bibcode:2006PNAS..103.1209G . doi:10.1073/pnas.0509498103 . PMC 1360560 . PMID 16432205 .
- [27] Gerst, Michael (2008). "In-Use Stocks of Metals: Status and Implications". Environmental Science and Technology. 42 (19): 7038–45. Bibcode:2008EnST...42.7038G . doi:10.1021/es800420p . PMID 18939524 .
- [28] Meylan, Gregoire (2016). "The anthropogenic cycle of zinc: Status quo and perspectives". Resources, Conservation and Recycling. 123: In press.
- [29] Stwertka 1998, p. 99 106. Lehto 1968, p. 829

[30] Bounoughaz, M.; Salhi, E.; Benzine, K.; Ghali E.; Dalard F. (2003). "A comparative

study of the electrochemical behaviour of Algerian zinc and a zinc from a commercial sacrificial anode". *Journal of Materials Science*. 38 (6): 1139–1145. Bibcode:2003JMatS..38.1139B .

doi:10.1023/A:1022824813564 .

[31] . Besenhard, Jürgen O. (1999). *Handbook of Battery Materials*. Wiley-VCH. ISBN 3-527-29469-4.

[32] Wiaux, J.-P.; Waefler, J. -P. (1995). "Recycling zinc batteries: an economical challenge in consumer waste management". *Journal of Power Sources*. 57 (1–2): 61–65. Bibcode:1995JPS....57...61W . doi:10.1016/0378-7753(95)02242-2 .

[32] Culter, T. (1996). "A design guide for rechargeable zinc-air battery technology". *Southcon/96. Conference Record*: 616. doi:10.1109/SOUTHCON.1996.535134 . ISBN 0-7803-3268-7.

[33] Whartman, Jonathan; Brown, Ian. "Zinc Air Battery-Battery Hybrid for Powering Electric Scooters and Electric Buses" (PDF). *The 15th International Electric Vehicle Symposium*. Archived from the original on March 12, 2006. Retrieved October 8, 2008.

[34] Cooper, J. F.; Fleming, D.; Hargrove, D.; Koopman, R.; Peterman, K. "A refuelable zinc/air battery for fleet electric vehicle propulsion" . *Society of Automotive Engineers future transportation technology conference and exposition*. Archived from the original on January 12,

2012. Retrieved October 8, 2008.

- [35] Xie, Z.; Liu, Q.; Chang, Z.; Zhang, X. (2013). "The developments and challenges of cerium half-cell in zinc– cerium redox flow battery for energy storage". *ElectrochimicaActa*. 90: 695–704. doi:10.1016/j.electacta.2012.12.066 .
- [36] Bush, Douglas Earl; Kassel, Richard (2006). *The Organ: An Encyclopedia* . Routledge.p. 679. ISBN 978-0-415-94174- 7.
- [37] "Coin Specifications" . United States Mint. Archived from the original on February 18, 2015. Retrieved October 8, 2008.
- [38] Jasinski, Stephen M. "Mineral Yearbook 1994: Zinc" (PDF). United States Geological Survey. Archived (PDF) from the original on October 29, 2008. Retrieved November 13, 2008.
- [39] Eastern Alloys contributors. "Diecasting Alloys" .Maybrook, NY: Eastern Alloys. Archived from the original on December 25, 2008. Retrieved January 19, 2009.
- [40] Apelian, D.; Paliwal, M.; Herrschaft, D. C. (1981)."Casting with Zinc Alloys". *Journal of Metals*. 33 (11): 12–19. Bibcode:1981JOM...33k..12A . doi:10.1007/bf03339527 .
- [41] Davies, Geoff (2003). *Materials for automobile bodies* . Butterworth-Heinemann.p. 157.ISBN 0-7506-5692-1.
- [42] Samans, Carl Hubert (1949). *Engineering Metals and Their Alloys*. Macmillan Co.
- [43] Porter, Frank (1994). "Wrought Zinc". *Corrosion Resistance of Zinc and Zinc Alloys* .CRC Press. pp. 6–7. ISBN 978-0- 8247-9213-8.[44] McClane, Albert Jules & Gardner, Keith (1987). [45] *The Complete book of fishing: a guide to freshwater, saltwater & big-game fishing* . Gallery Books. ISBN 978-0-8317-1565-6. Archived from the original on November 15, 2012. Retrieved June 26, 2012.

- [46] "Cast flywheel on old Magturbo trainer has been recalled since July 2000" .Minoura. Archived from the original on March 23, 2013.
- [47] Katz, Johnathan I. (2002). *The Biggest Bangs*. Oxford University Press. p. 18. ISBN 0-19-514570-4.
- [48] Zhang, Xiaoge Gregory (1996). *Corrosion and Electrochemistry of Zinc* . Springer.p. 93. ISBN 0-306-45334-7.
- [49] Weimer, Al (May 17, 2006). "Development of Solar-powered Thermochemical Production of Hydrogen from Water" (PDF). U.S. Department of Energy. Archived (PDF) from the original on February 5, 2009. Retrieved January 10, 2009.
- [50] . Heiserman 1992, p. 124 128. Blew, Joseph Oscar (1953). "Wood preservatives" (PDF). Department of Agriculture, Forest Service, Forest Products Laboratory.hdl:1957/816 .Archived (PDF) from the original on January 14, 2012.
- [51] . Frankland, Edward (1849). "Notiz übereineneueReiheorganischerKörper, welcheMetalle, Phosphor u. s. w. enthalten". *Liebig's Annalen der Chemie undPharmacie* (in German). 71 (2): 213– 216. doi:10.1002/jlac.18490710206 .
- [52] CRC 2006, p. 4-42
- [53] Paschotta, Rüdiger (2008). *Encyclopedia of Laser Physics and Technology* .Wiley-VCH.p. 798. ISBN 3- 527-40828-2.
- [54] Konstantinou, I. K.; Albanis, T. A. (2004). "Worldwide occurrence and effects of antifouling paint booster biocides in the aquatic environment: a review". *Environment International*. 30 (2): 235–248.doi:10.1016/S0160- 4120(03)00176-4 .
- [55] Boudreaux, Kevin A. "Zinc + Sulfur" . Angelo State University. Archived from the original on December 2, 2008. Retrieved October 8, 2008.
- [56] . "Technical Information" . Zinc Counters. 2008. Archived from the original on November 21, 2008. Retrieved November 29, 2008.

[57] Win, David Tin; Masum, Al (2003). "Weapons of Mass Destruction" (PDF). Assumption University Journal of Technology. Assumption University. 6 (4): 199. Archived (PDF) from the original on March 26, 2009. Retrieved April 6, 2009.

[58] David E. Newton (1999). Chemical Elements: From Carbon to Krypton . U. X.L. /Gale. ISBN 0-7876-2846-8. Archived from the original on July 10, 2008. Retrieved April 6, 2009.

[59] Ullmann's Agrochemicals . Wiley-Vch (COR). 2007. pp. 591–592. ISBN 3-527-31604-3.

[60] Walker, J. C. F. (2006). Primary Wood Processing: Principles and Practice. Springer. p. 317. ISBN 1-4020-4392-9.

[61] "ZDDP Engine Oil – The Zinc Factor" . Mustang Monthly. Archived from the original on September 12, 2009. Retrieved September 19, 2009.

[62] Overman, Larry E.; Carpenter, Nancy E. (2005). "The Allylic Trihaloacetimidate Rearrangement". Organic Reactions. 66: 1–107. doi:10.1002/0471264180.or066.01 .

ISBN 0-471-26418-0.

[63] . Rappoport, Zvi; Marek, Ilan (December 17, 2007). The Chemistry of Organozinc Compounds: R-Zn . ISBN 0-470-09337-4. Archived from the original on April 14, 2016.

[64] Knochel, Paul; Jones, Philip (1999). Organozinc reagents: A practical approach . ISBN 0-19-850121-8. Archived from the original on April 14, 2016.

[65] Herrmann, Wolfgang A. (January 2002). Synthetic Methods of Organometallic and Inorganic Chemistry: Catalysis . ISBN 3-13-103061-5. Archived from the original on April 14, 2016.

[66] E. Frankland, Ann. 126, 109 (1863); E. Frankland, B. F. Duppa, Ann. 135, 25 (1865)

[67] Kim, JeungGon; Walsh, Patrick J. (2006). "From Aryl Bromides to Enantioenriched Benzylic Alcohols in a Single Flask: Catalytic Asymmetric

Arylation of Aldehydes". *Angewandte Chemie International Edition*. 45 (25): 4175–4178. doi:10.1002/anie.200600741 . PMID 16721894 .

[68] . Łowicki, Daniel; Baś, Sebastian; Mlynarski, Jacek (2015). "Chiral zinc catalysts for asymmetric synthesis". *Tetrahedron*. 71 (9): 1339–1394. doi:10.1016/j.tet.2014.12.022 .

[69] DiSilvestro, Robert A. (2004). *Handbook of Minerals as Nutritional Supplements*. CRC Press. pp. 135, 155. ISBN 0-8493-1652-9.

[70] *Zinc Biochemistry: From a Single Zinc Enzyme to a Key Element of Life*. Wolfgang Maret 2013

[71] Mayo-Wilson, E; Junior, JA; Imdad, A; Dean, S; Chan, XH; Chan, ES; Jaswal, A;

Bhutta, ZA (May 15, 2014). "Zinc supplementation for preventing mortality, morbidity, and growth failure in children aged 6 months to 12 years of age". *The Cochrane Database of Systematic Reviews* (5): CD009384. doi:10.1002/14651858.CD009384.pub2 . PMID 24826920 .

[72] Swardfager W, Herrmann N, McIntyre RS, Mazereeuw G, Goldberger K, Cha DS, Schwartz Y, Lanctôt KL (June 2013). "Potential roles of zinc in the pathophysiology and treatment of major depressive disorder". *Neurosci.Biobehav. Rev.* 37 (5): 911–929. doi:10.1016/j.neubiorev.2013.03.018 . PMID 23567517 .

[73] Bhutta, Z. A.; Bird, S. M.; Black, R. E.; Brown, K. H.; Gardner, J. M.; Hidayat, A.;

Khatun, F.; Martorell, R.; et al. (2000). "Therapeutic effects of oral zinc in acute and persistent diarrhea in children in developing countries: pooled analysis of randomized controlled trials". *The American Journal of Clinical Nutrition*. 72 (6): 1516–22. PMID 11101480 .

[74] Evans JR, Lawrenson JG (2017). "Antioxidant vitamin and mineral supplements for slowing the progression of age-related macular degeneration". *Cochrane Database Syst Rev*. 7:

CD000254. doi:10.1002/14651858.CD000254.pub4 . PMID 28756618 . 154. Aydemir, T. B.; Blanchard, R. K.; Cousins, R. J. (2006).

[75] "Zinc supplementation of young men alters metallothionein, zinc transporter, and cytokine gene expression in leukocyte populations" . PNAS. 103 (6): 1699–704. Bibcode:2006PNAS..103.1699A . doi:10.1073/pnas.0510407103 . PMC 1413653 . PMID 16434472 .

[76] Valko, M.; Morris, H.; Cronin, M. T. D. (2005). "Metals, Toxicity and Oxidative stress" (PDF). *Current Medicinal Chemistry*. 12 (10): 1161–208. doi:10.2174/0929867053764635 . PMID 15892631 . Archived from the original (PDF) on August 8, 2017.

[77] Venkatratnam, Abhishek; Nathan Lents (July 1, 2011). "Zinc Reduces the Detection of Cocaine, Methamphetamine, and THC by ELISA Urine Testing". *Journal of Analytical Toxicology*. 35 (6): 333–340. doi:10.1093/anatox/35.6.333 . PMID 21740689 .

[78] Hosie AM, Dunne EL, Harvey RJ, Smart TG (2003). "Zinc-mediated inhibition of GABA(A) receptors: discrete binding sites underlie subtype specificity". *Nat. Neurosci*. 6 (4): 362–9. doi:10.1038/nn1030 . PMID 12640458 .

[79] "Zinc – Fact Sheet for Health Professionals" . Office of Dietary Supplements, US National Institutes of Health. February 11, 2016. Retrieved January 7, 2018.

[80] Singh M, Das RR (June 2013). "Zinc for the common cold". *The Cochrane Database of Systematic Reviews* (6): CD001364. doi:10.1002/14651858.CD001364.pub4 . PMID 23775705 .

[81] "Common Cold and Runny Nose" . United States Centers for Disease Control and Prevention. September 26, 2017. Retrieved January 7, 2018.

[82] . Roldán, S.; Winkel, E. G.; Herrera, D.; Sanz, M.; Van Winkelhoff, A. J. (2003). "The effects of a new mouthrinse containing chlorhexidine, cetylpyridinium chloride and zinc lactate on the microflora of oral halitosis patients: a dual-centre, double-blind placebo-controlled study".

Journal of Clinical Periodontology. 30 (5): 427–434. doi:10.1034/j.1600-051X.2003.20004.x .

[83] Marks, R.; Pearse, A. D.; Walker, A. P. (1985). "The effects of a shampoo containing zinc pyrithione on the control of dandruff". *British Journal of Dermatology*. 112 (4): 415–422.

doi:10.1111/j.1365-2133.1985.tb02314.x .

[84] Maret, Wolfgang (2013). "Chapter 12. Zinc and Human Disease". In Astrid Sigel; Helmut Sigel; Roland K. O. Sigel. *Interrelations between Essential Metal Ions and Human Diseases. Metal Ions in Life Sciences*. 13. Springer. pp. 389–414. doi:10.1007/978-94-007-7500-8_12 .

[85] Prakash A, Bharti K, Majeed AB (April 2015). "Zinc: indications in brain disorders". *FundamClinPharmacol*. 29 (2): 131–149. doi:10.1111/fcp.12110 . PMID 25659970 .

[86] Cherasse Y, Urade Y (November 2017). "Dietary Zinc Acts as a Sleep Modulator" . *International Journal of Molecular Sciences*. 18 (11): 2334. doi:10.3390/ijms18112334 .

[87] Prasad A. S. (2008). "Zinc in HumanHealth: Effect of Zinc on Immune Cells" *Mol. Med*. 14 (5–6): 353–7. doi:10.2119/2008-00033.Prasad . PMC 2277319 . PMID 18385818 .

[88] Zinc's role in microorganisms is particularly reviewed in: Sugarman B (1983). "Zinc and infection". *Review of Infectious Diseases*. 5 (1): 137–47. doi:10.1093/clinids/5.1.137 .

PMID 6338570 .

[89] Cotton 1999, pp. 625–629

[90] . Plum, Laura; Rink, Lothar; Haase, Hajo (2010). "The Essential Toxin: Impact of Zinc on Human Health" . *Int J Environ Res Public Health*. 7 (4): 1342–1365. doi:10.3390/ijerph7041342 . PMC 2872358 . PMID 20617034 .

[91]. Brandt, Erik G.; Hellgren, Mikko; Brinck, Tore; Bergman, Tomas; Edholm, Olle (2009). "Molecular dynamics study of zinc binding to cysteines in a peptide mimic of the alcohol dehydrogenase structural zinc site" (PDF). *Phys. Chem. Chem. Phys.* 11 (6): 975–83. Bibcode:2009PCCP...11..975B .doi:10.1039/b815482a . PMID 19177216 .

[92] Rink, L.; Gabriel P. (2000). "Zinc and the immune system". *Proc Nutr Soc.* 59 (4): 541–52.

doi:10.1017/S0029665100000781 . PMID 11115789 .

[93] Wapnir, Raul A. (1990). *Protein Nutrition and Mineral Absorption* . Boca Raton, Florida: CRC Press. ISBN 0-8493- 5227-4.

[94] Berdanier, Carolyn D.; Dwyer, Johanna T.; Feldman, Elaine B. (2007). *Handbook of*

Nutrition and Food . Boca Raton, Florida: CRC Press. ISBN 0-8493-9218-7.

[95] Bitanihirwe BK, Cunningham MG (November 2009). "Zinc: the brain's dark horse". *Synapse.* 63 (11): 1029–1049. doi:10.1002/syn.20683 . PMID 19623531 .

[96] . Nakashima AS; Dyck RH (2009). "Zinc and cortical plasticity". *Brain Res Rev.* 59 (2): 347–73. doi:10.1016/j.brainresrev.2008.10.003 . PMID 19026685 .

[97] Tyszka-Czochara M, Grzywacz A, Gdula-Argasińska J, Librowski T, Wiliński B, Opoka W (May 2014). "The role of zinc in the pathogenesis and treatment of central nervous system (CNS) diseases. Implications of zinc homeostasis for proper CNS function" (PDF). *Acta.Pol. Pharm.* 71 (3): 369–377. PMID 25265815 . Archived (PDF) from the original on August 29, 2017.

[98] PMID 17119290

[99] NRC 2000, p. 443

[100] Stipanuk, Martha H. (2006). *Biochemical, Physiological & Molecular Aspects of Human Nutrition*. W. B. Saunders Company. pp. 1043–1067. ISBN 978-0-7216-4452-3. 180. Greenwood 1997, pp. 1224–1225

[101] Kohen, Amnon; Limbach, Hans- Heinrich (2006). *Isotope Effects in Chemistry and Biology*. Boca Raton, Florida: CRC Press. p. 850. ISBN 0-8247-2449-6.

[102] Gadallah, M. A. A. (2000). "Effects of indole-3-acetic acid and zinc on the growth, osmotic potential and soluble carbon and nitrogen components of soybean plants growing under water deficit". *Journal of Arid Environments*. 44 (4): 451–467. Bibcode:2000JArEn..44..451G .

doi:10.1006/jare.1999.0610 .

[101] Ensminger, Audrey H.; Konlande, James E. (1993). *Foods & Nutrition Encyclopedia* (2nd ed.). Boca Raton, Florida: CRC Press. pp. 2368–2369. ISBN 0-8493-8980-1.

[102] . "Zinc content of selected foods per common measure" (PDF). USDA National Nutrient Database for Standard Reference, Release 20. United States Department of Agriculture. Archived from the original on March 5, 2009. Retrieved December 6, 2007.

[103] Allen, Lindsay H. (1998). "Zinc and micronutrient supplements for children". *American Journal of Clinical Nutrition*. 68 (2 Suppl): 495S–498S. PMID 9701167 .

[104] Rosado, J. L. (2003). "Zinc and copper: proposed fortification levels and recommended zinc compounds". *Journal of Nutrition*. 133 (9): 2985S–9S. doi:10.1093/jn/133.9.2985S .

PMID 12949397 .

[105] Hotz, C.; DeHaene, J.; Woodhouse, L. R.; Villalpando, S.; Rivera, J. A.; King, J. C.

(2005). "Zinc absorption from zinc oxide, zinc sulfate, zinc oxide + EDTA, or sodiumzinc

EDTA does not differ when added as fortificants to maize tortillas". *Journal of Nutrition*. 135 (5): 1102–5. PMID 15867288 .

- [106] Moshfegh, Alanna; Goldman, Joseph; and Cleveland, Linda. (2005). What We Eat in America Archived September 10, 2016, at the Wayback Machine.. NHANES 2001–2002: Usual Nutrient Intakes from Food Compared to Dietary ReferenceIntakes. U.S. Department of Agriculture, Agricultural Research Service. Table A13: Zinc.
- [107] What We Eat In America, NHANES 2013–2014 Archived February 24, 2017, at the Wayback Machine..208. NRC 2000, p. 442 209. Ibs, K. H.; Rink, L. (2003). "Zincaltered immune function". *Journal of Nutrition*. 133 (5 Suppl 1): 1452S–6S. PMID 12730441 .
- [110] "Position of the American Dietetic Association and Dietitians of Canada: Vegetarian diets" (PDF). *Journal of the American Dietetic Association*. 103 (6): 748–65. 2003. doi:10.1053/jada.2003.50142 . PMID 12778049 . Archived (PDF) from the original on January 14, 2017.
- [111] Freeland-Graves J. H.; Bodzy P. W.; Epright M. A. (1980). "Zinc status of vegetarians". *Journal of the American Dietetic Association*. 77 (6): 655–661. PMID 7440860 .
- [112] Hambidge, M. (2003). "Biomarkers of trace mineral intake and status". *Journal of Nutrition*. 133. 3 (3): 948S–955S. PMID 12612181 .
- [113] WHO contributors (2007). "The impact of zinc supplementation on childhood mortality and severe morbidity" . World Health Organization. Archived from the original on March 2, 2009. Retrieved March 1, 2009.
- [114] Shrimpton, R.; Gross, R.; Darnton-Hill, I.; Young, M. (2005). "Zinc deficiency: what are the most appropriate interventions?" . *British Medical Journal*. 330 (7487): 347– 9. doi:10.1136/bmj.330.7487.347 . PMC 548733 . PMID 15705693 .
- [115] Geoffrey Michael Gadd (March2010). "Metals, minerals and microbes: geomicrobiology and bioremediation" . *Microbiology*. 156 (3): 609–643. doi:10.1099/mic.0.037143-0 . PMID 20019082 . Archived from the original on October 25, 2014.

- [116] Alloway, Brian J. (2008). "Zinc in Soils and Crop Nutrition, International Fertilizer Industry Association, and International Zinc Association" . Archived from the original on February 19, 2013.
- [117]. Eisler, Ronald (1993). "Zinc Hazard to Fish, Wildlife, and Invertebrates: A Synoptic Review" (PDF). Contaminant Hazard Reviews. Laurel, Maryland: U.S. Department of the Interior, Fish and Wildlife Service (10). Archived from the original on March 6, 2012.
- [118] Muysen, Brita T. A.; De Schamphelaere, Karel A. C.; Janssen, Colin R. (2006). "Mechanisms of chronic waterborne Zn toxicity in *Daphnia magna*". *Aquatic Toxicology*. 77 (4): 393–401. doi:10.1016/j.aquatox.2006.01.006 . PMID 16472524 .
- [119] Bothwell, Dawn N.; Mair, Eric A.; Cable, Benjamin B. (2003). "Chronic Ingestion of a Zinc-Based Penny". *Pediatrics*. 111 (3): 689–91. doi:10.1542/peds.111.3.689 . PMID 12612262 .
- [220] . Johnson AR; Munoz A; Gottlieb JL; Jarrard DF (2007). "High dose zinc increases hospital admissions due to genitourinary complications". *J. Urol*. 177 (2): 639–43. doi:10.1016/j.juro.2006.09.047 . PMID 17222649 .
- [121] "Lawsuits blame denture adhesives for neurological damage" . Tampa Bay Times. February 15, 2010. Archived from the original on February 18, 2010.
- [122] Oxford, J. S.; Öberg, Bo (1985). *Conquest of viral diseases: a topical review of drugs and vaccines* . Elsevier. p. 142. ISBN 0-444-80566-4.
- [123] "FDA says Zicam nasal products harm sense of smell" . Los Angeles Times. June 17, 2009. Archived from the original on June 21, 2012.
- [124] Lamore SD; Cabello CM; Wondrak GT (2010). "The topical antimicrobial zinc pyrithione is a heat shock response inducer that causes DNA damage and PARP-dependent energy crisis in human skin cells" . *Cell Stress Chaperones*. 15 (3): 309–22. doi:10.1007/s12192-009- 0145-6 . PMC 2866994 . PMID 19809895 .
- [125] Barceloux, Donald G.; Barceloux, Donald (1999). "Zinc". *Clinical Toxicology*. 37 (2): 279–292. doi:10.1081/CLT- 100102426 .

- [126] Bennett, Daniel R. M. D.; Baird, Curtis J. M.D.; Chan, Kwok-Ming; Crookes, Peter F.; Bremner, Cedric G.; Gottlieb, Michael M.; Naritoku, Wesley Y. M.D. (1997). "Zinc Toxicity Following Massive Coin Ingestion". *American Journal of Forensic Medicine and Pathology*. 18 (2): 148–153. doi:10.1097/00000433-199706000-00008 .
- [127] . Fernbach, S. K.; Tucker G. F. (1986). "Coin ingestion: unusual appearance of the penny in a child". *Radiology*. 158 (2): 512. doi:10.1148/radiology.158.2.3941880 . PMID 3941880 .
- [128] . Stowe, C. M.; Nelson, R.; Werdin, R.; Fangmann, G.; Fredrick, P.; Weaver, G.; Arendt, T. D. (1978). "Zinc phosphide poisoning in dogs". *Journal of the American Veterinary Medical Association*. 173 (3): 270. PMID 689968 .
- [129] Reece, R. L.; Dickson, D. B.; Burrowes, P. J. (1986). "Zinc toxicity (new wire disease) in aviary birds". *Australian Veterinary Journal*. 63 (6): 199. doi:10.1111/j.1751-0813.1986.tb02979.x
- [134] Vijaya Pandurang Dhawale¹, *, VaideiBalraj Khobragade², Satish Damodar Kulkarni² - Synthesis and Characterization of Aluminium Oxide (Al₂O₃) Nanoparticles and its Application in Azodye Decolourisation - *International Journal of Environmental Chemistry* - 2018; 2(1): 10-17 <http://www.sciencepublishinggroup.com/j/ijec> doi: 10.11648/j.ijec.20180201.13].
- [135] Chienwen Huang¹, Jiechao Jiang¹, Chivarat Muangphat¹, Xiankai Sun², Yaowu Hao^{1*}- Trapping Iron Oxide into Hollow Gold Nanoparticles - Huang et al. *Nanoscale Res Lett* 2011, 6:43 <http://www.nanoscalereslett.com/content/6/1/43>
- [136] Elena F. Sheka - Reduced Graphene Oxide and Its Natural Counterpart Shungite Carbon - *Russian Peoples' Friendship University of Russia Moscow, 117198 Russia*- sheka@icp.ac.ru.
- [137] Tiago Zozi* Fábio SteinerI Rubens FeyII Deise Dalazen CastagnaraII Edleusa Pereira SeidelIII - Response of wheat to foliar application of zinc - *Ciência Rural, Santa Maria*, v.42, n.5, p.784-787, mai, 2012- ISSN 0103-8478.

[138] Osman Sivrikaya- Adana Science and Technology University, Dept. of Mining and Mineral Processing Eng., Adana Turkey *a. Corresponding author (osmansivrikaya@gmail.com)*/ SULFIDIZATION FLOTATION OF A LOW GRADE OXIDE Pb-Zn ORE- Proceedings of 14th International Mineral Processing Symposium – Kuşadası, Turkey, 2014 .

[139] Guido Panzarasa 1,*,† , Giovanni Consolati 2,3 , Marco Scavini 4 , Mariangela Longhi 4 and Fiorenza Quasso 2. Convenient Preparation of Graphene Oxide from Expandable Graphite and Its Characterization by Positron Annihilation Lifetime Spectroscopy – C Journal of Carbon Research - C **2019**, 5, 6; doi:10.3390/c5010006 www.mdpi.com/journal/carbon .

[140] K.I. Bogutskaya*, Yu.P. Sklyarov2, Yu.I. Prylutskiy1 Zinc and zinc nanoparticles: biological role and application in biomedicine -*Ukrainica Bioorganica Acta 1 (2013) 9–16-* www.bioorganica.org.ua .

[141] 1Ch.Bimola Devi, 2Th. Nandakishore, 3Sangeeta N, 4Gomi Basar, 5N.Omita Devi, 6Sungdirenla Jamir, 7M.Amuba Singh- Zinc in Human health - *IOSR Journal of Dental and Medical Sciences (IOSR-JDMS) e-ISSN: 2279-0853, p-ISSN: 2279-0861. Volume 13, Issue 7 Ver. II (July. 2014), PP 18-23* www.iosrjournals.org .

[142] T.V. Perevalov1,a, V.A. Gritsenko1,b, and V.V. Kaichev2,c - Electronic structure of aluminum oxide: ab initio simulations of α and γ phases and comparison with experiment for amorphous films / *Eur. Phys. J. Appl. Phys.* 52, 30501 (2010). DOI: 10.1051/epjap/2010159 .

[143] Peyman Hassanpour1,2, Yunes Panahi3, Abbas Ebrahimi-Kalan4, Abolfazl Akbarzadeh1,3,5 Soodabeh Davaran1,5, Aygun N. Nasibova5,6, Rovshan Khalilov5,6, Taras Kavetskiy5,7,8/ Biomedical applications of aluminium oxide nanoparticles / *Micro & Nano Letters*, 2018, Vol. 13, Iss. 9, pp. 1227–1231 doi: 10.1049/mnl.2018.5070& The Institution of Engineering and Technology 2018 .

[144] .T. A. Denisova, L. G. Maksimova, O. N. Leonidova, and N. A. Zhuravlev / *Physical and Chemical Properties of Zinc Cyanoferrates(II) /ISSN 0036-0236, Russian Journal of Inorganic Chemistry, 2009, Vol. 54, No. 1, pp. 6–12.* © Pleiades Publishing, Ltd., 2009. Original Russian Text © T.A. Denisova, L.G.

Maksimova, O.N. Leonidova, N.A. Zhuravlev, 2009, published in Zhurnal Neorganicheskoi Khimii, 2009, Vol. 54, No. 1, pp. 8–14.

[145] A.K. Bhattacharjee . J. P´erez-Conde /Optical properties of semiconductor nanocrystals: A symmetry-based tight-binding approach /MATERIA CONDENSADA REVISTA MEXICANA DE F´ISICA 49 SUPLEMENTO 3, 168–171 NOVIEMBRE 2003 .

[146] Mayuree Jaisai¹, Sunandan Baruah^{*1,2} and Joydeep Dutta^{*1,3}/Paper modified with ZnO nanorods – antimicrobial studies /*Beilstein J. Nanotechnol.* 2012, 3, 684–691.

[147] Sunandan Baruah, Mayuree Jaisai, Reza Imani¹, Mousa M Nazhad and Joydeep Dutta/**Photocatalytic paper using zinc oxide nanorods** / IOP PUBLISHING SCIENCE AND TECHNOLOGY OF ADVANCED MATERIALS -Sci. Technol. Adv. Mater. **11** (2010) 055002 (7pp) doi:10.1088/1468-6996/11/5/055002 .

[148] Ananthu C Mohana, Renjanadevi Bb* -Preparation of Zinc Oxide Nanoparticles and its Characterization Using Scanning Electron Microscopy (SEM) and X-Ray Diffraction(XRD) - 2212-0173 © 2016 The Authors. Published by Elsevier Ltd. This is an open access article under the CC BY-NC-ND license (<http://creativecommons.org/licenses/by-nc-nd/4.0/>).

[149] F V Molefe¹, L F Koao¹, B F Dejene¹, H C Swart² - Influence of zinc acetate concentration in the preparation of ZnO nanoparticles via chemical bath deposition - SA Institute of Physics ISBN: 978-0-620-65391-6 -Proceedings of SAIP2014 .